Task rule and choice are reflected by layer-specific processing in rodent auditory cortical microcircuits

Dissertation

for the degree of

doctor rerum naturalium (Dr.rer.nat.)

approved by the Faculty of Natural Sciences of
Otto-von-Guericke-University Magdeburg

by **MSc. Maria Zempeltzi**

born on: 25th February 1987 in: Larisa, Greece

Reviewers: PD Dr. Max F.K. Happel

Prof. Dr. Simon Rumpel

submitted on: 23rd June 2020, Magdeburg

defended on: 25th January 2021, Magdeburg

Abstract

Title: *Task rule and choice are reflected by layer-specific processing in rodent auditory cortical microcircuits*

Author: *Maria Zempeltzi*

Keywords: *auditory cortex, rodents, sensory processing, learning, behavior, cortical microcircuits, current source density (CSD) analysis*

The primary auditory cortex (A1) is an essential node in the integrative brain network that encodes the behavioral relevance of acoustic stimuli, predictions, and auditory-guided decision making. Previous studies have revealed task-related information being present at both the single-unit and population activity. However, its realization with respect to the cortical microcircuitry is less well understood. In this study, we used chronic, laminar current source density (CSD) analysis from the A1 of behaving Mongolian Gerbils *(Meriones unguiculatus*) in order to characterize layer-specific, spatiotemporal synaptic population activity. Animals were trained to first detect and subsequently to discriminate two pure tone frequencies in consecutive training phases in a Go/NoGo shuttle-box task.

We demonstrate that not only sensory but also task- and choice-related information is represented in the mesoscopic neuronal population code distributed across cortical layers. Based on a single-trial analysis using generalized linear-mixed effect models (GLMM), we found infragranular layers to be involved in auditory-guided action initiation during tone detection. Supragranular layers, particularly, are involved in the coding of choice options during tone discrimination. Further, we found that the overall columnar synaptic network activity represents the accuracy of the opted choice. Moreover, cognitive flexibility was represented in the A1 during multiple reversal of choice-outcome contingency

task. During those cognitive processes, the infragranular layer VI continuously updates the network in order to optimize of the discrimination performance, while the supragranular layers promote the choice accuracy, especially at states with higher task-engagement and performance.

Our study thereby suggests a multiplexed cortical representation of stimulus features in dependence of the task, action selection, and the behavioral options of the animal in preparation of correct choices. The findings expand our understanding of how individual layers contribute to the integrative circuit of the A1 in order to code task-relevant information and guide sensory-based decision making.

Zusammenfassung

Title:*Schichtspezifische Repräsentation der Aufgabe und Entscheidung in Schaltkreisen des primären auditorischen Cortex bei Nagetieren*

Author:*Maria Zempeltzi*

Strichwoerter: *auditorischer Kortex, Nagetiere, sensorische Verarbeitung, Lernen, Verhalten, kortikale Schaltkreise, Analyse der Stromquellendichte (CSD)*

Der primäre auditorische Kortex (A1) ist eine zentrale Integrations-Schaltstelle des Hirns bei der Kodierung der Verhaltensrelevanz akustischer Reize, der Vorhersagen und akustisch bedingter Entscheidungsfindungen. Frühere Studien haben gezeigt, dass aufgabenbezogene Informationen sowohl auf Ebene von Einzelaktivität, als auch in der Populationsaktivität reflektiert sind. Die mechanistische Realisierung in Bezug auf die kortikalen Mikroschaltkreise ist jedoch bisher wenig verstanden. In der vorliegenden Arbeit wurde mittels chronischer Ableitungen die laminare Stromquellendichte (CSD) in A1 bei sich verhaltenden Wüstenrennmäusen *(Meriones unguiculatus*) die schichtspezifische, raumzeitliche synaptische Populationsaktivität charakterisiert. Die Tiere wurden in aufeinander folgenden Trainingsphasen in einer Go/NoGo-Shuttle-Box-Aufgabe darauf trainiert, zunächst zwei Reintonfrequenzen zu erkennen und anschließend zu diskriminieren.

Die Arbeit konnte zeigen, dass nicht nur sensorische, sondern auch aufgaben- und wahlbedingte Informationen im mesoskopischen neuronalen Populationscode, der über kortikale Schichten verteilt ist, repräsentiert werden. Auf der Grundlage von Single-trial Analysen konnte mittels generalized linear-mixed effect models (GLMM) gezeigt werden, dass die Aktivität in infragranulären Schichten an der auditorisch ausgelösten Motorreaktion bei der Tondetektion eine zentrale Rolle spielen. Des Weiteren konnte gezeigt

werden, dass insbesondere die supragranularen Schichten an der Kodierung von Wahloptionen während der komplexeren Tonunterscheidung beteiligt sind. Ferner fanden wir heraus, dass die gesamte kolumnäre synaptische Netzwerkaktivität in A1 bei der Kodierung der Antwortgenauigkeit eine zentrale Rolle spielt. In einem letzten Schritt wurde untersucht, wie die Schaltkreise in A1 während der mehrfachen Umkehr der Kontingenz in einer Diskriminationsaufgabe involviert sind. Während der Änderung der Kontingenz und einem erzwungenen Strategiewechsel zeigt sich vor allem ein wichtiger Beitrag der Aktivität in der infragranularen Schicht VI. Die supragranularen Schichten hingegen waren bester Prädiktor für die korrekte Verhaltensauswahl vor allem während Phasen höherer genereller Leistung. Die vorliegende Arbeit zeigt damit auf, dass der auditorische Kortex eine multiplexe Darstellung von Reizmerkmalen in Abhängigkeit von der Aufgabe, der Handlungsauswahl und den Verhaltensoptionen eines Tieres zur Vorbereitung korrekter Entscheidungen und der Anpassung von Verhaltensstrategien ermöglicht. Die Ergebnisse erweitern unser Verständnis darüber, wie einzelne Schichten zum integrativen Schaltkreis in A1 beitragen, um aufgabenrelevante Informationen zu kodieren und sensorisch basierte Entscheidungsfindung zu steuern.

Dedicated to my grandmother, in memoriam.

"Brick walls are there for a reason. And once you get over them—even if someone has practically had to throw you over—it can be helpful to others to tell them how you did it."

— Randy Pausch, The Last Lecture

Contents

List of Tables

List of Figures

Index of Notation

A1 Primary Auditory Cortex

AVREC Averaged Rectified Current Source Density

CR Conditioned Response

Cor.Rej. Correct Rejection of a conditioned response

CS Conditioned Stimuli

CS+/CS- Conditioned stimuli for retrieving the animals' Go/NoGo behavior

CSD Current Source Density

d' D-prime Sensitivity index

FA False Alarm - Incorrect conditioned response

FM Frequeny Modulation

GLMM Generalized Linear Mixed Model

Hit Correct conditioned response

LFP Local Field Potential

Miss Delayed conditioned response

mPFC medial Prefrontal Cortex

RMS Root Mean Square

ROC Receiver Operator Curve

SDT Signal Detection Theory

S1 Primary somatosensory Cortex

SVM Support Vector Machine

V1 Primary Visual Cortex

US Unconditioned Stimulus

1 | Introduction

"Since we perceive that we are seeing and hearing, it is necessary that one perceives that one sees either by sight or by some other sense... Further, if the sense which perceived sight were to be other than sight, then either this will carry on into infinity or there will be some sense which will be of itself, with the result that one should grant this in the case of the first sense."

— Aristotle, De Anima, 425b22 ff, trans. Shields

1.1 Sensory processing: From auditory perception to action

Awareness of perception and sensory processing is not recent; it has been described at least as early as Aristotle's treatise 'De Anima' (c. 350 BCE). In the De Anima passage above, Aristotle said that there are no perceptions of perceptions. Perception exists as such and does not carry its own awareness. On this understanding the first perception would be how an organism perceives an object, while the second perception would be the organism's awareness of the perception of the object. One can recognize that with this Aristotle sets the ground basis of the modern neuroscientific theories regarding sensory perception with the bottom-up and top-down processing, as we know them today. Bottom-up processing refers to processing sensory stimuli as they come from our environment and they built up the sensory information. Top-down processing, on the other hand, is the cognition-driven perception, the internal representation of environmental key aspects/features relevant for the organism, and its consequential action-selection. Organisms must be capable of adapting their responses to sensory stimuli and developing proper behavioral strategies in order to survive and evolve. In recent years, there has been an increasing amount of

literature emphasizing that sensory cortices can facilitate such required flexibility. In fact, there is still considerable uncertainty with regard to the representation of task-relevant and choice-related information in the sensory cortices. In this doctoral thesis, I will be focusing on a data driven approach to find layer-specific activity patterns from the primary auditory cortex region and their involvement in auditory learning and flexible decision-making processes.

1.1.1 The auditory pathway and laminar organization of the primary auditory cortex

Overview of the auditory pathway

Sounds are one of the main external stimuli into our environment. To perceive sounds and initiate behaviors, for instance movements towards the source of the sound, the auditory system needs to transform the sound waves into neuronal activity patterns. The auditory pathway consists of several stations of transformation starting with the external and middle ears which collect the sound waves (Figure 1.1, anatomical details are described in Purves). Then, the amplified sound pressure is transmitted via the inner ear's fluid, wherein the signal characteristics (frequency, amplitude, and phase) are decomposed. Biomechanical processes at the sensory hair cells result in the signal decomposition and then it reaches the auditory nerve to get encoded. As next, the signal arrives to the cochlea where it is represented by its frequency, a phenomenon known as *tonotopy*.

The next station is the cochlear nucleus which is the merging point of the peripheral auditory information into central pathways. Further, the outputs of the cochlear nucleus are the superior olivary complex and the inferior colliculus of midbrain. At the first branch the signal of two ears interacts and it contributes to the proper sound localization. The second branch is one of the crucial locations where integration of auditory and motor system happens. From this station the auditory signal is forwarded to the thalamus (specifically the medial geniculate body (MGB)) and to the auditory cortex. The auditory cortex consists of the core area, with the primary and secondary areas. The primary auditory cortex (A1), the main part of the core area, plays an important role in integration of neuronal signals from multiple brain areas. Compared to other sensory systems, the

auditory has the largest numbers of stations from periphery to the cortex (Purves). The pivotal role of auditory processing in survival and development of all the mammals, as well as, the large numbers of stations makes sound perception a highly interesting neural phenomenon.

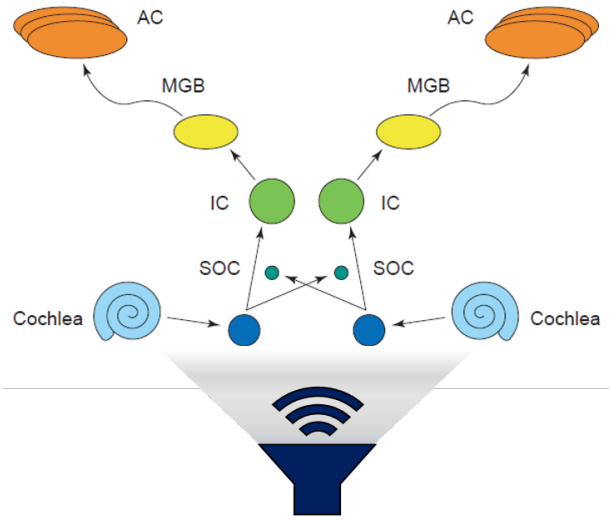

Figure 1.1: The auditory pathway. A schematic illustration (adapted from Patterson, 1999) of the primary components of the auditory pathway: the cochlea (or inner ear); the three brainstem structures - the cochlear nucleus (CN), the superior olivary complex (SOC) and the inferior colliculus (IC); the auditory thalamus or medial geniculate body (MGB); and the auditory cortex (AC).

First cortical station: The primary auditory cortex's microcircuits

The A1 is the first cortical station of auditory representation and it is tonotopically organized. This means that neurons found in several locations of the A1 respond differently at specific sound frequencies (Figure 1.2, b). Although the exact tonotopic gradient shows species-related differences, the principle mechanism is similar across species. In the last decades an increasing volume of published studies describe the complexity of the A1 and its multi-functionality. For example, the A1 is crucial for sound processing and auditory scene analysis, but also it contributes to learning-related functions (Bizley and Cohen, 2013; Francis et al., 2018b; King et al., 2018)

Like all the other sensory cortices, the primary auditory cortex is also columnar, into the 3-dimensional volume of the temporal neocortex. The auditory cortex consists of the classical six-layer architecture forming a specific microcircuitry between layers (Winer, 1992). The columnar organization allows neurons to get connected via synapses vertically and horizontally creating a functional unit called cortical column (Mountcastle VB,

1955; Haueis, 2016; Hawkins et al., 2017). Understanding the function of the cortical column(s) under certain conditions is a major area of interest within the field of neuroscience (Markram et al., 2015).

The focus of the present study is the cortical column of the A1 area (Figure 1.2, c), which consists of the layers I/II called supragranular, layer III/IV are the granular and layers Va, Vb and VI, which are the infragranular layers (Budinger and Kanold, 2018; Happel et al., 2014a). The first bottom-up driven input, from the tonotopically organized lemniscal pathway via the ventral division of the ventral MGB (MGBv), goes to layer IV. From this point, the neural information flows then to other layers of the same column and subsequently to next columns and cortical areas.

Additionally, there are descending projections mainly from the deeper layers of A1 to the thalamus (Figure 1.2, c). This corticothalamic feedback loop in A1 is important for shaping the receptive field properties of the neurons in the ventral auditory thalamus (MGBv) (He, 1997; Hackett et al., 2011). Recently, it has been also reported that the corticothalamic feedback loop plays a crucial role in perception of complex sounds and scene analysis (Homma et al., 2017). Further, the supragranular layers (I/III) consist of a complex, non-homogeneous subdivision of the microcircuitry which is involved in cortico-cortical communication and offers a diverse functionality (Meng et al., 2017).

The tonotopic and laminar organization of the A1 has been investigated by using a variety of mammals' brains (Figure 1.2), from rodents or cats to primates, and their features show many homologies anatomically, histologically, but also fascinatingly functional differences. One of the best examples is the auditory cortex of the echolocating bats, which has been extensively studied due to its highly specialized functions (Suga, 1984). Bats are the only taxon among all other mammals whose auditory cortex shows a *chronotopy*. Chronotopy is an innate feature which enable the cortical neurons to respond in specific time points using the echo-delay information from the surrounding environment (Kössl et al., 2012; Hechavarría et al., 2013). Such cortical features and complex hippocampal navigation systems are natural benefits dedicated to help bats preying and surviving (Geva-Sagiv et al., 2015; Moss and Surlykke, 2010).

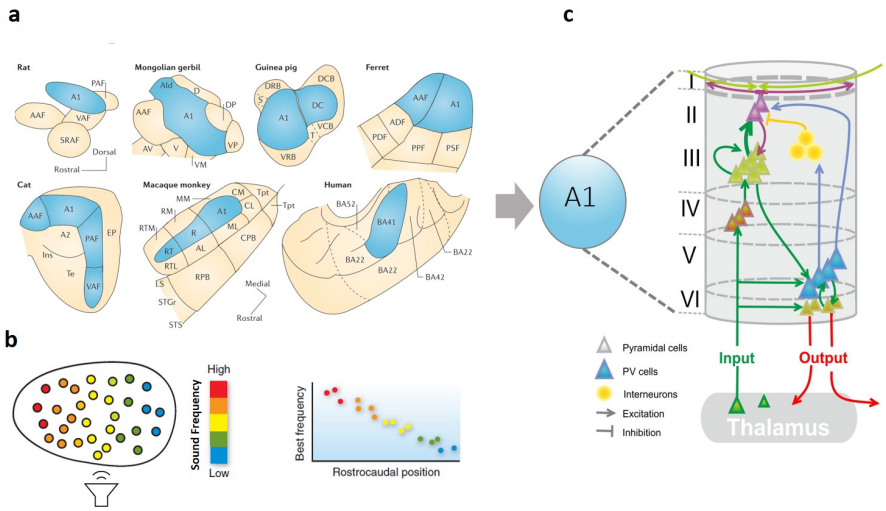

Figure 1.2: The primary auditory cortex across species: tonotopical and columnar organization. a. Illustration of the organization of the A1 across different species. **b.** Example of a tonotopic gradient where neurons respond differently along the rostocaudal axis depending on the preferred frequency. **c.** Schematic overview of the A1 cortical column, which consists of the layers I-VI. Cortico-thalamic and cortico-cortical interactions happen and generate a specific microcircuritry with the involvement of different types of cells. (adapted from a.Bizley and Cohen, b.Castro and Kandler, 2010 and c.Happel et al., 2014a)

Comparative studies across animal systems and modalities may help to deepen our understanding of basic neuronal mechanisms during the multiple interactions with the external or natural environments. Studying the A1 area allows us to understand more about the sound perception, the analysis of the acoustic scene, the formation of the auditory objects, but also other complex cognitive processes such as learning and decision making (King et al., 2018).

1.1.2 The role of the primary auditory cortex in learning and decision-making

In the history of auditory neurophysiology, the A1 has been often described as the key factor for auditory scene analysis (Bizley and Cohen, 2013; King et al., 2018). Many studies have shown that the A1 is crucial for analyzing the spectral, spatial, or temporal features of sounds (Fishman et al., 2014; Teki et al., 2013; Shiell et al., 2018).Thus, the formation of perceptual representations from the acoustic environment leads to the creation of auditory objects. For example, the receiver of a visual stimulus is able to directly extract information about the features of an object (eg. shape, size, color etc.), while in the auditory modality a prior experience to the auditory stimulus is required

in order to assign the semantics and adapt behaviors (Scheich et al., 2011). Much of the early research on how sound is encoded in the A1 has been explored by cortical inactivation (lesions) and observation on its effects to the behavior of the subjects (Ohl et al., 1999).

Existing research recognises that learning and behavioral engagement play a critical role in shaping the tuning properties – either by shifting the best frequency of neurons towards the task-relevant frequency or by increasing the slope of the tuning curve near to that specific frequency (Weinberger and Weinberger, 2007; Ohl and Scheich) – and expanding the tonotopic maps of the A1 (Guo et al., 2017a; Bao et al., 2004; Carcea et al., 2017a). Moreover, an increasing amount of literature reports the importance of A1 neuronal networks beyond tonotopy in a more learning-related fashion. In a recent report, Bagur et al. (2018) examine the extent to which task-engagement is encoded in the A1 using spike recordings in behaving ferrets. They found task-engagement-induced changes in cortical activity, which also depend on the task-design (appetitive or aversive). Moreover,they conclude that A1 and frontal cortex responses share strong similarities on a population level. By now more evidence supports the idea that the central function of the A1 is the integration of auditory stimulus features (eg. pitch, frequency etc.) and cognitive aspects of behavioral contexts, especially via connections between the A1 and other higher cortical areas such as the prefrontal cortex (Caras and Sanes, 2017; Polley et al., 2006; Rodgers and DeWeese, 2014; Runyan et al., 2017; Steinmetz et al., 2019; Plakke and Romanski, 2014; Fritz et al.). However, the underlying integrative circuit mechanisms are still only partially understood.

To date, several studies have demonstrated that the A1 integrates sensory information with other contextual and motor signals. Those studies highlight that such an integrative network enables subjects to facilitate higher cognitive demands, which are related to the prediction (Kamarajan et al., 2015; Parras et al., 2017; Town et al., 2018), choice accuracy (Caras and Sanes, 2017; Niwa et al., 2012) and auditory-guided decision-making (Ohl and Scheich, 2005; Brosch et al., 2005; Tsunada et al., 2015; King et al., 2018). Similarly, such integrative task-dependent coding and motor feedback have been reported in other sensory cortical areas across different species, as the primary visual cortex (V1) (Pakan et al., 2018; Henschke et al., 2020; Tajima et al., 2017) and the somatosensory cortex (S1) (Yang et al., 2015; McNiel et al., 2016).

Until today, the exact role of sensory cortices for sensory-guided decision-making has been subject to considerable discussion. In a recent review, Romo and Rossi-Pool (2020) argue that decision-making is not represented directly within the primary sensory areas. For example, during a tactile experiments in monkeys they did not find decision-related activity in the S1. They support the idea that primary sensory cortices, including the A1, promote decision-making by transforming the sensory information into a percept, which is represented mainly in higher frontal areas, such as the mPFC. However, a very recent report has implicated considerable recurrent feedback processing between prefrontal and auditory cortical areas suggesting cross-regional distributions of complex task-dependent representations (Yin et al., 2020).

Additionally, the salience of behaviorally relevant sounds critically depends on the exact reinforcement regimes and task rules (Bagur et al., 2018; Huang et al., 2019; David et al., 2012), which renders the auditory cortex a multifarious integrative circuit. In cases of novelty learning, uncertainty, task rule changes or other cognitive complex processes, A1 activity appears to be positively related with the dopamine release and cortical plasticity at cellular level (Stark et al., 2004; Happel et al., 2014c).

Under such circumstances, the columnar microcircuit of the A1 is an excellent integrative system to explore combined bottom-up and top-down processes, from pure auditory perception to cognitively demanding action-selection (Figure 1.3). However, the aforementioned and other studies have described corresponding neural correlates on the level of single neuron or population activity recordings. Some studies have suggested layer-specific differences in the representation of auditory information along the vertical axis of the auditory cortex, with granular layers revealing more accurate tonotopic response properties due to the dominant lemniscal inputs compared to supragranular and infragranular layers (Bandyopadhyay et al., 2010; Li et al., 2014; Tischbirek et al., 2019). Recently, Francis et al. (2018b) examined the layer-specific differences during task performance using 2-photon imaging technique. They found that behavior-relevant stimuli enhanced particularly the activity in supragranular layers and the formation of small neuronal networks helped in decoding precise behavioral choices. In addition, a growing body of human imaging studies has shown attention and task-related modulation of auditory processing in the A1 (Petkov et al., 2004; Puschmann et al., 2017; Deike et al., 2015) based on gross neural or metabolic response measures. However, how the canonical principles of

the columnar processing are reflected in the aforementioned multiplexed function of the A1 remain unclear (King et al., 2018; Ohl, 2015).

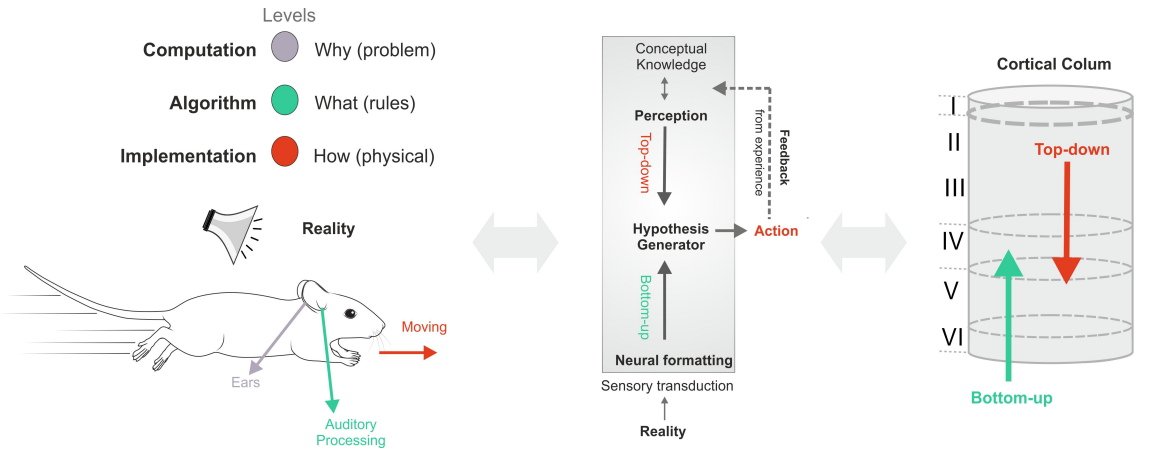

Figure 1.3: Cortical column: from auditory perception to action. Marr's three levels of analysis (Stevens, 2012): a mouse listens to a warning sound via its ears, after auditory processing (algorithmic realization) attempts to run away from the source of sound (goal) by using its limbs and muscles (physical implementation). This reality conceptual framework consists of bottom-up and top-down processes (middle). We propose the cortical column and its integrative function as a realistic model to explore such multifarious processes for the auditory modality. (illustration inspired by Krakauer et al. and Frégnac et al., 2015, mouse image adapted from E.Tyler and L.Kravitz SciDraw.io).

1.2 Approaches to explore the relationship between the primary auditory cortex and cognitive flexibility

Central to the entire discipline of neuroscience is the concept of understanding neuronal structure and function. However, in a perspectives review, Yuste (2015) discusses the challenges and strategies for shifting neuroscientific investigations from the single-neuron doctrine to neural ensembles and networks - the so-called mesoscopic level. Recent advances in neurophysiological recording methods have facilitated investigation of multiple neurons in multiple areas of the brain (eg. multi-array electrodes and neuropixels). According to Yuste (2015), focusing on the mesoscopic level will help us to understand how neurons and neuronal circuits give rise to specific behaviors, cognition and mental disorders. The ability to record from multiple neurons is a tremendous technological step forward. In addition, to understand the relationship 'brain-behavior' there is a necessity of well-designed behavioral paradigms (Krakauer et al.; Gomez-marin et al., 2014).

Hypothesis-based behavioral experiments are crucial because they help us establishing conceptual frameworks where we can link neuronal activity to behavior and learning. In this vein, to explore the relationship between the A1 cortical circuit and flexible behaviors, we combined an auditory, 2-way avoidance shuttle-box task with chronic cortical recordings from the A1 using Mongolian gerbils.

1.2.1 Model system: Mongolian gerbil in a shuttle-box auditory task

Key ethological characteristics

In the present study, the model system of choice is the Mongolian gerbil *(Meriones unguiculatus)*. The Mongolian gerbil is a rodent who belongs to the family Muridae, subfamily Gerbillinae, which is a native of Mongolia and northern China. A gerbils' size is roughly between the size of mice and rats (60-100 g). In the wild, gerbils live in desert or steppe environments in family groups. They build extended burrow systems and a vast network of tunnels with nest-champers for specific functions eg. pups, sleeping, or food nest (Hurtado-Parrado et al., 2015; Waiblinger and König, 2004). Under laboratory conditions animals usually develop stereotypies such as extensive digging and gnawing cage lids. Waiblinger and König (2004) examined the impact of housing to gerbil's behavior and they proposed a cage refinement with burrows, tunnels and chewable cardboard tubes. Further, gerbils show individual behaviors in their way of communication such as noise bursts or frequency-modulated syllables in vocalization or foot-stomping as a warning signal during arousal states. In our experiments we considered those species-specific needs and we adapted the housing conditions in accordance to the existing literature.

The Mongolian gerbil in auditory research

The Mongolian gerbil is a popular animal model with a long history in multiple research topics such as animals' social cognition (Tchabovsky et al., 2019), neurological diseases - epilepsy (Cutler and Mackintosh, 1989), auditory processing and hearing loss (Scheich, 1991; Otto and Jürgen, 2011). The Mongolian gerbil has become one of the key species in auditory research (Scheich, 1991; Ohl and Scheich, 1997; Deliano et al., 2009a; Happel et al., 2010b; Wrobel et al., 2018). One of the main reasons is its excellent sensitivity to low frequency sounds similar to humans. In comparison, other laboratory animals (mice and rats) show hearing sensitivity in much higher frequencies (Otto and Jürgen,

2011; Figure 1.4). Additionally, gerbils have large middle ear cavities through which the cochlea can be reached easily. This is extremely beneficial for experimental interventions. Their cochlea shows a frequency range from 200Hz to 50 kHz which are represented in the tonotopically organized auditory cortex (Thomas et al., 1993; Gerd and Frank, 2016). Furthermore, previous research has proved that gerbils are able to adapt in experimental conditions and learn complex auditory behavioral tasks (Ohl and Scheich, 1997; Ohl et al., 2001a; Deliano et al., 2009b; Happel et al., 2014b). Besides those physiological features, the Mongolian gerbils are convenient laboratory animas due to their small size, easy breeding, and low cost. Considering all those advantages, and especially the translational perspectives to human research, Mongolian gerbil and its primary auditory cortex was selected as a suitable model system for our experiments.

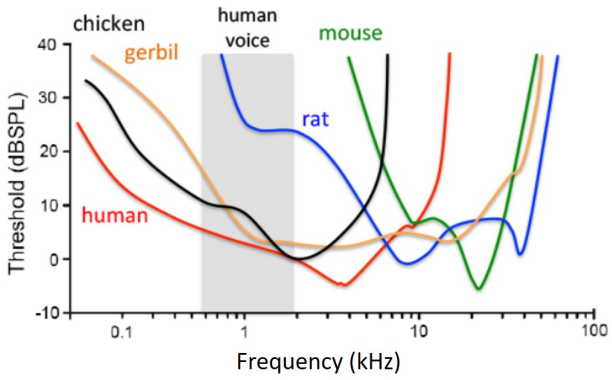

Figure 1.4: A comparative audiogram among species. Audiograms of several laboratory species including gerbils and humans. The lower the threshold (y-axis) is, the higher the sensitivity is to a particular frequency of the sound (x-axis). Gerbils' audiogram (yellow line) is very similar to human's (red line), which shows high sensitivity at frequencies below 4 kHz, low frequencies. For comparison, the normal human voice range (100 Hz - 2 kHz) is shown at the grey shaded area. (image adapted from https://med.fsu.edu/wangyuanlab/research).

Two-way active avoidance learning in the shuttle-box

For the purpose of this hypothesis-driven research, we designed a new auditory experimental protocol which takes place in a well-established behavioral arena: the shuttle-box (Stark et al., 2008; Ohl et al., 2001a; Deliano et al., 2009b; Happel et al., 2014b; Happel et al., 2015). The shuttle-box provides an ideal environment to carry out operant conditioning experiments and study behavior and learning with rodents. The shuttle-box consists of two identical compartments separated by a middle hurdle, allowing the animals to move from one side to the other depending on the presented stimuli (conditioned or

unconditioned). In fact, this apparatus is designed to investigate behavioral concepts as active avoidance (instrumental learning). Usually, shuttle-box paradigms are described as negative reinforcement regimes where avoidance occurs.

Avoidance conditioning is a two-part process; first, subjects learn a neutral stimulus (eg. a tone) and second, they associate it with an aversive stimulus (eg. foot-shock), based on the *Two-factor theory* (Mowrer, 1951). Active avoidance learning is the outcome of such processes, meaning the subjects develop certain behavioral strategies and learn to prevent an aversive stimulus. Usually, a prior stage of avoidance learning is the escaping behavior where subjects learn to just terminate the noxious stimuli (Wadenberg, 2010; Krypotos et al.). Especially, in the 2-way active avoidance procedure subjects are able to shuttle back and forth in the equal compartments of the box because they learn that they have to cross upon a stimulus presentation or o not cross upon upon another stimulus (eg. Go/NoGo paradigms). Additionally, the shuttle-box arena is often combined with stimulus emitters (eg. loudspeakers) to allow neurobiological investigations in relation to specific modalities (eg. auditory) and neuronal systems. Over the past decades, 2-way active avoidance protocols have been used broadly as they are unique and useful to examine attention, memory, perceptual learning, and decision making. In the following chapters, it will be discussed how auditory avoidance learning paradigms can be adapted in order to address questions related to cognitive flexibility (eg. auditory discrimination and contingency reversal learning, subsection 2.3.2). This dissertation seeks to explore the dipole 'brain-behavior', and more specific the link between A1 microcircuits and the auditory-guided behavior. Therefore, we combine the shuttle-box task with chronic multichannel-recordings from the A1 (subsection 2.2.3) aiming to investigate the neuronal observables of learning on a mesoscopic level (Happel et al., 2015).

1.2.2 Mesoscopic observations: local field potentials and chronic current source density profiles from A1

Traditionally, neural activity has been assessed by recording either single neuron or multi-neuron spike activity. Besides those measures, over the last decade local field potential (LFP) recordings have gained importance in the field of *in vivo* electrophysiogy. LFPs are generated by transmembrane current flow in ensembles of neurons with synchronous

activity. Those signals are related to processes and events that are causal to action potentials (Kajikawa and Schroeder, 2011). Therefore, LFP-based recordings provide a means of investigation at a larger scale of the mesoscopic level as they describe excitatory and inhibitory synaptic processes (Einevoll et al., 2013).

For example, in the A1 cortical column, ensembles of neurons are activated after an auditory event. Consequently, at the neuron's cellular membrane positive currents leave the extracellular space (influx of positive ions) - named *sinks* - whereas positive ions entering the extracellular medium and are called current *sources* (Einevoll et al., 2013). Those LFPs can be measured by micro-electrodes implanted intracortically, along the laminar space. Furthermore, it is known that LFPs are sensitive to sub-threshold integrative processes, which allows us to draw conclusions about the state of local cortical network and neuromodulatory pathways under specific circumstances (eg. sensory stimulation or behavioral context). However, direct LFP measurements do not portray spatial information until extracted by using current source density (CSD) analysis (Mitzdorf, 1985; Freeman and Nicholson, 1975; Mazzoni et al., 2013).

Current source density analysis was developed in the 1950s, and over the last decades have neuroscientists started using it more often (Schroeder, 1998; Lakatos et al., 2005; Happel et al., 2010b; Schaefer et al.). Briefly, CSD is a second spatial derivative transformation of the LFP signal (Mitzdorf, 1985; Freeman and Nicholson, 1975, see details in subsection 2.4.3). This approach is advantageous because it eliminates the effects of volume conduction and it allows direct interpretations regarding the synaptic activity in the local cortical networks (Schroeder, 1998). Another, major advantage of CSD analysis is that it contains high spatiotemporal information about the neuronal activity at the recording location (Kajikawa and Schroeder, 2011). Therefore, it is possible to relate the recorded neuronal activity to specific anatomical information, such as the cortical layers of the A1. Those activity readouts enable us to describe the synaptic circuits within the distinct cortical layers (Happel et al., 2010a; Szymanski et al., 2009). In the present study, chronically implanted electrodes in the A1 allow us to implement a long-term CSD analysis (subsection 2.2.3) . The investigation of chronic CSD profiles was chosen to allow a deeper insight into the layer-specific processing during auditory cognitive complex tasks.

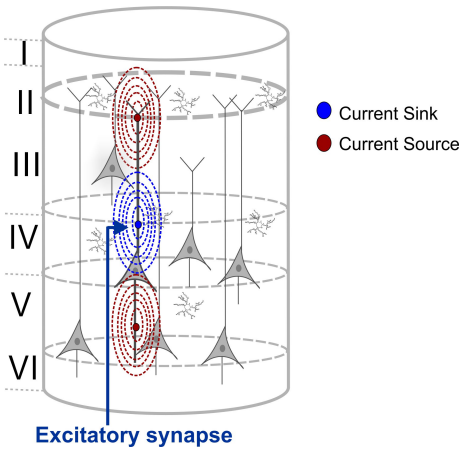

Figure 1.5: Current source density distributions along the cortical column. Illustration of a local postsynaptic event of excitatory synaptic neuronal populations along the cortical column. Transmembrane currents generate dipoles of sources (red) and sinks (blue), which can be recorded and measured by CSD analysis. (Neuron image items adapted from J. Shin and J.Chilton SciDraw.io).

1.3 Aims and objectives of the study

The aim of this thesis is to explore the role of the primary auditory cortex of Mongolian gerbils during their engagement in a complex auditory decision-making task. This study attempts to expand our knowledge of how individual cortical layers contribute to the integrative circuit in the A1, in order to code task-relevant information and guide sensory-based decision making. The main focus is to achieve a deeper understanding of the underlying neuronal observables on a mesoscopic level. The current dissertation is designed in four main parts, which reflect the specific objectives:

1. The first part investigates the behavioral aspects of the newly established, long-term, auditory Go/NoGo shuttle-box task. This allows the combination of a behavioral training paradigm with simultaneous in-vivo chronic LFP recordings from the A1 of Mongolian gerbils. During this protocol, the animals are required to learn the behavioral relevance of the two conditioned stimuli (pure tones: 1 kHz and 4 kHz) which change their contingencies (Go or NoGo) in the respective blocks of training (detection, discrimination and multiple reversals). In this section, I systematically review the behavioral data to better understand the learning strategies of the animals, aiming to provide more evidence on the ability of the gerbils to re-adapt their strategies even after several reversals of the choice outcome contingency. Also, the

new approach suggests an important tool to study multiple aspects of sensory-guided decision-making processes in combination with neurophysiological recordings.

2. The second part focuses on the chronic CSD recordings, a mathematical tool to gain further insights into auditory cortical circuits and the plastic changes over the learning progress in the shuttle-box Go/NoGo task. Due to the novelty of this approach, explicit evidence about the quality and stability of the chronic CSD recordings are provided. Further, I attempt to broaden the current understanding on a circuit level, on how changes in the task rule are represented in the A1. For this I will apply statistical tests of variance in order to quantify existing differences of the overall columnar activity strength based on the stimuli, contingencies and choices for several time windows of the trials.
3. The third main objective is to determine whether the relative contribution of cortical layers to the canonical columnar response is modulated by task-dependent features such as the behavioral relevance of the stimulus, its particular contingency and required action, as well as direct decision variables and the choice accuracy. In order to achieve that I will analyze the electrophysiological data of binary classes (1kHz vs 4kHz, Hit vs Miss, Correct vs Incorrect etc.) on a single-trial level using generalized linear-mixed effect models (GLMM) in relation to the observed behavioral effects for several time windows within the trials. Evaluation of the applied models will allow us to draw conclusions about the contribution of the cortical layers to the observed behavior, especially in relation to the actual decisions.
4. Besides the aforementioned objectives, the established experimental paradigm with the chronic CSD recordings provides the frame for numerous other analytical approaches. In the later parts of the thesis, I will discuss about the ongoing collaborative projects and perspectives which will help us to to better understand the cortical mechanisms underlying auditory learning and decision making. For example, I have worked closely with scientists from the Computer Science faculty in order to apply machine learning algorithms to the obtained CSD data. This project was set out to investigate whether a linear support vector machine classifier, which was trained for targets reflecting either stimulus-related aspects of auditory processing or processing of task-dependent information is able to separate the layer-specific and time-limited subsets of the CSD profiles.

2 | Materials and methods

In this study, we used chronic, laminar current source density (CSD) analysis of the primary auditory cortex (A1) of behaving Mongolian gerbils (Meriones unguiculatus) in order to characterize layer-specific, spatiotemporal synaptic population activity. Animals were trained to first detect and subsequently to discriminate two pure tone frequencies in consecutive training phases in a Go/NoGo shuttle-box task. A following block of training with multiple reversals of the choice-outcome contingency allows us to investigate cortical circuit mechanisms underlying flexible auditory guided behaviors.

2.1 The animal model: Mongolian gerbil

Experiments were carried out with adult male Mongolian gerbils (4 to 8 months of age, 70-90 g body weight, total n=9, in-house breeding). All experiments presented in this study were conducted in accordance with ethical animal research standards defined by the German Law and approved of an ethics committee of the State of Saxony-Anhalt.All animals were housed at a temperature 25°C and humidity 30-50% under a 12-hr dark/light non-inverted cycle. We used conventional cages (Type IV) with raised wire lids, which allows nesting. Their cages were filled with hay, woodchips and paper-based bedding. For the enrichment of their environment we used tunnels and wheels. All animals had free access to food and water. Due to the gerbil's genetic tendency to develop epileptic seizures a 3-days behavioral screening protocol (established by Gonzalo Arias Gil and Dr.Dr.Kentaroh Takagaki at the SPL Department - LIN, based on Seto-Ohshima et al., 1992) was taking place before the start of surgery and training. Only animals that did not show an epileptic seizure during those tests were used for the experiments.

2.2 Neural recordings from the area A1

2.2.1 Surgical preparation and electrode chronic implantation

Surgery - right A1 area

For chronical in vivo electrophysiological recordings a multichannel electrode (Neuronexus, A1x32-6 mm-50-177_H32_21mm) was surgically implanted into the A1.Gerbils were initially anesthetized by an intraperitoneal (i.p.) injection (0.004 ml/g) consisting of 45% ketamine (50 mg/ml, Ratiopharm GmbH), 5%xylazine (Rompun 2%, Bayer Vital GmbH) and 50%of isotonic sodium-chloride solution (154 mmol/1, B. Braun AG). Anesthesia during the surgery was maintained with around 0.15 ml/g*h i.p. infusion. Anesthetic status was regularly checked (10-15 min) by the paw withdrawal-reflex and breathing frequency. Body temperature was continuously measured and kept stable at 34°C.

The primary field A1 of the right auditory cortex was exposed by a small trepanation through the temporal bone (Ø 1mm). This avoids tissue damage and guarantees stable fixation of the implanted electrode on the skull. The positioning of the electrode array is indicated based on the characteristic vascularization pattern formed by the ascending branches of the inferior cerebral vein (icv) and the descending branches of the middle cerebral artery (mca). The primary cortical field A1 is typically located at a characteristic area between them (Ohl et al., 2000). Another small hole for the reference wire (stainless steel, Ø 200-230 µm) was drilled into the parietal bone on the contralateral side. Animals were head-fixed with a screw-nut glued to the rostral part of the exposed nasal bone plate by UV-curing glue (Plurabond ONE-SE and Plurafill flow, Pluradent) that was temporally attached to a metal bar. The recording electrode with a flexible bundle between shaft and connector was inserted perpendicular to the cortical surface into A1 via the small hole (cf. Figure 2.1)

Chronic fixation of the multichannel probes

Before enclosing the exposed A1 with UV-glue an antiseptic lubricant (KY-Jelly, Reckitt Benckiser-UK) was applied to the exposed cortex. After the surgery, the wounds were treated with a local antiseptic tyrothricin powder (Tyrosur, Engelhard Arzneimittel GmbH

& Co.KG). Directly after the surgery and over the next 2 days, animals received analgesic treatment with Metacam (i.p. 2mg/kg bw; Boehringer Ingelheim GmbH) substituted by 5% glucose solution (0.2 ml). Animals were allowed to recover for at least 3 days before the first session of awake electrophysiological recording (Figure 2.1).

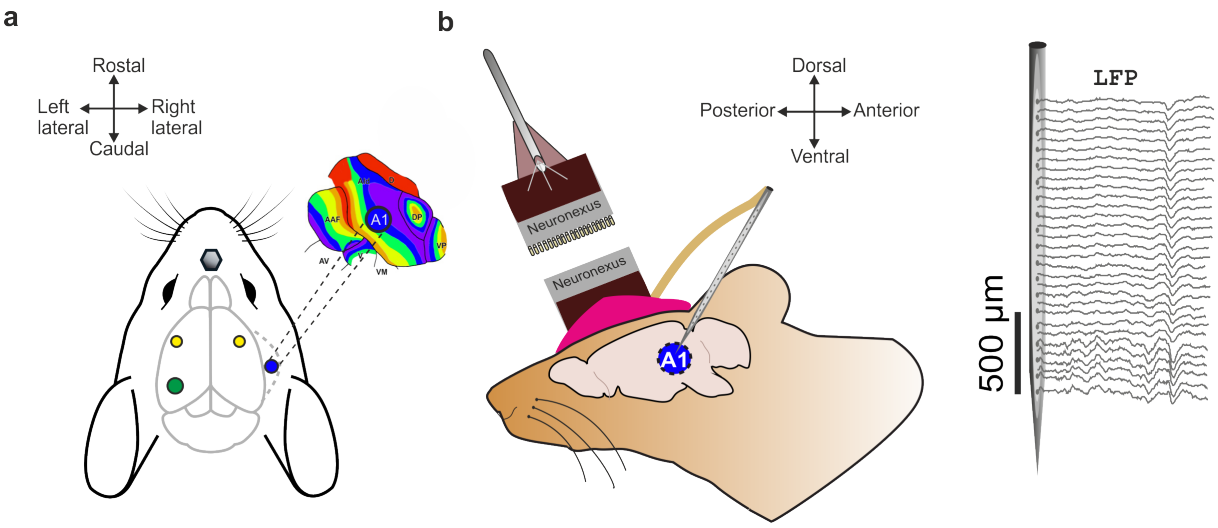

Figure 2.1: Implantation and chronic fixation of the multichannel electrodes in A1. **a.** Dorsal view of the brain (adapted from Luigi Petrucco, SciDraw.io): Animals are fixated via a screw nut (gray hexagon) and a metal bar. The blue circle illustrates the implantation position to reach the right A1 field. The position of the reference electrode is shown by the green circle, at the left side of the skull. To increase the stability of the fixated implant we use two small screws, indicated by the yellow circles. **b.** Lateral view of the brain (adapted from Ann Kennedy, SciDraw.io): The multichannel (32 channels) Neuronexus silicon probe was inserted perpendicular to the cortical surface (A1). The electrode together with the flexible bundle and the connector are chronically fixated onto the skull by using UV-glue. Before the start of the behavioral experiment the dry UV-glue is painted with a bright magenta colour which is detectable for later video analysis and tracking of animals′ movements. Over the course of the behavioral experiment the headstage is connected via the Neuronexus pre-amplifier to acquire LFP signals.

2.2.2 Verification and characterization of the recording location A1

A very crucial step of this experiment was to verify and characterize the recording location. Therefore, during the implantation and before the chronic fixation of the electrode animals were placed in a Faraday-shielded acoustic soundproof chamber. Sounds were presented from a loudspeaker (Tannoy arena satellite KI-8710-32) in 1 m distance to the animal.

For verification of the implantation site in A1, a series of pure-tones covering a range of at least 7 octaves were presented (0.25–32 kHz; tone duration 200 ms, inter-stimulus-

interval (ISI) 800 ms, 50 pseudorandomized repetitions, sound level 65 dB SPL). Stimuli were generated in Matlab (MathWorks, R2006b), converted into an analog signal by a data acquisition card (sampling frequency 1 kHz, NI PCI-BNC2110, National Instruments), rooted through an attenuator (gPAHGuger,Technologies), and amplified (Thomas Tech Amp75). A measurement microphone and conditioning amplifier were used to calibrate acoustic stimuli (G.R.A.S. 26AM and B&K Nexus 2690-A, Bruel&Kjaer, Germany). By the end of the acoustic stimulation protocol the recording signal was evaluated and the best frequencies were identified. Finally, the chronic fixation of the multichannel probe took place (see above).

2.2.3 The shuttle-box apparatus combined with electrophysiology

Operant conditioning was trained in a two-way avoidance shuttle-box task (Figure 2.2 and Figure 2.3). The shuttle-box (E15, Coulbourn Instruments) was placed in an acoustically and electrically shielded chamber and contained two compartments separated by a hurdle (3 cm height).

Conditioned stimuli (CS). The auditory stimuli were generated in Matlab (MathWorks, R2012b), converted into an analog signal by a data acquisition card (NI PCI-6733, National Instruments), rooted through an attenuator (gPAH Guger, Technologies), and amplified (Black Cube Linear, Lehman). Two electrostatic loud speakers positioned 5cm at both sides of the shuttle-box (Figure 2.2). A measurement microphone and conditioning amplifier were used to calibrate acoustic stimuli (G.R.A.S. 26AM and B&K Nexus 2690-A, Bruel& Kjaer, Germany).

Unconditioned stimuli (US). The mild foot-shock (US) was conditionally delivered by a grid floor and generated by a stimulus generator (STG-2008, Multi-Channel Systems MCS GmbH, Figure 2.2). Depending on the individual animal sensitivity and performance the shock intensity was adjusted (starting at 200 µA) in steps of 50µA until the escape latencies were below 2s, in order to achieve a successful association of conditioned stimuli (CS) and US (**?**).

Chronic LFP recordings during training. Multichannel recordings were performed with connecting the head-connector of the animal to a preamplifier (20-fold gain,

band-pass filtered, HST/32V-G20; Plexon Inc.) and a data acquisition system (Neural Data Acquisition System Recorder Recorder/64; Plexon Inc.). The cable harness was wrapped by a metal mesh for bite protection. Tension of the cable was relieved by a spring and a turnable, motorized commutator (Plexon Inc.) that permits free movement and rotation of the animal in the box. Broadband signals were recorded continuously using a preamplifier (Plexon REC/64 Amplifier; 1Hz-6 kHz) during the training with a sampling frequency of 12 kHz. Local field potentials were sampled with 2 kHz, visualized online (NeuroExplorer, Plexon Inc. Recording Controller) and stored offline for further analysis (Figure 2.2). To avoid ground loops between recording system, shuttle-box and the animal we ensure proper grounding of the animal via its common ground and leave the grid floor on floating voltage (**?**).

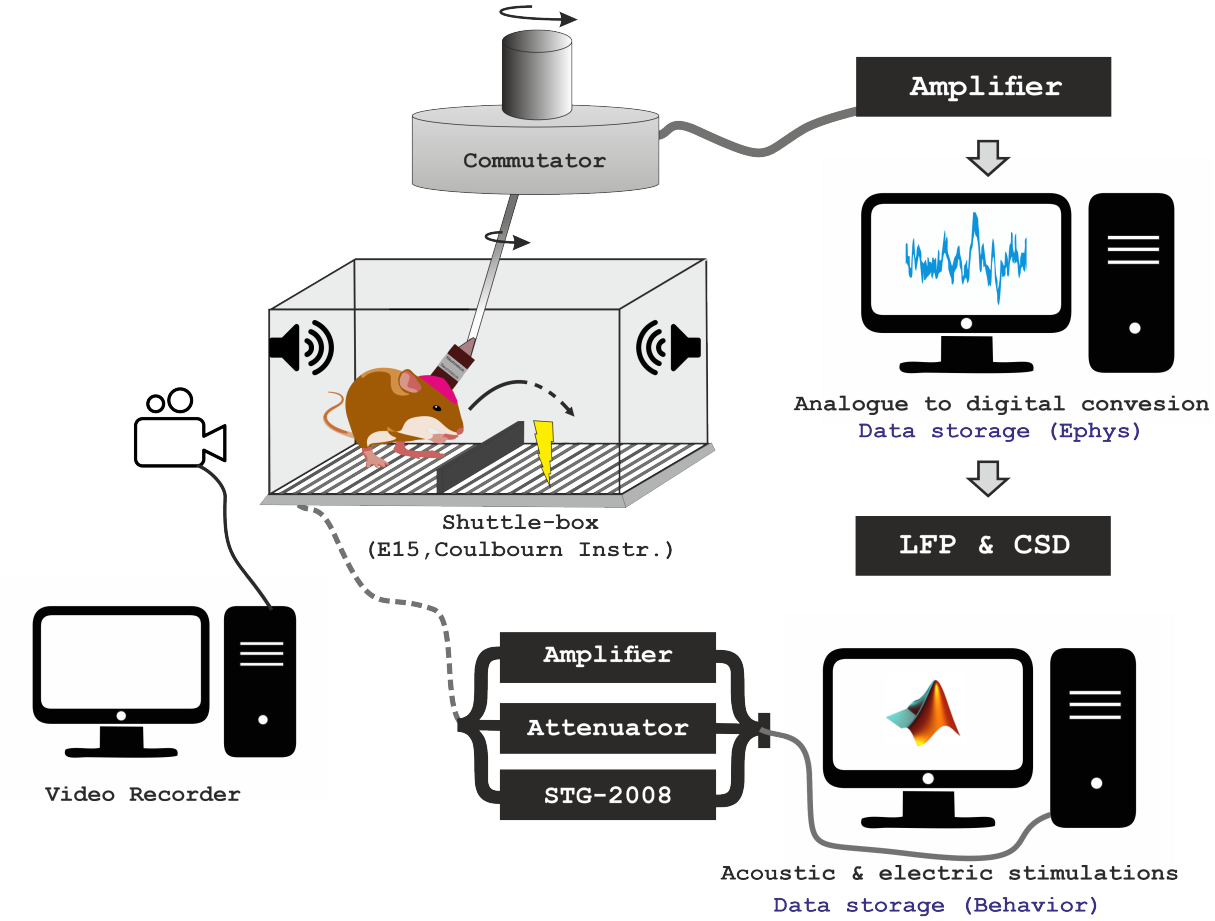

Figure 2.2: Schematic representation of the the setup for chronic electrophysiological recordings in behaving animals. The gerbil is placed at one side of the box and connected with the pre-amplifier. Due to the commutator the animal can freely move into the shuttle-box. Broadband signals are recorded continuously during the training session. The behavioral experimental settings, acoustic and electric stimuli, are controlled via the stimulation computer. During the training session video is recorded continuously. The collected data (Ephys, behavioral and video) are saved in proper formats for further offline analysis.

2.3 The experimental design

2.3.1 The awake passive listening condition

After the recovery period, animals were placed in a 1-compartment box in an electrically shielded and sound-proof chamber in order to re-characterize the tuning properties of the chronically implanted electrode. Acoustic stimuli were presented in a pseudo-randomized order of pure-tone frequencies covering a range of 7 octaves (0.25-16kHz; tone duration: 200 ms, ISI 800 ms, 50 pseudo-randomized repetitions, sound level 70 dB SPL), while laminar LFP signals were recorded. After each training phase (detection, discrimination, reversals) the frequency response tuning was recorded again.

2.3.2 The auditory Go/NoGo behavioral task

The animals (max. n=9) were trained twice a day with a break of at least 5 hours in between both training sessions. In each training session subjects were allowed to habituate for 3 minutes within the shuttle-box. In the first training phase two pure tones with frequencies 1 kHz and 4 kHz were presented both as 'Go' conditioned stimuli (CS+). Subjects needed to detect any tone event and respond with a compartment change in order to avoid a mild foot shock (200-500 μA) presented as the unconditioned stimulus (US). We therefore call this phase the detection phase.

Within each trial (12-15s), the CS+ tones were repeatedly presented (tone duration 200 ms, ISI of 1.5 s, 70 dB SPL) in a 6 s observation window during which subjects are required to change the compartment in order to make a correct 'hit' response. When subjects shuttled into the other compartment in response to the CS before US onset, this was counted as conditioned response (CR). In case animals did not show a CR within the 6 s observation window this defined a so-called miss trial. Here, the animal received an overlapping presentation of the CS+ and the US until an escape to the other compartment terminated the US/CS presentation. Subjects thereby learned to escape the aversive foot shock within a couple of trials. In each session we presented each CS+ for 30 times in a pseudo-randomized order.The time point at which we changed the task rule from detection to discrimination and afterward to the first reversal was oriented at the behavioral performance of each subject individually. Later reversal discrimination blocks

lasted one week (9 sessions) per block.

Once animals reached a stable detection performance (threshold critirion d' , see below) for 3 consecutive training sessions, we introduced a change of the task rule and switched to a discrimination task by assigning the former 4 kHz 'Go' tone with a 'NoGo' (CS-) contingency (n=8; one subject excluded due to epileptic seizure during training). Subjects needed to report on the 'NoGo' condition by staying within the compartment to avoid an US, which we call a 'correct rejection' (Corr. Rej.). In 'NoGo' trials, animals had to stay in the compartment for 12-15 s, while the CS- was continuously played with an ISI of 1.5 s to prevent animals from developing a time estimate of the observation window length over the long training period. If subjects incorrectly crossed within this 12-15 s, the behavioral choice was counted as 'false alarm' (FA).When animals achieved high discrimination performance we reversed the rule of the choice-outcome contingencies (Go vs NoGo) of the two stimuli over consecutive training phases.

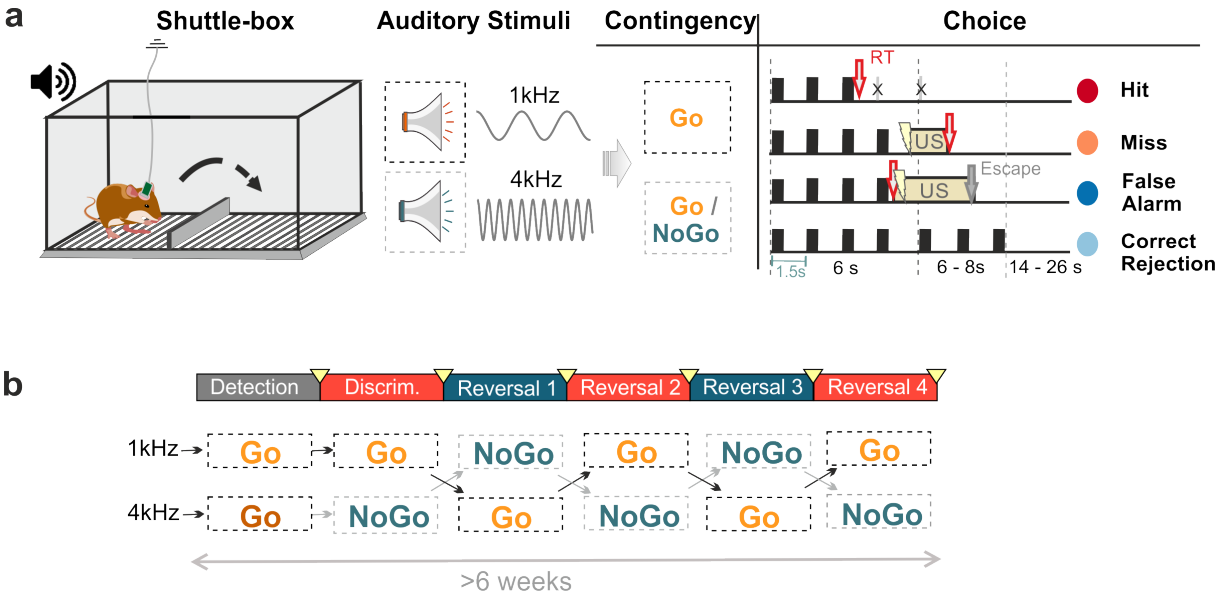

Figure 2.3: Experimental design of the auditory Go/NoGo task.a. Illustration of the two-way avoidance shuttle-box training with chronic recordings in behaving Mongolian gerbils. Subjects were trained to respond to two different pure tone frequencies (1 kHz and 4 kHz; conditioned stimulus - CS) in a Go/NoGo task design to avoid an unconditioned stimulus (US - mild foot shock). During the discrimination phase the contingency of the CS can be either 'Go' (CS+) or 'NoGo' (CS-) leading to four possible behavioral outcomes (hit, miss, correct rejection – Corr. Rej., false alarm - FA). Right, Illustration of consecutive CS within a trial, length of the observation window (6 s), inter-stimulus interval (1.5 s) and behavioral choices. **b.** Task design separated in blocks of different training tasks-rules. The initial block is the detection phase (both stimuli have 'Go' contingency), as next comes the discrimination phase (only 4kHz changes contingency to 'NoGo'), and finally the multiple reversals of choice-outcome contingencies blocks took place over several weeks.

2.3.3 The experimental timeline

To investigate the role of the A1 during a Go/NoGo auditory task with multiple reversal of choice-outcome contingencies a precise protocol has been introduced (**?**. The experimental protocol is represented in a Gantt chart (Figure 2.4) with all crucial steps and training blocks. All the animals (n=9) were behaviorally screened for three consecutive days. Only animals showed normal behavior, in terms of epilepsy, underwent the surgery and chronic implantation of the electrode. Three days of post-operative treatment and recovery followed.

Before the start of the training phase gerbils were habituated in the shuttle-box for 10 -20 minutes and then the first passive listening recording session started.Following the active training phases with the blocks of detection (1 week), discrimination (1-2 weeks) and multiple reversals (1 week per block). Eventually, after the end of each block a passive listening session was taking place. Finally, all animals were sacrificed and the brains were extracted in order to perform histology. Most of the animals underwent the complete protocol, but three of them not due to technical difficulties (training phase starts with n= 9 and it ends n= 7).

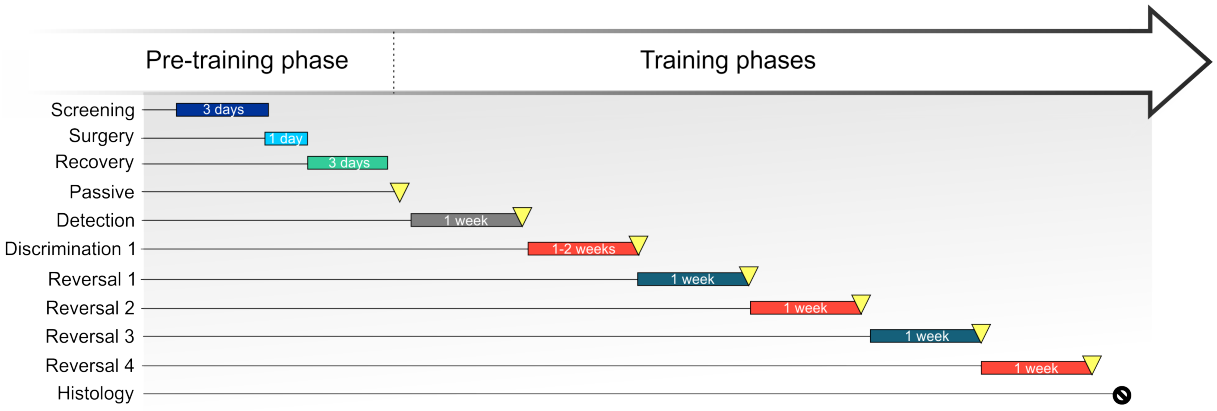

Figure 2.4: Timeline of the experimental protocol. The Gantt chart represents the timeline of the experimental protocol. The pre-training phase consisted of the behavioral screening, surgery and the recovery period. The training phase started with habituation and the passive listening recording (into the shuttle-box), which is shown with the yellow triangle. Followed by the fist session of the detection block (grey box) in the next day. Next, blocks of discrimination and reversal tasks (red and dark green boxes) were following. Animals were trained twice per day. Almost all animals underwent the complete protocol (training phase start: n= 9; training phase end n= 7). The end point was the histology.

2.4 Data analyses

2.4.1 Data storage and analysis pipeline

Two types of raw data : were acquired: the behavioral data in text format (.txt) and the electrophysiological recording dat in plexon format (.plx). The size of the raw signals reaches 178 GB. To reduce the complexity and to combine the two types of data of each session, a conversion step is needed. The converted matlab file (.mat, $\sim$ 37GB) contains information about the epochs of interest at the LFP level and a complete description of the behavioral variables. The converted data structure is stored in a 3-dimensional matrix (32x12400x60): first the spatial domain (channel index); second, the temporal domain (time from the beginning to the end of the trial) ; and third, the index of each individual trial.

As next, preprocessing of each single-session converted .mat file is executed via a custom made Graphical User Interface (GUI) for a trial-by-trial inspection of the signal quality and definition of the cortical layers. Once the LFP signal is manually evaluated and the layers are assigned, data are saved. A following conversion routine creates a data container with information for all animals, all sessions and all the variables that we are interested in. The size of this output data file depends on whether we save the CSD matrices ($\sim$ 80 GB) or not ($\sim$ 41 MB). In the end, those data containers can be feed in the custom made scripts in Matlab, R studio or Python for further different analysis approaches Figure 2.5. All data are stored at LIN′s servers and backed-up in multiple hard drives.

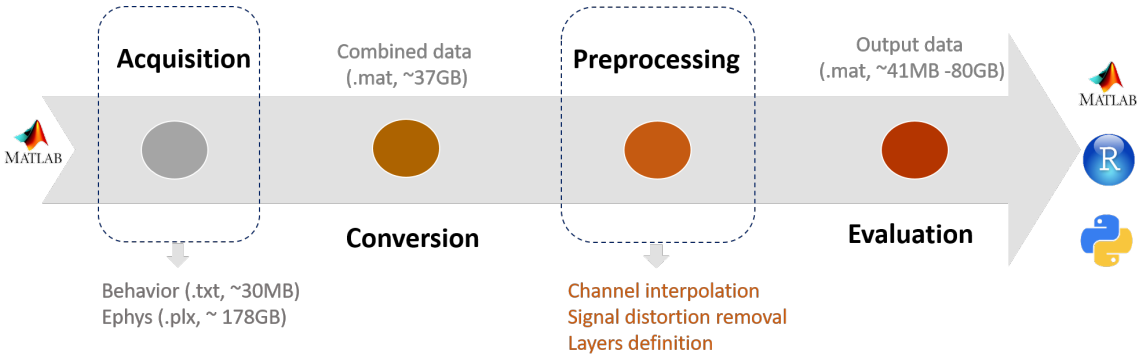

Figure 2.5: Schema of the workflow and data pipeline. The arrow illustrates the workflow and the coloured circles the individual process steps from the acquisition of the data (left) to the final evaluation steps (right). The final output data are used in a variety of analysis methods using Matlab, R studio or Python programming languages.

2.4.2 Behavioral analysis

The behavioral training data output (.txt/ files) includes all the required information to investigate and reconstruct the behavior of each animal during the shuttle-box Go/NoGo paradigm. For example, all compartment changes, reaction time, escape latencies, spontaneous inter-trial shuttles are recorded.

Reaction Time. First important behavior-related factor is the reaction time, which is defined as the time period between the CS (+/-) onset and the animal 's decision to jump over the shuttle-box hurdle - complete compartment change. Single-trial reaction time calculations help the experimenter to understand if the animal is under shock control (escaping or avoiding) and adapt the intensity of the US during the session. Additionally, given the fact that the reaction time / motor response is the outcome of a decision, it is crucial to look at the neuronal observables in relation to that.

Conditioned Responses. A first approach to evaluate the learning progress and dynamics is the session-wise calculation of the conditioned response rates for the CS+ and the CS-:

$$\textit{Hit rate} = \text{hits/ number of CS+ trials}$$
$$\textit{False alarm rate} = \text{false alarms/ number of CS- trials}$$

Signal Detection Theory. Since the animals in this paradigm have the choice of responding to two different stimuli, another tool to quantify the behavioral sensitivity independent of experimental conditions and bias is the d' values based on Signal Detec-

tion Theory (SDT) (Green and Swets, 1966 ; Carandini and Churchland, 2013). For the detection phase the d' was calculated as the differences of the z-transforms of the hit rate and the z-transform of the relative inter-trial shuttles (ITS) derived from the inverses of a standardized normal distribution.

$$d' = Z(hits) - Z(ITS) \tag{2.1}$$

For the next phases (discrimination and reversals) the d' was calculated as the differences of the z-transforms of the hit rate and the z-transform of the false alarm rate, similarly (Figure 2.6).

$$d' = Z(hits) - Z(FA) \tag{2.2}$$

The learning threshold criterion was defined as the perceptual signal strength being one standard deviation above noise, meaning having values of d' above 1 for at least 3 consecutive sessions (in detection and discrimination phase).

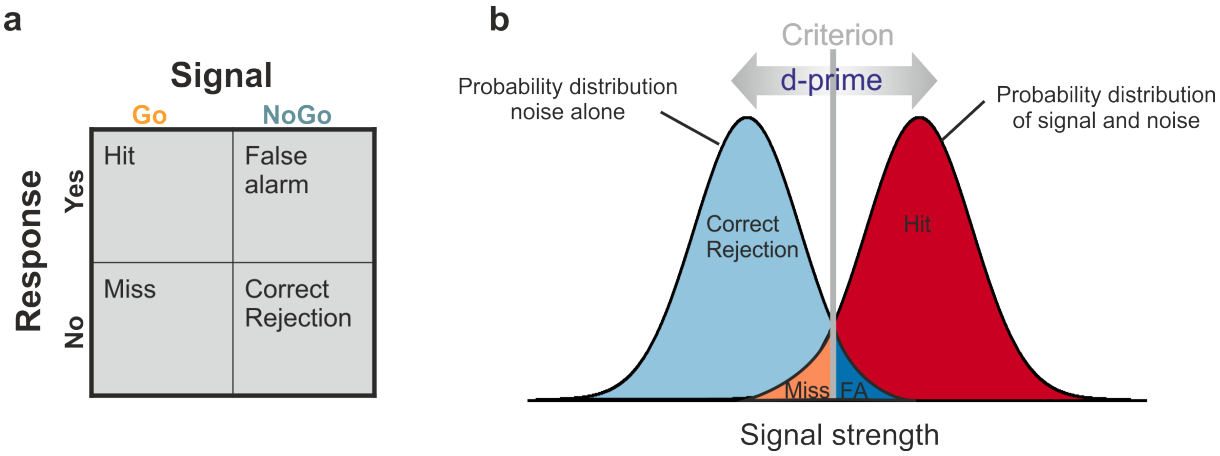

Figure 2.6: Signal Detection Theory for the Go/NoGo paradigm.. a. The table shows the four possible behavioral outcomes after the presentation of an auditory stimulus in the shuttle-box, depending on the contingency 'Go' or 'NoGo' and the response, eg. crossing the hurdle 'Yes' or 'No'. **b.** Illustration of Signal Detection Theory (SDT) in this experimental design. The 'Correct Rejection' responses are treated as 'noise' or true negative (in light blue) and the 'Hit' responses as 'signal and noise' or true positive (in red). The sensitivity d' measures the ability of one animal to discern signal from noise. The criterion is set by the experimenter and defines the decision tendency (our criterion was $d' = 1$). The effect of training could be to make the subjects increase discrimination sensitivity, by separating the two distributions to the sides, by increasing correct choices and minimizing incorrect choices.

Strategy plane - ROC curves. In the interest of characterizing individual learning strategies over the course of the training I have used a method that combines the conditioned response rates and the SDT - d' information. Specifically, every session is plotted as a unique point consisting of hit response (x-axis) and false alarm response (y-axis). All the session points are placed onto a Receiver Operator Characteristic (ROC) space (Fawcett), where the ROC curves represent the d' levels with the diagonal being $d' = 0$. The ROC space is divided in four sub-spaces (squares) that describe the strategy the animal shows at a given session: *"conservative", "liberal", "correct" or "wrong"*. By connecting the unique session points, we get a trajectory which allows us to observe the strategy shifts and the learning dynamics individually and for each phase separately (cf. Figure 2.7). Thus, throughout this thesis, the term 'strategy plane' will refer to this specific approach. The ultimate goal of such a detailed behavioral analysis is to correlate the perceptual decisions with the recorded the neuronal activity.

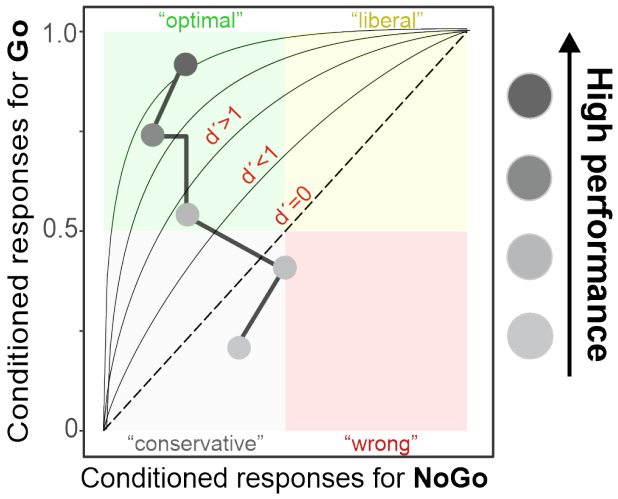

Figure 2.7: Behavioral strategies: Receiver operator curve (ROC). Example receiver operator characteristic (ROC) curve based on the discrimination performance placed in a behavioral strategy plane, grey dots show the different sessions in one single phase of training. Sequential decisions form a strategy trajectory on a plane with four equal quarters describing a characteristic behavior: optimal (in green); liberal (in yellow); wrong (in red); and conservative (in gray).

Video material. Finally, a valuable source of information regarding the entire behavior can be acquired by the video analysis and tracking of the animal in the shuttle-box. In a next data set of a similar experiment (data not shown here), we have developed an accurate tracking technique as well as synchronization with the electrophysiological recordings (Auer et al., in preparation).

2.4.3 Current Source Density (CSD) analyis

Based on the recorded laminar local field potentials, the second spatial derivative was calculated yielding an estimate of the current-source density distribution, as seen in equation:

$$-\,\mathrm{CSD} \approx \frac{\delta^2 \Phi(\mathrm{z})}{\delta \mathrm{z}^2} = \frac{\Phi(z + n\Delta z) - 2\Phi(z) + \Phi(z - n\Delta z)}{(n\Delta z)^2} \tag{2.3}$$

where ϕ is the field potential, z is the spatial coordinate perpendicular to the cortical laminae, Δz is the spatial sampling interval, and n is the differential grid (Mitzdorf, 1985). LFP profiles were smoothed with a weighted average (Hamming window) of 9 channels which corresponds to a spatial kernel filter of 400 µm (Happel et al., 2010a).
CSD distributions reflect the local spatiotemporal current flow of positive ions from extracellular to intracellular space evoked by synaptic populations in laminar neuronal structures. CSD activity thereby reveals the spatiotemporal sequence of neural activation across cortical layers as ensembles of synaptic population activity (Mitzdorf, 1985 ; Happel et al., 2010a).

One advantage of the CSD transformation that it is reference-free and hence less affected by far-field potentials and referencing artifacts. It allows to observe the local synaptic current flow with high spatial and temporal precision (Kajikawa and Schroeder, 2011). Current sinks thereby correspond to the activity of excitatory synaptic populations, while current sources mainly reflect balancing return currents. The CSD thus provides a functional readout of the cortical microcircuitry function, encompassing a wider, mesoscopic field of view than for instance single- or multi-unit approaches26. Early current sinks in the auditory cortex are therefore indicative of thalamic input in granular layers III/IV and infragranular layers Vb/VI (Happel et al., 2010a ; Szymanski et al., 2009). In order to describe the overall columnar processing, the CSD profiles were transformed by averaging the rectified waveforms of each channel:

$$AVREC(t) = \frac{\sum_{i=1}^{n} |CSD_i|\,(t)}{n} \tag{2.4}$$

where n is the number of recording channels and t is time. The AVREC reflects the temporal overall local current flow of the columnar activity (Givre et al., 1994 ; Schroeder, 1998).

2.4.4 Data preprocessing

subsection:Data preprocessing) Single-trial data were analyzed via a custom-written graphical user interface (MathWorks, R2016a & R2017b) that visualized the LFP, CSD and behavioral parameters to inspect and mark two types of artifacts: 1) affected recording channels and 2) foot-shock or movement induced signal clipping and distortions. Affected channels were substituted by a linear interpolation method across neighboring, unaffected channels on the level of the LFP (Happel et al., 2010a). Shock induced clipping was rejected from the overall signals. Trials with artifacts were also discarded from further analysis.

2.4.5 Extraction of signal parameters

Cortical layers were assigned to the recording channels based on the averaged auditory-evoked spatiotemporal CSD current flow in response to the first CS presented during a session and compared to the awake measurement before the training (Figure A.1). Identification of cortical layers was based on previous studies by Happel et al., 2010a and Szymanski et al., 2009, where the early dominant current sinks in the auditory cortex are indicative of thalamic input in granular layers III/IV and infragranular layers Vb/VI and allow to identify supragranular layers I/II and infragranular layers Va and VI in the CSD recordings (Figure 2.8).

In this study, we determined trial-by-trial root-mean-square (RMS) values of averaged CSD traces within each of the five cortical depths from tone onset of each CS presentation in a time window of 500 ms. Also, the RMS value of the AVREC was calculated within the same time windows for the corresponding overall columnar response. We did not inspect the time-points after a CR, as the CS presentation was terminated. For statistical analysis, single-trial values were z-normalized across trials.

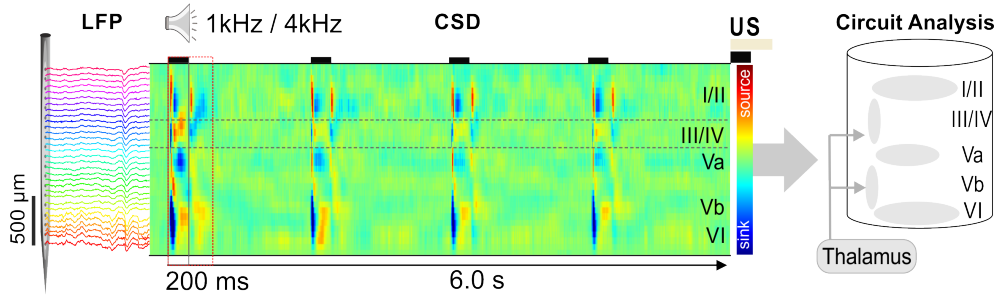

Figure 2.8: Chronic CSD recordings from the A1 in awake behaving gerbils. In vivo multichannel LFP recordings were obtained by single-shank (32 channels) silicon probes chronically implanted perpendicular to the surface of the auditory cortex targeting all cortical layers (I – VI). From laminar LFP signals single-trial current source density (CSD) distributions were calculated offline (here shown is a CSD averaged over 30 repetitions). During CS-presentation (200 ms, black frame) tone-evoked CSD components appeared as current sink (in blue) and source (in red) activity reflecting the well-known feedforward information flow of sensory information in the A1 (Happel et al., 2010a). Activity from 500ms (red frame) after the CS-presentation was used for the following analysis. A simplified schematic illustration of the cortical column and its layers is shown at the right part of the figure.

2.4.6 Statistics - Test of variance

Statistical test of variance. Statistical difference between groups was tested by one-factorial repeated measures ANOVA (rmANOVA) to account for the hierarchical structure of the data using R Studio (R 3.5.1.). We used an overall significance level of $\alpha = 0.05$ and paired-sample t-tests with a Holm-adjusted significance level (Holm, 1979) for post-hoc testing. Before testing, data was generally z-normalized within each animal and session. The generalized eta squared η^2_{gen} is reported as measure of effect size calculated using the R package DescTools (Bakeman, 2005 ; Olejnik and Algina, 2003). In general, we interpret effect sizes to be small for $\eta^2_{gen} \leq 0.1$, as medium for $0.1 < \eta^2_{gen} < 0.25$, and large for $\eta^2_{gen} \geq 0.25$ (Bakeman, 2005).

2.4.7 Generalized linear mixed model

Mixed-effects logistic regression. For statistical comparison between two-choice classes, parameters of interest were analyzed on a single-trial level using generalized linear-mixed effect models (GLMM) with a logistic link function (Chang et al., 2018) GLMM calculation in in R Studio (R 3.5.1) was done with the lme4 package for model estimation and ggplot2 and sjplot for plotting. Logistic regression was used for predicting the probability of the binary (0/1) dependent variables $\pi_i = E(\boldsymbol{y}_i)$. The predictions were then wrapped

by the logistic link function: $g(x) = \frac{1}{1+\exp(-x)}$ to map the predictions of the model to the interval between 0 and 1. In the mixed-effects logistic regression, random effects were additionally introduced to model subject-specific variance by:

$$g\left(E\left(\boldsymbol{y}_i\right)\right) = \boldsymbol{X}_i\boldsymbol{\beta} + \boldsymbol{Z}_i\boldsymbol{v}_i \tag{2.5}$$

where ψ_i is the vector of all responses of the i^{th} animal, $\boldsymbol{X}_i$ and $\boldsymbol{Z}_i$ are design matrices, β the fixed effects and $\boldsymbol{v}_i$ the animal-specific random effects. The parameters of the estimated model can be interpreted as logarithmic odds ratios $\log\left(\frac{\pi_{ij}}{1-\pi_{ij}}\right)$, where π_{ij} corresponds to the probability of the outcome to be 1 for animal i in trial j. The GLMM thus allows for an intuitive interpretation of its predicted values (choice probabilities) and its estimated coefficients (logarithmic odds ratios). As such, GLMMs are optimally suited to compare data on a trial-by-trial-level while accounting for within-subject variability. Random intercepts were introduced to account for the general variability in overall activity across subjects and random slopes to allow for the fixed effect to vary between animals. We z-normalized the AVREC RMS values for the GLMM to facilitate the estimation procedure.

Evaluation of the model. Calculation of the marginal (R^2m) and conditional (R^2c) coefficient of determination was done using the MuMIn package (Barton, 2019). The R^2m represents the variance in the dependent behavioral variable (on the logistic link scale) explained by the fixed effect of the respective CSD variable (across subjects), while the R^2c reflects the total variance explained by the model's fixed and random effects, respectively (Muff et al., 2016). In a binary GLMM, the R^2m is independent of sample size and dimensionless, which allows comparing fits across different data-sets (Nakagawa and Schielzeth, 2013). An R^2m of 0.2 thus means that 20% of the variance in the binary outcome can be explained by the cortical activity variable, which was used as the model's predictor. If the corresponding R^2c is 0.35, the whole model explains 35% of the variance, meaning that an additional 15% of the variance in the outcome can be explained by the variability between animals. The R^2m can hence be used to estimate the effect size, which we did in accordance with the η^2_{gen} from rmANOVA tests and report small effects for $R^2m \leq 0.1$, as medium for $0.1 < R^2\text{m} < 0.25$, and large for $R^2m \geq 0.25$ (Bakeman, 2005).

3 | Results

The present work has investigated the role of the primary auditory cortex (A1) in the encoding of behaviorally relevant acoustic stimuli, predictions, and auditory-guided decision making. For this, chronic laminar CSD analysis from the A1 was used in order to characterize layer-specific, spatiotemporal synaptic population activity while freely moving gerbils were performing a Go/NoGo auditory learning task in a shuttle-box.

This chapter contains two sections. The first section summarizes the findings on the level of the behavioral training and several learning estimates while animals perform cognitively demanding tasks. The second section, describes the stability of our new established method and the findings on how individual layers contribute to the integrative circuit of the A1 in order to code task-relevance and guide sensory-based decision making.

Based on the learning curves and careful examination of the results, I have decided to investigate the electrophysiological results in two parts. In the first part (***Part I***) , results from the detection and first discrimination phase are shown. While, in the second part (***Part II***) results from the multiple reversals are shown. To draw conclusions for the cortical microcircuits, a plethora of electrophysiological parameters have been extensively analysed. However, due to the quantity and complexity of the data, here the focus is the neuronal observable AVREC, which is a robust measure of the overall columnar activity. Additionally, in order to investigate the layer-specific changes during learning, the RMS values of the single layer (I/II, III/IV,Va, Vb, VI) cortical traces were used. These results go beyond previous reports, showing that by using generalized linear-mixed effect models (GLMM) on a single-trial level we can predict cortical layer-specific contributions during an auditory-guided action initiation and choice accuracy.

3.1 Auditory decision making with multiple reversals of the choice-outcome contingency in a shuttle-box - behavioral analysis

Mongolian gerbils were trained in an auditory cued two-way active avoidance shuttle-box task to respond to two pure tones (1 and 4 kHz) presented as conditioned stimuli (Figure 2.3). Gerbils were trained in six separate phases: detection, discrimination, and four reversal phases. First, in a detection training phase, both CS were assigned with a 'Go' contingency and required subjects to change the compartment to actively avoid the unconditioned stimulus (mild electric foot shock). The animals were trained over consecutive sessions until they reached a stable detection of both stimuli significantly above chance level Figure 3.1. In the subsequent training phase - discrimination, the contingency of the 4 kHz pure tone was changed to a 'NoGo' stimulus (CS-), while 1 kHz was maintained as CS+ ('Go' stimulus). Following, in the first reversal phase the contingencies of the two pure tones were switched, meaning that 1 kHz was a 'NoGo' stimulus (CS-) and 4 kHz was a CS+ ('Go' stimulus). Another three consecutive blocks of reversal tasks followed. During the phases of discrimination and multiple reversals, animals needed to discriminate the two pure tones in order to avoid the US. As it is mentioned in the Methods chapter, we classified behavioral choices depending on the response of the animal and the contingency as hit, miss, correct rejection, or false alarm (Figure 2.3).

3.1.1 Learning curves - Conditioned response rates

In the interest of describing the development of learning and cognitive flexibility during the auditory experiment in the shuttle-box, we used learning curves based on the conditioned response rates. Averaged conditioned response curves across training sessions for all training phases showed gradual and significant improvement of task performance Figure 3.1. During the detection phase averaged hit rates reached almost 80% for both 'Go'-stimuli (1 kHz and 4 kHz). During the initial discrimination phase, conditioned response rates dropped significantly for both stimuli (<10% hit rate). This indicates lack in the transferal of behavioral choice for the 1 kHz pure tone from the detection phase,

but the animals completely abandoned their detection-based avoidance strategy. Despite the significant drop, they quickly re-associated the 1 kHz CS with a 'Go' contingency by showing increasing hit responses within 1-2 sessions, while false alarm rates in response to the 'NoGo' 4 kHz tone were significantly lower (10-20%). When the contingency of the two pure tone stimuli was reversed for first time (Reversal 1), hit rates dropped significantly (<10% rate) while the false alarm rates were at the first session about 45-50% and reduced gradually. The following reversal phases showed a similar learning pattern. Usually lasted three to four sessions until animals were able to re-associate the conditioned stimuli with the respective contingency in each block of reversal training. Over the course of the long training, gerbils were adapted in the shuttle-box environment and they showed an increased avoidance behavior, which will be discussed in the next section. Hence, although the reversal is a quite demanding task, finally subjects were able discriminate the two pure tone frequencies even over four reversals of the contingency (Figure 3.1, above).

3.1.2 Learning curves - Sensitivity index d'

The learning progress can be evaluated by the averaged d' values (Figure 3.1, below) calculated based on the SDT (see Methods). As it is described above, high learning performance is defined when animals show increased conditioned responses for the 'Go' contingency and less for the 'NoGo' contingency. The threshold value to be reached for the detection and discrimination criterion was selected as $d' > 1$. During the initial detection phase the d' values are defined session-wise, as the difference of the z-transformed values for the responses to the Go stimulus and the spontaneous inter-trial jump rates. Animals were able to reach $d' > 1$ within four sessions. For the rest of the training phases d' values are defined as the difference of the z-transformed values for the jumps to the Go stimulus and the jumps to the NoGo stimuli. When the 'NoGo' 4 kHz tone was introduced for the first time during the discrimination phase, animals dropped their performance with $d' = 0$ but increased and reached $d' > 1$ already in the second session. It is interesting to note that d' values for the initial sessions of the reversal phases are very low, even $d' < 0$ and gradually reach the criterion threshold level. This implies there is a cognitive effort to re-adapt the learning strategy and finally to reach good discrimination performance in such auditory paradigm. At this point, consider that the number

of animals decreased (n=9, at initial phase till n=7 at the last phase, Figure 3.1) due to technical challenges to guarantee high-quality recordings over such long time periods.

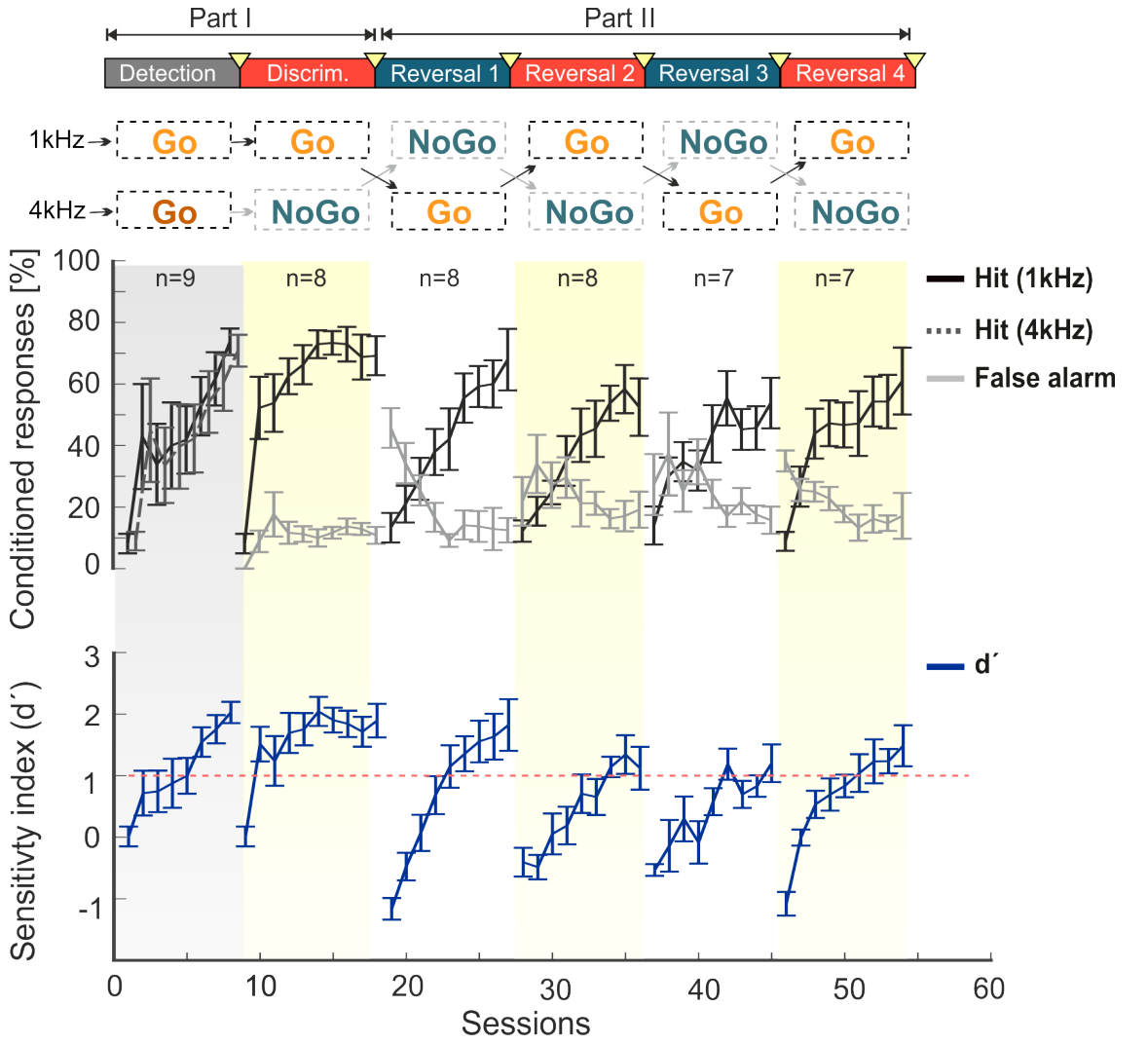

Figure 3.1: Learning curves during the multiple reversal Go/NoGo auditory task. Averaged conditioned responses to both CS in the detection, discrimination and reversal phases (top) and averaged sensitivity index d' (bottom) as a function of the individual training sessions. During detection phase (grey area, n=9), hit rates (shown in black lines) reach almost 80% for both 'Go'-stimuli (1kHz and 4kHz) and $d' > 1$ (shown in blue lines) after the fourth session. At the beginning of the discrimination phase (first yellow area, n=8), conditioned responses dropped for both stimuli (<10% hit rate). The performance gradually increased reaching again almost 80% for the hit rates and significantly decreased and stayed around 20% for the false alarm rates (grey lines). During reversal 1 and at least for two sessions, hit rates are <20% and false alarm rates are 40-50%, which gives also d' values under criterion threshold. After four sessions, the discrimination ability is re-acquired. Similarly, for the subsequent three reversal phases (n=8/7) but with reduced d' values.

3.1.3 Reaction time and learning progress

In the current shuttle-box Go/NoGo experiment, the reaction time is calculated as the time period between the presentation of the auditory stimulus and the animal 's decision to show a response with a complete compartment change. Specifically, conditioned responses were counted in time bins of 250ms and the distributions of reaction times over all animals and trials for each training phase (Detection to Reversal 4) were plotted in histograms (Figure 3.2, a). Due to the fact that the observation time window is 6 seconds (from the tone onset) we are mainly interested for the reaction times below 6 seconds, which correspond to hit (shown in red) and false alarm choices (shown in blue). From these results, it is clear that during the detection and discrimination phase (left part) the correct behavioral choices (Hits) are generally executed after the 2nd to 4th tone, and less frequent already after the first tone, while the reaction time of the wrong choices (FA) are equally distributed over the trial duration. Note, that the tones are presented four times within the observation time window (delayed conditioning). This suggests that the task design allows the subjects to use at least the presentation of a second CS to evaluate their planned behavioral choice. The results from the reversal phases demonstrate two things. First, again the reaction times were found to be mainly after the second CS was presented within a trial in an equally distributed manner. Second, the conditioned responses showed a reduction, which can be explained either by the decrease of group size (n = 8/7) and sessions compared to the previous phases (detection and discrimination) or by the tendency of the animals to switch their strategy from avoidance to escaping after the long training protocol. The latter is in line with the results we get from the learning curves based on conditioned response rates and the sensitivity index.

Another way to illustrate the possible switch of animal 's behavior from active avoidance to escaping strategy is to count all possible behavioral choices (hit, miss, false alarm and correct rejections) over the course of the complete trial duration (Figure 3.2, b) for each training phase separately. This test revealed that indeed most of the conditioned responses happened during the first two phases of training. The number of false alarm responses stays always relative low. However, during the multiple reversal tasks there is an increase of the miss responses comparing to the number of hit trials of the same phase. This is a

clear indicator for an escaping behavior. Because of this potential limitation, in later sections of this thesis the electrophysiological analysis will be treated in two parts. The first part will include CSD analysis of the detection and discrimination phase, while the second will deal with CSD data from the multiple reversal tasks.

Finally, in order to prove the exact relationship between the reaction time and the discrimination performance Pearson 's correlation coefficient was used. In this case, each data point in x-coordinate represents the d' values from each session during the discrimination phase, while each data point in y-coordinate represents the mean reaction time of each particular session. This allows us to plot the data from all animals in a scatter-plot and to calculate the correlation coefficient of those two variables (Figure 3.2, c). This analysis showed that when the mean reaction time tends to decrease, the sensitivity index d' variable increases. Therefore, there is a significant negative correlation between discrimination learning performance and the reaction time, which is in line with the existing literature (Donders, 1969; Young, M.E. & *Crumer, 2006).

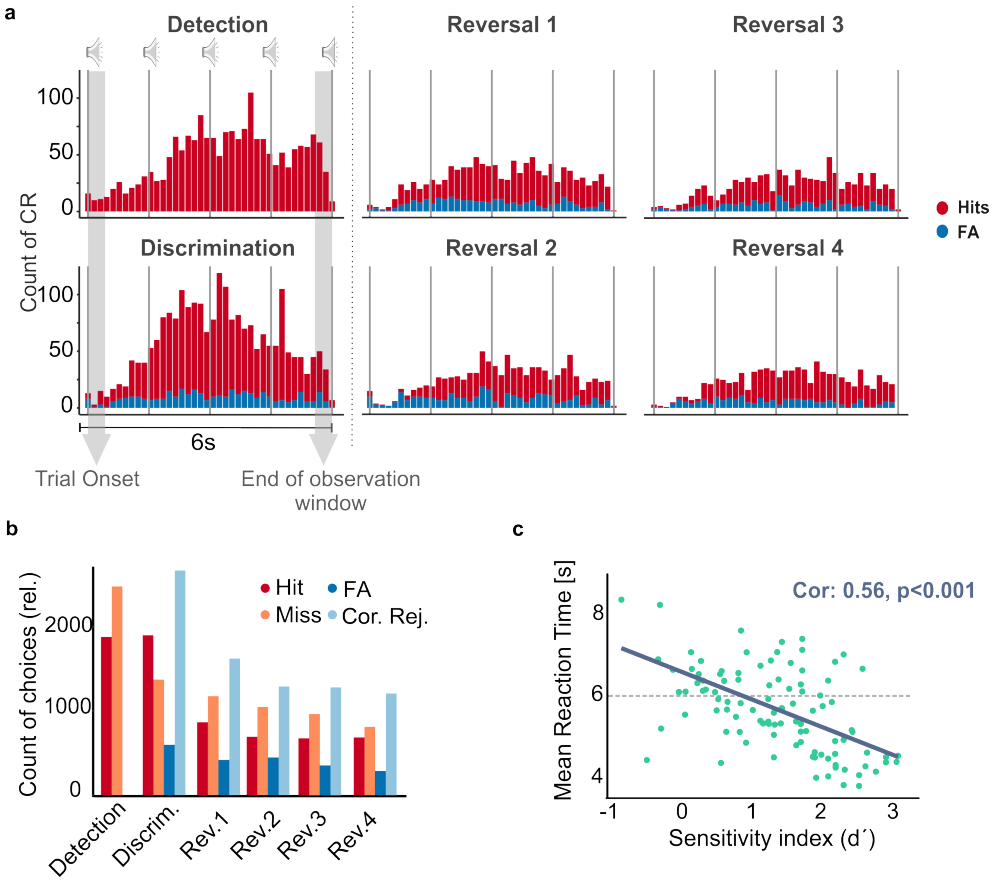

Figure 3.2: Correlation of reaction time with the learning progress. a. Histograms with distributions of the conditioned responses - reaction times over all trials of the phases detection, discrimination (left part) and reversal 1-4 (right part). The observation window is 6s and each tone (CS+/CS-) is presented 4 times with ISI 1.5s, if there is no conditioned response before that period. The responses are counted in relation to the tone presentation and in time bins of 250ms. Hits responses are shown in red bars and false alarms in blue bars. **b.** Histograms with distributions of the relative count of behavioral choices: hit (red); miss (orange);false alarm (FA, dark blue);and correct rejection (Cor.Rej., light blue) over the course of the complete trial duration and per training phase. **c.** Scatter-plot represents the relationship of the variables d' values (x-axis) and mean reaction time (y-axis) of each session in discrimination phase (n = 8). There is a significant negative correlation between the variables with Pearson 's r = 0.56 and p<0.001.

3.1.4 Characterization of individual learning strategies

In order to distinguish between individual learning strategies, the receiver operator curves (ROC) were placed on a strategy plane (see, 2.4.2, *Strategy plane - ROC curves*) for each animal and phase separately. Representative examples of two different subjects are shown in Figure 3.3. The one animal (Figure 3.3, a) could be characterized as a "quick learner". During the first session of the discrimination task (light grey dot- start) it showed low jumping rate for both stimuli (Go and NoGo) with $d' < 0$, a strategy that can be

described as conservative (grey plane).

However, by following the trajectory on the graph, one can observe that the animal very quickly (2 sessions after) achieved $d' > 1$ (on ROC lines) with an optimal performance (green plane). This strategy remained till the end of this phase. As it is mentioned above, the task switch (reversal 1) caused drop in performance. In this case, at the start point the animal kept the strategy that developed during the previous task, which is now wrong due to different contingencies. It took, again, only two sessions till the new meaning of the stimuli was re-associated and the discrimination performance became optimal. In contrast, the graph shown in the Figure 3.3 and panel b (left) illustrates a completely different learning strategy from another gerbil. This animal showed increased amount of conditioned responses for both stimuli (Go and NoGo) in the beginning of the discrimination phase (start point). This strategy can be characterized as liberal (yellow plane) because the animal seemed to generalize the given conditions.

In next sessions, the jump rates were reduced and his strategy changed to a more conservative. Looking at the ROC curve trajectory it is obvious that although this animal reached $d' > 1$ there were many fluctuations in its discrimination performance. Interestingly, after the contingency reversal, its strategy changed again. The reversal task caused a significant reduction to the jumping rates (conservative plane - start) and it lasted for two sessions. Finally, the animal achieved the optimal discrimination performance ($d' > 1$, dark gray dots- end) within three consecutive training sessions. Hence, it can be concluded that although the animals reach the criterion threshold to learn the Go/NoGo paradigm the way they do it differs from subject to subject.

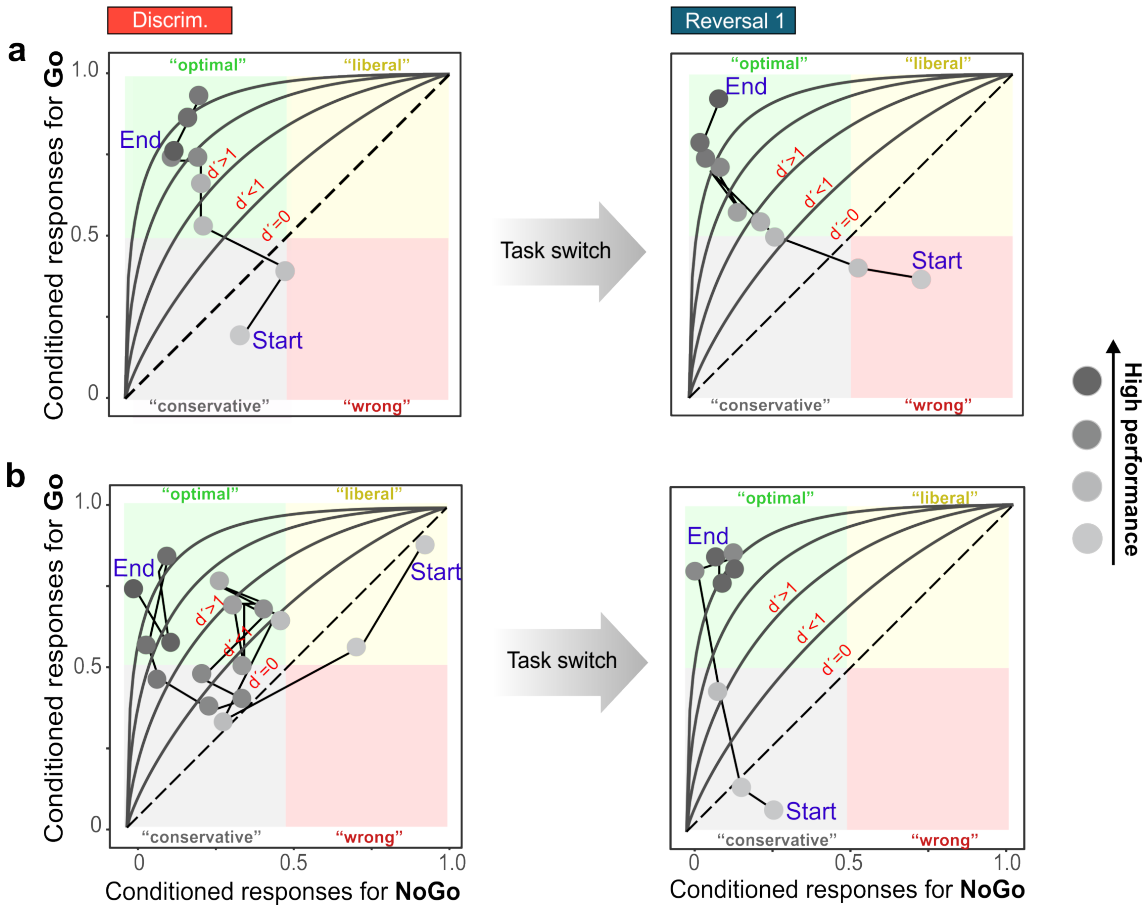

Figure 3.3: Behavioral variability and unique learning strategies (ROC). Representative examples of receiver operator characteristic (ROC) curves based on discrimination and first reversal learning performance placed in a behavioral strategy plane. The diagonal and ROC lines indicate the d' value levels. The grey dots show the different sessions. The initial session (start) is shown with the lightest gray dot while the final session (end) with the darkest grey dot. Each point represents the total amount of conditioned responses to the Go (y-axis) and NoGo (x-axis) stimuli at that session. Based on the relationship of those two variables, the behavior can be characterized as "conservative" (gray plane), "wrong"(red plane), "liberal" (yellow plane), and "optimal" (green plane). **a.** The single subject learning trajectory during discrimination revealed a quick (within 2 sessions) transition from the conservative to the optimal state ($d' > 1$). Task switch caused a drop in performance. Initially, the animal showed a "wrong" strategy which changed to the "optimal" after two sessions. **b.** Trajectories from another single subject revealed a different learning strategy. It started from the "liberal" and reached the "optimal" state but after many fluctuations during the training. The reversal task reduced dramatically the conditioned responses but the animal re-acquired the task quickly, after two consecutive sessions reaching again the "optimal" state.

3.2 Chronic CSD recordings during the auditory learning paradigm in the shuttle-box - a cortical circuit analysis.

The first set of analyses examined the impact of the designed auditory Go/NoGo paradigm on the behavior of the animals and it focused on the behavioral parameters. Turning now to the experimental evidence on how task-related information is represented in the cortical microcircuitry in the A1, the results from the chronic LFP/CSD recordings will be described in the following sections.

3.2.1 Establishment of stable chronic CSD recordings.

The ability to chronically record LFP/CSD signals from the A1 during the long-term experiment is one of the advantages of this newly established method (Happel et al., 2015). In order to prove the stability of the long-term recordings, averaged CSD profiles (n=1) across 30 trials from the first and 30 trials from the last training sessions (after 6 weeks) are compared, qualitatively (Figure 3.4, a). In this representative example, the CSD quality remains stable, allowing the detection of physiological sink-source activity patterns across the cortical layers of the trained animal. Based on the relationship of cortical depth with the sink-activity patterns, identification of the cortical layers (I-VI) was possible and it was controlled over the course of the complete training.

Despite the stable CSD quality, in a long-term experiment, which combines electrophysiological data with behaving, freely-moving animals, the sources of artifacts cannot be ignored. As it is mentioned in the methods section, data preprocessing on a trial-by-trial level is an important step to get artifact-free data. One common type of artifacts is the distortions on the recording channels, which generate non-physiological signals. In order to eliminate such channel-dedicated artifacts, the method of linear interpolation was used (**??**). To quantify the quality of the recordings in respect to the channels, averages (n=9/7) of the interpolated recording channels are shown per session over the course of the training protocol (multiple reversals, Figure 3.4, b - top). From the Figure 3.4, b can be seen that the maximum number of affected channels is 10 out of the 32 recording

channels. Even after the long-term use of the recording sites only a few channels needed to be interpolated. Similarly, Figure 3.4, b - bottom illustrates the averaged (n=9/7) number of trials which were excluded from the analysis due to non-physiological signals. The maximum number of excluded trials was 5 out of 60 trials per session and it happened in the later phases of the training. Furthermore, the quality of the data can be also controlled in respect to the artifacts caused by the conditioned responses (CR or no CR) during a session. Thus, in Figure 3.4, c the y-axis represents the percentage of the affected signal per session (100% corresponds to all trials of that session) while the x-axis shows the training sessions. Trials with CR (purple line) are plotted separately from the trials with no CR (green line). Interestingly, at least until the end of phase 3 (reversal 1) there is no significant difference in the amount of artifacts between trials with or without CR. In later phases, indeed, CR-trials showed an increased amount of artifacts compared to no-CR trials. However, what stands out from the Figure 3.4, c is that even in later phases about 80% of the data in each session can be used as they are artifact-free. Thus, despite the existing cases of non-physiological data, the newly established techniques enable us to control the data quality and perform valuable data analysis.

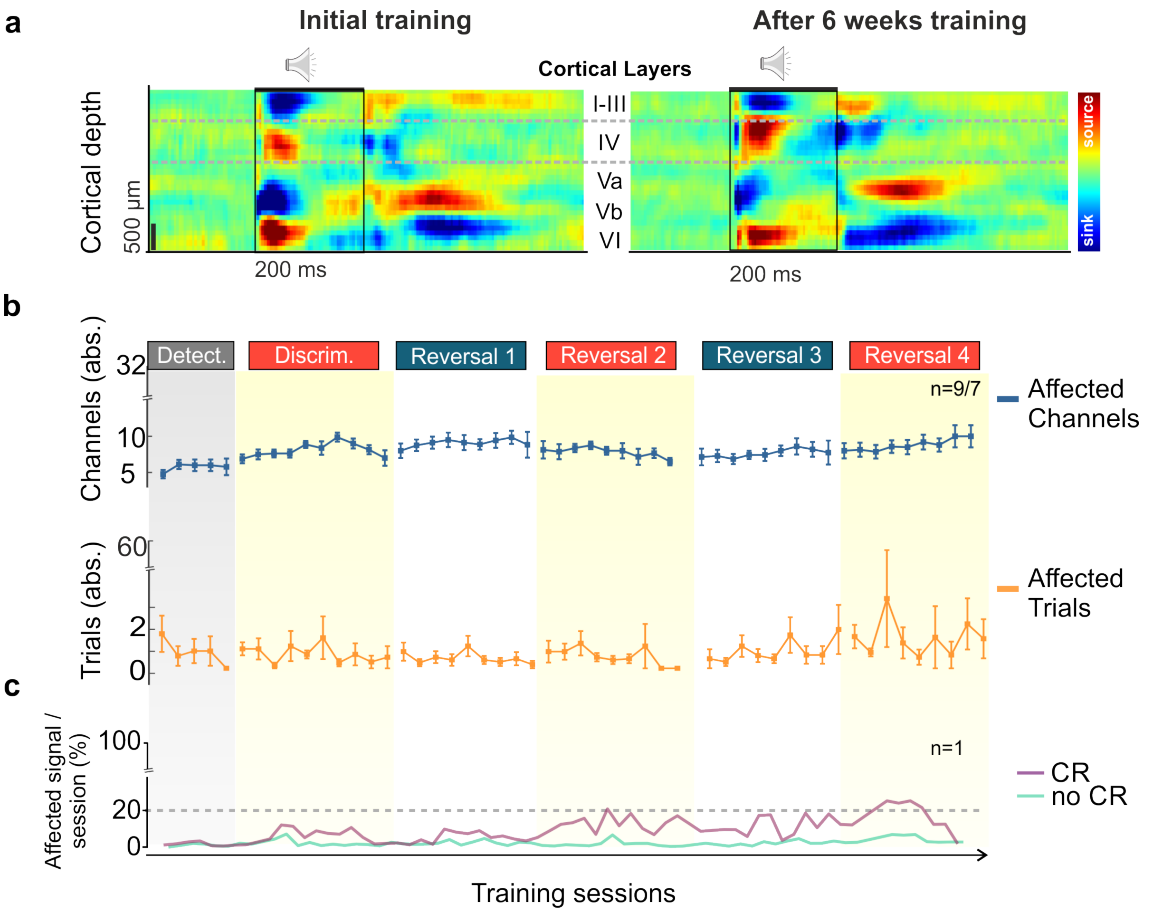

Figure 3.4: Long-term stable CSD recordings from all cortical layers in A1. a. Representative example of an averaged (across 30 trials) CSD profile from one subject of the first training session (detection; left) and the last discrimination session (right), after 6 weeks of training. Based on the averaged auditory-evoked activity in response to the first presentation of the conditioned stimuli within a trial (time window: 500ms; tone duration: 200 ms; indicated by the black frames) we assign the cortical input layers (I/II-VI) to the respective recording channels (indicated with the dashed lines). The example illustrates the stability of the electrode positioning over the course of the training. **b.** Averaged number of interpolated channels (top, blue line) and affected trials (bottom, orange line) over the course of multiple-phase training (n=9/7 animals,error-bars show the SEM). **c.** Example of a single animal data (n=1) showing the percentage of artifacts on trials with conditioned responses (CR - in purple) and those without conditioned responses (no CR- in turquoise) over the course of the training.

3.2.2 Task rule impacts on the columnar representation of sound frequency

Previous research has established that in an averaged CSD trace, the tone-evoked activity in response to the repetitive CS presentation, reflects the spatiotemporal feedforward flow of sensory information across cortical layers in the A1 (Happel et al., 2010a; Sakata and Harris; Hickmott and Merzenich, 1998). This is marked as the most prominent laminar response pattern. To compare the difference between different conditions of the experiment, we used the averaged CSD trace information. For example, during the detection phase, the two pure tones (both 'Go' stimuli) generated highly similar CSD patterns with respect to the spatiotemporal current flow (Figure 3.5, a). Initial current sink activity was observed within granular layers III/IV and infragranular layer Vb, reflecting cortical depths of main thalamocortical inputs from the ventral medial geniculate body. Subsequent synaptic activity is then routed to supragranular layers I/II and infragranular layers Va and VI (Happel et al., 2010a; Szymanski et al., 2009; Schaefer et al.). Given the fact that the pure tone duration was 200ms, the overall columnar response showed a prolonged activation. In awake passive listening subjects CSD profiles were generally also very similar in response to both pure tones (Figure A.1). This is due to considerably similar and flat frequency tuning properties across the entire group of animals measured (Figure A.1).

In contrast, during the discrimination phase, the two physically identical stimuli evoked considerably different CSD patterns. While the overall tone-evoked columnar activity in Go-trials showed a marked increase, the activity in NoGo-trials was rather unchanged or slightly decreased (Figure 3.5, a). More evidence is provided after quantification of the overall columnar activity strength. For this, I compared the root mean square values of the AVREC (AVREC RMS; z-normalized) calculated for the entire trace in each trial (Figure 3.5, b). The applied one-way repeated-measures ANOVA (rmANOVA) revealed that, during the detection phase, the overall activity over the trial between the two CS+ did not differ ($F_{1,8} = 0.20$, $p = 0.668$). During discrimination, the CS+ evoked significantly more cortical overall current flow compared to the CS- ($F_{1,7} = 143.63$, $p < 0.001$). Thus,

these findings show that the activation strength of the auditory cortex in response to pure tones depends on the task rule (Figure 3.5,b in grey insets, find full AVREC traces at Figure A.2).

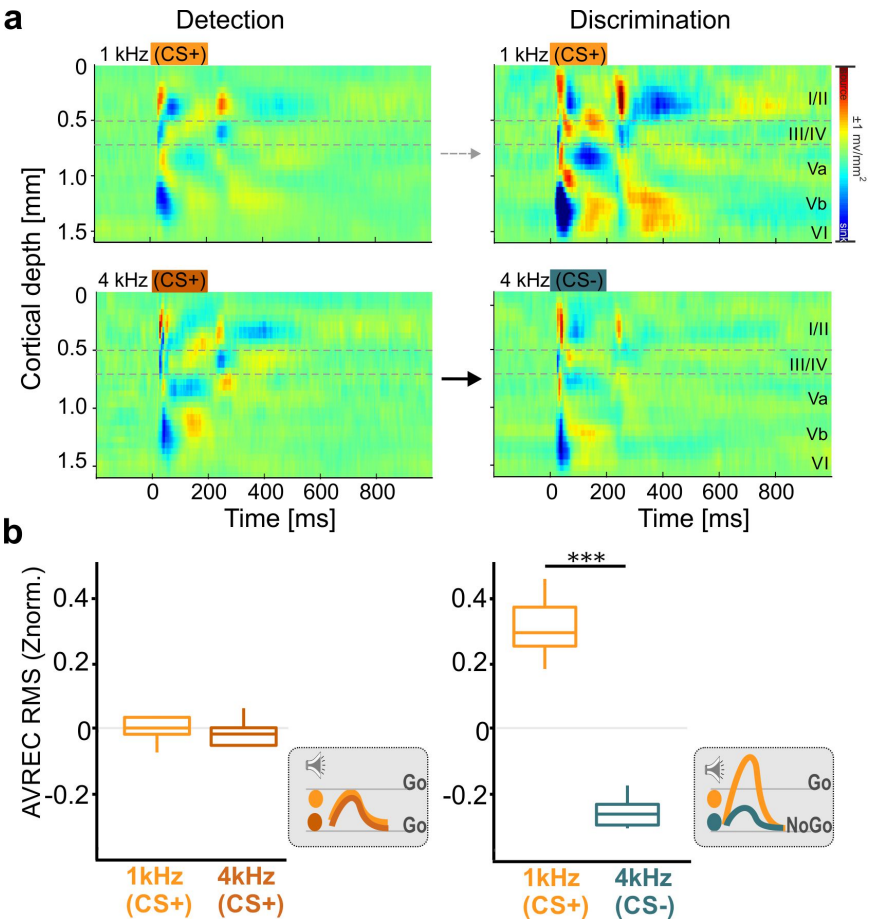

Figure 3.5: Stimulus-related activity during different training phases. a. Representative example of an averaged CSD profile across all trials of the detection (left) and discrimination (right) phase of one subject. The CSD profiles show the tone-evoked activity after the first presentation of both conditioned stimuli within a trial (top: 1 kHz, bottom: 4 kHz; tone duration: 200 ms; indicated by dashed bar in upper left panel). Evoked CSD patterns between the two pure tones frequencies showed no obvious differences during the detection phase but yielded considerably different CSD patterns during discrimination for the CS+. **b.** RMS values of the AVREC (time window of 500 ms beginning at each tone presentation and z-normalized) shown for each of the four consecutive CS and separated by the different behavioral outcomes during the two task phases(detection/discrimination= 9/8). Box plots represent median (bar) and interquartile range, and bars represent full range of data. Significant bar indicate differences revealed by pairwise testing. Schematic illustration of the evoked cortical activity in dependence of stimulus frequency and task rule are shown in grey inserts (see Figure A.2).

3.2.3 The auditory cortex represents decision and choice accuracy

The next question asked was whether the decision made by the animal is represented within the A1 and how the cortical recruitment depends on that. For this, we compared the AVREC RMS values during a 500 ms window beginning with each CS onset. In a first step, we tested the dependence of the animals' choice options and the time bins throughout the trial, by a 2-way rmANOVA with the main factors outcome and tone order (Figure 3.6). Significant effects were found for both main factors, outcome and tone order, as well as their interaction in both the detection and discrimination phase (Detection: outcome $F_{3,24}= 40.63$, $p < 0.001$, $\eta^2_{gen}= 0.66$;tone order $F_{3,96}= 26.58$, $p < 0.001$, $\eta^2_{gen}= 0.25$; interaction $F_{9,96}= 10.05$, $p < 0.001$, $\eta^2_{gen}= 0.27$; Discrimination: outcome $F_{3,21}= 31.67$, $p < 0.001$, $\eta^2_{gen}= 0.68$; tone order $F_{3,84}= 26.39$, $p < 0.001$, $\eta^2_{gen}= 0.23$; interaction $F_{9,84}= 17.52$, $p < 0.001$, $\eta^2_{gen}= 0.38$). In order to test the differences of the behavioral outcomes at each time point separately, we used restricted Holm-corrected post-hoc comparisons at each of the CS+ presentations. During detection training, post-hoc tests revealed that the evoked AVREC RMS values (z-norm.) after the first CS presentation are similar for hit and miss trials. Consecutive CS+ presentations evoked significantly higher RMS values during hit trials compared to miss trials (Figure 3.6, a-left, Table A.1).

These findings were independent of the actual stimulation frequency (1 or 4 kHz). In the discrimination phase, we found a significantly different recruitment of auditory cortex columnar activity depending on frequency and choice of the subjects at the second and ongoing CS presentations throughout a trial (Figure 3.6, a-right). Cortical activation in the 500 ms time window around the first CS showed only minor differences. During later CS presentations, we found a stable pattern of columnar activity. During hit trials, cortical activation was significantly highest compared to all other classes. Correct rejections showed the lowest cortical recruitment. In contrast, cortical activation during miss and false alarm trials did not differ at any CS presentation throughout the trial.

Note that cortical recruitment was generally stronger during trials in which animals reported a compartment change (hits > misses; false alarms > correct rejections), comparable to findings in the detection phase. However, as the cortical activity during miss and false alarm trials did not differ significantly, the variability of cortical activation in

our data cannot be explained by a mere correlate of motor responses or motor planning, but must also depend on the contingency of a stimulus. Indeed, the strongest difference observed was between the two correct choice options of the animal, namely between hits and correct rejections. Hence, cortical recruitment during detection was influenced to a larger degree by the behavioral action taken by the animal, rather than the physical stimulus. During discrimination, cortical recruitment was influenced by the frequency, coding for the contingency of the stimulus, and the choice accuracy of the taken action (Figure 3.6, b).

In addition, data from a time window of 500-1000 ms after each stimulus presentation (stimulus duration: 200 ms) were analyzed. The reason behind it was to separate the relative modulation of cortical layer activity by sensory-driven effects from the task-related, but potentially temporally distributed information. This analysis revealed a similar pattern of cortical activity being modulated by the choice accuracy, which is hence present also independently from the stimulus-dominated auditory response (Figure A.3).

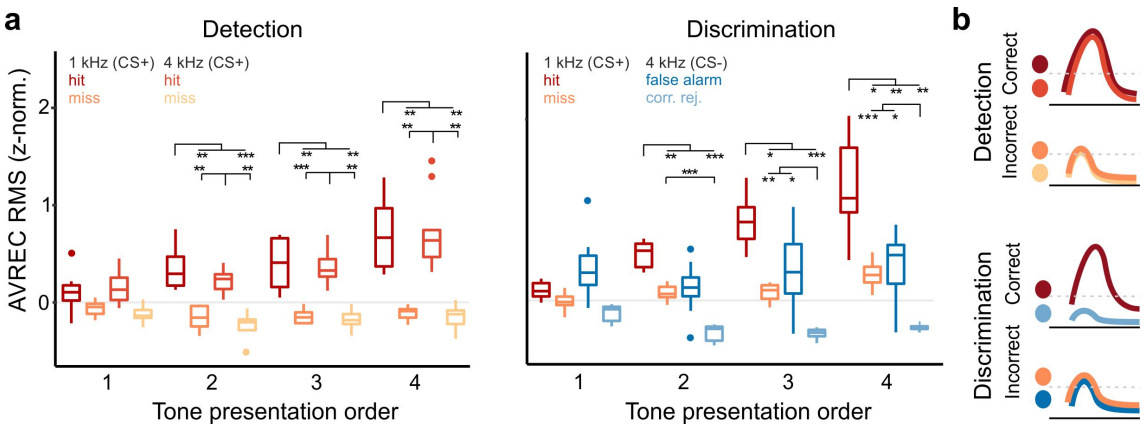

Figure 3.6: Behavioral choices and contingency are both reflected in population activity of the A1. Averaged AVREC RMS values (500 ms window at CS onsets) plotted with respect to the conditioned stimuli and behavioral choice. **a.** Left, During the detection phase evoked activity was significantly higher during hit trials compared to miss trials independent of the stimulation frequency (detection/ discrimination: n=9/8). Right, In the discrimination phase, cortical activity was strongest during correct hit trials and lowest during correct rejections. During trials of incorrect behavioral choices (miss/false alarm) tone-evoked activity was characterized by intermediate amplitudes and did not differ. Box plots represent median (bar) and interquartile range, and bars represent full range of data.Dots represent outliers. Significant bars indicate differences revealed by a 2-way rmANOVA and corresponding posthoc tests with Holm-corrected levels of significance (see Table A.1) **b.** In summary, cortical activity was generally higher in trials in which animals showed a conditioned response in comparison to trials where animals stayed in the compartment. Cortical activity differed strongest between correct behavioral choices, namely hits and correct rejections.

3.2.4 Representation of contingency is layer-specific and differs with task rule

Further steps of the analysis were concerned with examining the contribution of cortical layers to the observed effects. In order to investigate this, I analyzed binary classes on a single-trial level using generalized linear-mixed effect GLMM (Chang et al., 2018; Bakeman, 2005). The GLMM analysis revealed that in the detection phase, the AVREC trace RMS (z-norm.) was not dependent on the presented frequency of the two conditioned stimuli (left, $R^2m = 0$, ns.; Figure 3.7, left). During the discrimination phase, an increase in the AVREC trace RMS was a reliable predictor that the 1kHz 'Go' stimulus was presented ($R^2m = 0.17$, $p < 0.001$; Figure 3.7, right). Hence, the columnar activity in the auditory cortex in response to the same conditioned stimuli differed in dependence of the task and was only separable when both had contrasting contingencies.

We further applied the GLMM to the RMS value measured over the entire trace activity within single cortical layers (I/II, III/IV, Va, Vb, VI) in order to reveal the source of the aforementioned results on a layer-specific level (Figure 3.7). In the detection phase, the two CS+ used as binary class in the GLMM could not be predicted significantly for any particular cortical layer. Then, the GLMMs were applied for the two conditioned stimuli during the discrimination phase. Remember that in discrimination, the two stimuli reflect two distinct contingencies (CS+ and CS-). In this case, a moderate prediction of the model with an R^2m of 0.12 for only the granular input layers was observed. Detailed results for each model are reported in Table A.2.

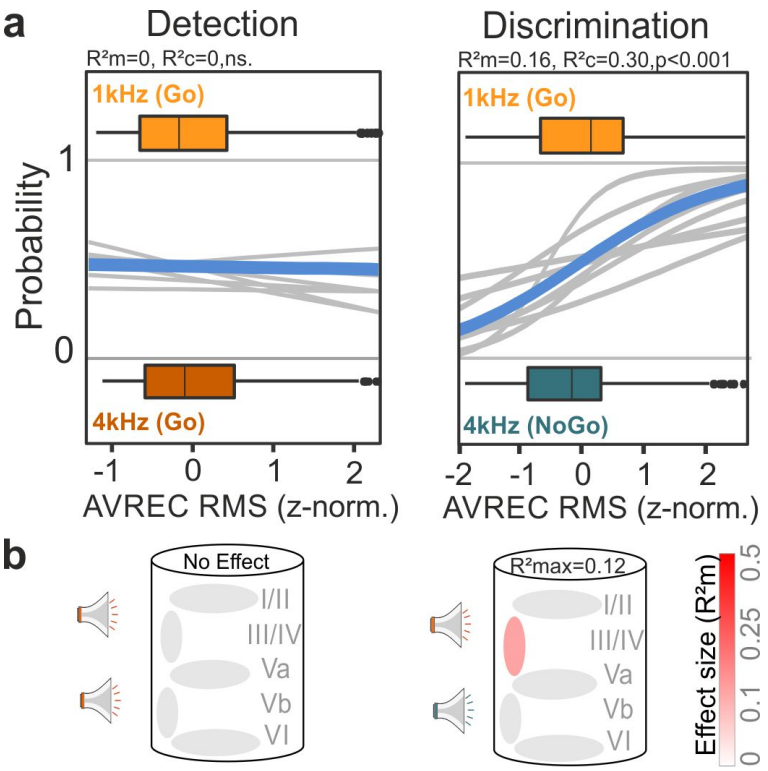

Figure 3.7: Representation of contingency, not frequency revealed in synaptic population activity of granular input layers. Parameters of interest were analyzed on a single-trial level using generalized linear-mixed effect models **a.** Logistic regression curves show the probabilities of the presented CS (1kHz and 4kHz as the dependent variable) for individual subjects (gray) and as an average (blue). The boxplots above and below the curves represent the mean (bar), interquartile range (box) the full range of data (whiskers). The AVREC trace RMS did not predict the frequency of the conditioned stimuli (1 kHz and 4 kHz) during the detection phase (left, R^2m=0, R^2c=0, ns.). During discrimination an increase in the AVREC trace RMS significantly indicated that the 1 kHz 'GO' stimulus was played (R^2m=0.16, R^2c=0.30, p<0.001). Hence, auditory cortical activity in response to the same conditioned stimuli differed in dependence of the task. **b.** GLMMs were applied to RMS values measured within single cortical layers (I/II, III/IV, Va, Vb, VI). The illustration of the cortical column below indicates the GLMM predictability based on data from corresponding layers to the binary behavioral choice combinations. The color illustrates the effect size for the model-based R^2m (grey= no effect to red=strong effect). The top R^2m value (R^2max) depicts the best fit result for all layers tested. In the detection phase, the two CS+ used as binary class in the GLMM revealed no significant prediction for any particular cortical layer. During the discrimination phase we observed a moderate prediction of the model with R^2m = 0.12 for the granular input layers. The detailed results for each GLMM are reported in Table A.2.

Following, the GLMMs were used to predict the behavioral choices rather than the stimulus frequency (Figure 3.8). Therefore, the AVREC RMS values (z-norm.) of the 500 ms windows around the tone presentation that preceded an active avoidance response of the animal (hit/false alarm) or around the last CS in the observation window in trials without a CR (miss/correct rejection) were used. During the detection phase, a higher AVREC RMS was a robust predictor for trials with a correct hit response compared

to miss trials with lower overall cortical activity ($R^2m = 0.32$, $p < 0.001$; Figure 3.8, left). In order to test the contribution of distinct cortical layers to the coding of different behavioral choices, GLMMs predictions were calculated for the RMS values of each layer separately.

Those results demonstrate that during the detection phase, cortical activity in infragranular layers was a good predictor ($R^2m = 0.2 – 0.25$, $p < 0.001$), while supragranular and granular layers were less accurate ($R^2m = 0.11 – 0.19$, $p < 0.001$; Figure 3.8, left; cf. Table A.3). Again, during the discrimination phase the AVREC RMS also predicted choice outcome during 'Go'-trials (hits vs. misses) with a moderate effect size ($R^2m = 0.18$, $R^2c = 0.38$, $p < 0.001$; Figure 3.8 a, right). Additionally, for the 'NoGo'-trials the GLMM was able to predict the outcome with a high effect size: false alarms were effectively predicted by stronger cortical recruitment than measured during correct rejections ($R^2m = 0.27$, $p < 0.001$; Figure 3.8 a, right). During discrimination, granular and supragranular layers appear to be important for the differential representation of the behavioral choice in 'Go'-trials ($R^2m = 0.14$-0.18). During 'NoGo'-trials, the RMS value of all cortical layers except of layer VI were good predictors for the trial outcome ($R^2m = 0.10$-0.17, $p<0.001$), while supragranular layers were also the best predictor between false alarms and correct rejections (see Table A.3).

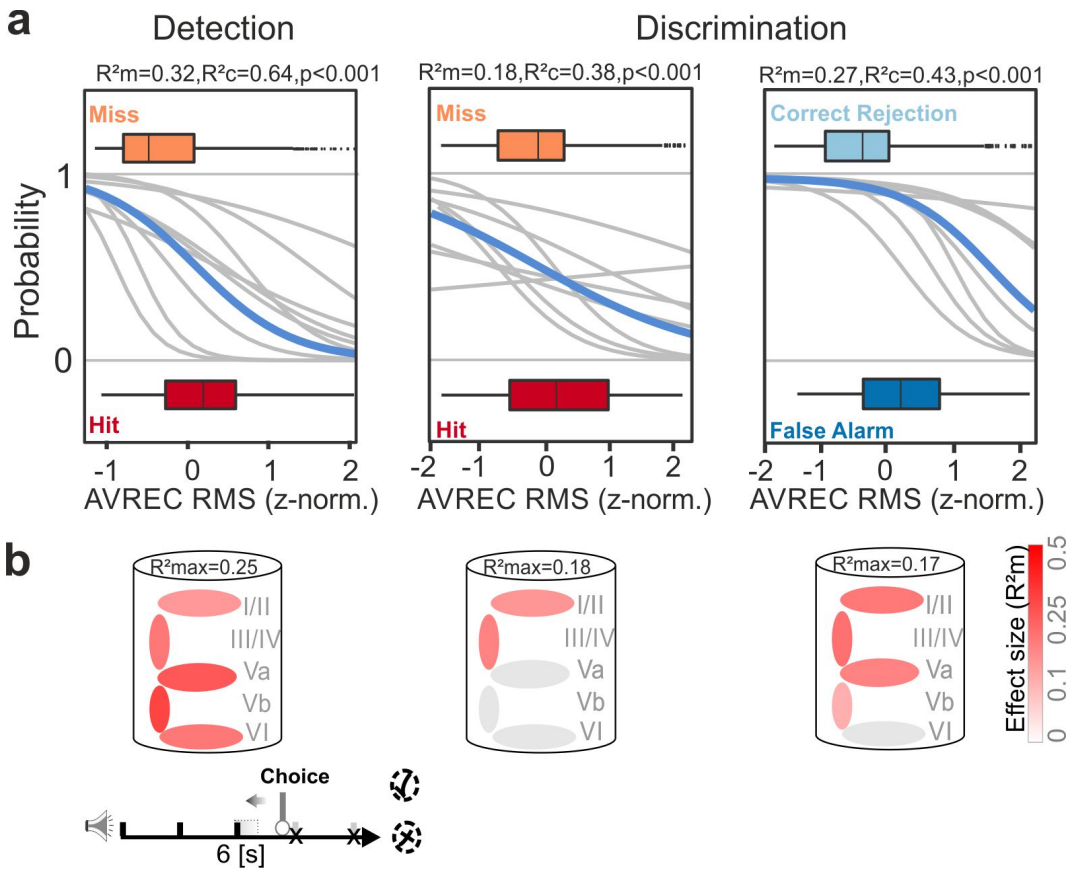

Figure 3.8: Layer-specific contribution to behavioral choice. a. GLMM and logistic regression analysis was used to predict the behavioral choice of the subjects. Left, During the detection phase RMS values of the AVREC (z-norm.) in the 500 ms time window around the CS presentation which was initiating a hit response was significantly higher compared to the fourth CS during miss trials (R^2m=0.32, p<0.001). Middle, this was also true for the discrimination phase, although with only a moderate effect size (R^2m=0.18, p<0.001). When comparing data from 'NoGo' trials, false alarm and correct rejections could be predicted with a high effect size (R^2m=0.27; p<0.001). **b.** The illustration of the cortical column below indicates the GLMM predictability based on data from corresponding layers to the binary behavioral choice combinations. The color illustrates the effect size for the model-based R^2m (grey/red scale). GLMM predictions for each layer showed that cortical activity from all layers were good predictors (R^2m=0.1-0.25), especially higher effect we observed at deeper layers Va, Vb, and VI, for the two possible choices (hit/miss). This finding was independent of the actual spectral content of the presented stimulus (1 kHz/4 kHz; see Figure 3.6). During the discrimination phase, granular and supragranular layers appear to be important for the differential representation of the behavioral choice in 'Go'-trials (R^2m=0.14-0.18). For 'NoGo'-trials, the GLMM revealed that false alarms are accompanied by significantly higher activity in all cortical layers except of layer VI compared to correct rejections (R^2m=0.17, p<0.001). Supragranular layers were also the best predictor between false alarms and correct rejections classes. The detailed results for each GLMM are reported in Table A.3.

3.2.5 Choice accuracy is robustly represented throughout cortical layers

Finally, in order to obtain more evidence regarding the A1 cortical recruitment during decision-making, data from accurate and inaccurate choices were compared. To test this, similar analysis with GLMM was done but this time with binary class being the correct and incorrect choice options of the subjects.

From this analysis, it can be seen that only correct choices lead to a distinguishable cortical circuit activation (Figure 3.9). The AVREC RMS could predict the outcome in correct trials with a high effect size: Correct 'hit' responses can be predicted by higher RMS values of the AVREC trace in the time window before the actual decision compared to the time window at the trial end during correct rejections ($R^2m = 0.45$, $p<0.001$). On the other hand, the two incorrect choices 'false alarms' and 'miss' were not predictable by the GLMM ($R^2m = 0.04$; n.s.; Figure 6A). The layer-specific analysis further revealed that particularly supragranular layer activity contributed to the differential cortical activation between the correct choice classes ($R^2m = 0.18$-0.51; $p<0.001$; cf. Table A.4; Figure 3.9, left).

Nevertheless, all cortical layers were recruited in a distinct way, so that the whole cortical column differs in activity during correct hit and correct rejection choices. In accordance with the insignificant GLMM result on the overall columnar activity measured by the AVREC RMS, also no cortical layer activity could predict the two incorrect choices (false alarm/miss; Figure 3.9, right).

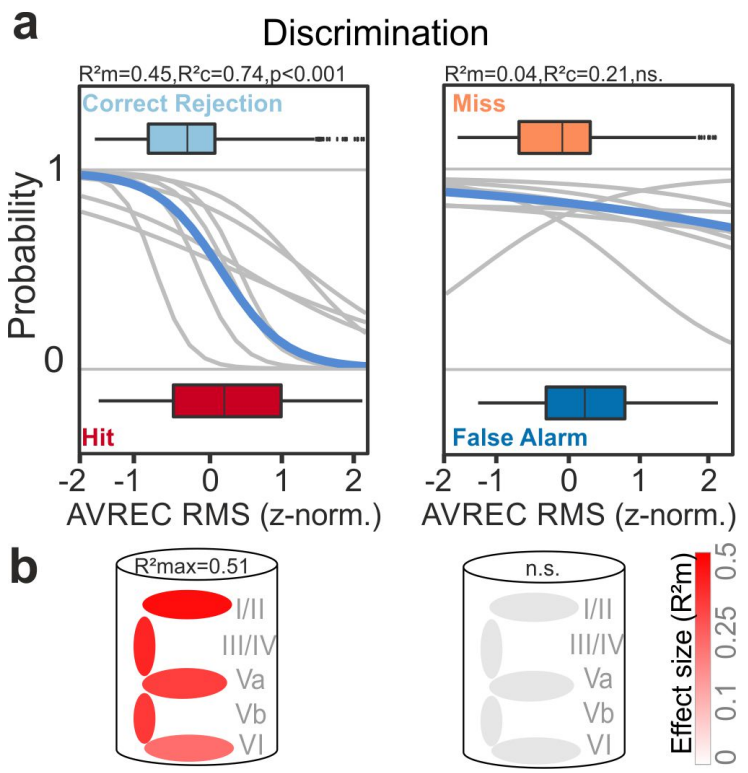

Figure 3.9: Representation of choice accuracy across layer-specific population activity in A1. a. Predictability of correct (left) and incorrect (right) choices during the discrimination phase were modelled by GLMM and logistic regression. Correct 'hit' responses can be predicted by higher RMS values of the AVREC trace in the time window before the actual decision compared to the time window at the trial end during correct rejection responses (R^2m=0.45, p<0.001). In contrast, the two incorrect choices 'false alarms' and 'miss' were not predictable by the GLMM (R^2m=0.04; n.s.). **b.** The illustration of the cortical column below indicates the GLMM predictability based on data from corresponding layers to the binary behavioral choice combinations. The color illustrates the effect size for the model-based R^2m (grey/red scale). Activity from all cortical layers contributed to the differential cortical activation between the correct choice classes, while the largest effect size was found for supragranular layers (R^2m=0.51; p<0.001). In accordance with the insignificant GLMM result on the overall columnar activity measured by the AVREC, also no cortical layer activity could predict the two incorrect choices (false alarm/miss). The detailed results for each GLMM are reported in Table A.4.

3.2.6 Accumulating evidence of task-related information across auditory cortical layers

Another set of analyses examined the build-up of evidence for behavioral choices along the trial duration and how this can be predicted based on the layer-specific adaptations we observe with the use of GLMMs. In order to reveal the temporal accumulation of such task-dependent information during a trial, we further analyzed time-resolved R^2m values for the four behavioral choices, which generally increased over the trial duration preceding an animal's reaction (Figure 3.10).

While infragranular layers Va-VI showed moderate R^2m values even 2 – 3 CS+ presentations before the actual response (up to 3 – 4.5 seconds), layers III/IV and I/II only allowed moderate predictions of the animal's choice. During discrimination, activity in cortical layers I/II and III/IV, however, allowed us to correctly predict the occurrence of correct rejections up to 3 CS-presentations before the animal's reaction. This is particularly pronounced in contrast to false alarm trials. The largest effects were found when comparing hit vs. correct rejections, revealing the accumulating evidence of choice accuracy over the trial duration.

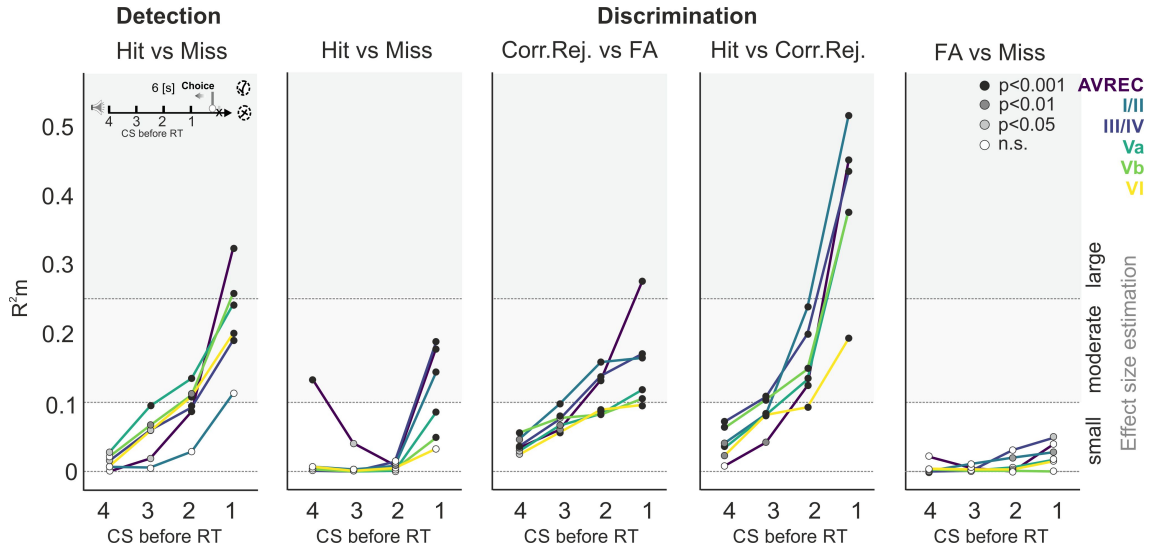

Figure 3.10: Time-resolved GLMM-based effect sizes of behavioral outcomes reflecting accumulating evidence over the trial duration. GLMM-based R^2m values for behavioral choices are plotted for time bins before an animal's reaction (small inset top left). Dashed lines indicate small, moderate and large effect sizes, while the color of circles indicates the corresponding p-value of each GLMM (black: $p<0.001$, dark grey: $p<0.01$, light grey: $p<0.05$ and white: n.s.). We found R^2m values to generally increase over the trial duration until a behavioral choice option was made. During detection, infragranular layers Va - VI showed moderate R2m values even at 2-3 CS+ presentations before the actual response was commuted. Layers III/IV and I/II only allowed moderate predictions of the animal's choice at the CS+ presentation preceding the reaction. During discrimination, the predictability between hits and misses were considerably less pronounced and time-resolved. Activity in cortical layers I/II and III/IV, however, allowed to correctly predict the occurrence of correct rejections of up to 3 CS-presentations before the animal's reaction. Such temporally dispersed evidence was particularly pronounced in upper layers in contrast to false alarm trials. Largest effects were found when comparing hit vs. correct rejection responses revealing the accumulating evidence of choice accuracy over the trial duration. For incorrect decisions, the model showed no change of low predictability over the trial length.

Part II

3.2.7 Cortical recruitment in A1 during the multiple reversals of choice-outcome contingencies

In this section, I illustrate some experimental results related to the multiple reversals of choice-outcome contingencies (Part II: Reversal 1-4). As it is shown in Figure 3.1 subjects showed similar CR-based behaviors across all blocks of reversals. The question then was how the cortical adaptations during those multiple behavioral switches can be investigated. Initially, we compared averaged CSD activity patterns (800ms after the 4th stimulus presentation of both conditioned stimuli) from one representative example animal (n=1). The CSD patterns are placed in a chronological matrix showing the level of performance based on the sensitivity index d' (low to high, x-axis) and the phases of experimental training (early to late reversal phase, y-axis) so that they can be compared in Figure 3.11, a , qualitatively. In all cases clear tone-evoked activation patterns with stable layer indications were observed.

During the early phases of the reversal training, the tone-evoked columnar activity in low performance sessions showed a similar pattern to that of the high performance stage, with only sightly stronger prolonged layer VI sink (Figure 3.11, a, top). If we now turn to the late reversal phases (eg. reversal 4) reduced infragranular (layer VI) activity was observed (Figure 3.11, b, bottom). While there was stable CSD activity between the different levels of performance, supragranular layers I/II appeared to be stronger during later reversals with low performance. One can recognize that in general the CSD profiles are stable and our analysis targets to find out those small difference between conditions. Therefore our approach was to pool the data of all phases of reversals and split them again based on the performance level (d') creating three different subsets: low, medium and high performance. Due to the fact that the pure tones (1 kHz and 4 kHz) were switching their contingencies in each block of reversal, before pooling the data we tested and verified that there is no statistical difference in cortical activity caused by the frequency itself but rather by the contingency and the task-rule (Figure A.5 and Figure A.4).

Following, the three performance level-based pooled data were used for further investi-

gation. The choice-related columnar activity strengths were compared as in the analysis at the subsection 3.2.3. This means that we compared for each of the three subsets (low, medium and high performance) the AVREC RMS values during a 500 ms window beginning of each CS onset testing the dependence of the animals' choice options and the time bins throughout the trial, by a 2-way rmANOVA with the main factors the choice outcome, the tone order and the interaction (with restricted Holm-corrected post-hoc comparisons at each of the CS presentations). For simplification reasons, I demonstrate here the rmANOVA plots only after the 4th CS onset where we found the most prominent effects for the three performance states (Figure 3.11, b). The interpretation does not change by restricting ourselves to the last stimulus as seen in the 2-way rmANOVA in the appendix (Figure A.6).

During sessions with low discrimination performance ($d' < 0$) the evoked AVREC RMS values (z-norm.) during only incorrect responses (miss and false alarm) were significantly different from those induced by correct rejection trials (Low performance - outcome: $F_{3,21}= 30.39$, $p < 0.001$, $\eta^2_{gen}= 0.57$; tone order: $F_{3,84}= 5{,}24$, $p < 0.001$, $\eta^2_{gen}= 0.1$; interaction: $F_{9,84}= 2.57$, $p = 0.001$, $\eta^2_{gen}= 0.14$). Averaged choice-related cortical columnar activity during medium performance stage ($0 < d' < 1$) revealed significant differences between all behavioral choices except of trials where animals showed conditioned responses (hit and false alarm, medium performance - outcome: $F_{3,21}= 76.98$, $p < 0.001$, $\eta^2_{gen}= 0.68$; tone order: $F_{3,84}= 12.04$, $p < 0.001$, $\eta^2_{gen}= 0.23$; interaction: $F_{9,84}= 6.3$, $p < 0.001$, $\eta^2_{gen}= 0.32$). This changed at the state of high discrimination performance ($d' > 1$) where during hit trials, the cortical activation was significantly highest compared to all other classes while correct rejections showed the lowest cortical recruitment (High performance - outcome: $F_{3,21}= 152.41$, $p < 0.001$, $\eta^2_{gen}= 0.86$; tone order: $F_{3,84}= 47.80$, $p < 0.001$, $\eta^2_{gen}= 0.45$; interaction: $F_{9,84}= 28.11$, $p < 0.001$, $\eta^2_{gen}= 0.59$). Now, these results provide even more evidence to the hypothesis of choice-related representation in the A1 which seems to be also related with the level of the engagement to the task. (Table A.8).

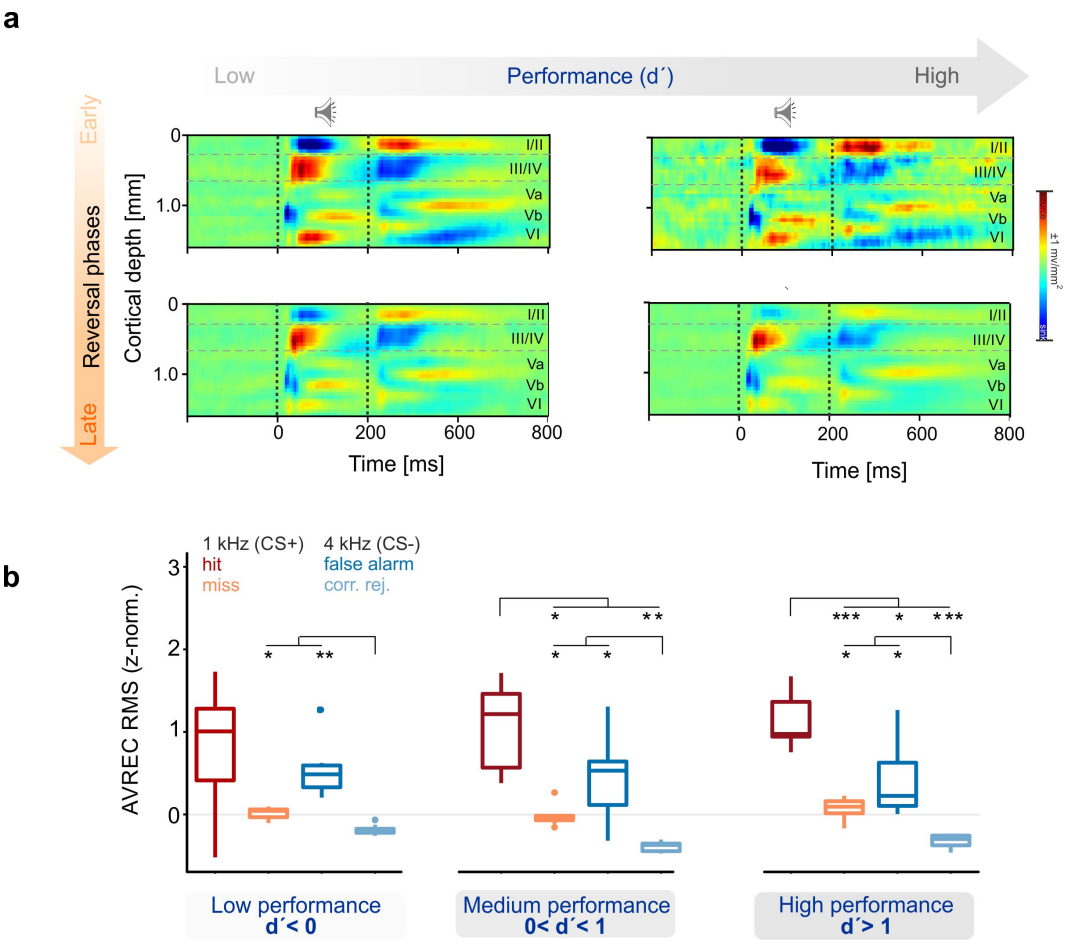

Figure 3.11: Cortical CSD activity during multiple reversal tasks at different performance levels. a. Representative example averaged CSD profiles across all trials of all reversal phases (Reversal 1-4) of one subject (n=1) placed in a matrix of performance level (low or high based on d') and phase of the reversal training (early or late). The CSD patterns show a stable layer-specific activity. The CSD profiles show the tone-evoked activity after the 4th presentation of both conditioned stimuli across multiple sessions and trials with RT $>$ 4.5 s (tone duration: 200 ms; indicated by dashed bars). At early stages of the reversal training evoked CSD patterns show a prolonged layer VI sink and only minor qualitative differences between the performance levels (averaged trials from : top left - early averaged trials with low performance $d' < 1$, top right - high performance $d' > 1$). At later stages of the multiple reversals CSD sink activity was considerably different comparing to the early stages (averaged trials from:bottom left - late low performance $d' < 1$,bottom right - late high performance $d' > 1$). **b.** Averaged AVREC RMS values (500 ms window at the 4th CS onsets) plotted with respect to the behavioral choices (n=8) after pooling the data of all reversal blocks (Reversal 1-4) and split them again based on the sensitivity index d'. In the low performance stage (left: $d' < 0$), only miss and false alarm trials were significant different from the correct rejection trials. During the medium performance stage (middle: $0 < d' < 1$) cortical activity differs significantly across all behavioral choices except of hit versus false alarm trials. When animals perform highly (right: $d' > 1$) cortical activity was strongest during correct hit trials and with a significant difference comparing to all other behavioral choices. Box plots represent median (bar) and interquartile range, and bars represent full range of data. Dots represent outliers. Significant bars indicate differences revealed by a 2-way rmANOVA and corresponding posthoc tests with Holm-corrected levels of significance. The complete (at all the 4 CS onsets) 2-way rmANOVA plots are shown in the appendix (Figure A.6)

3.2.8 Strategy switch and performance level are reflected in layer-specific activity during multiple reversals

In the final part of the analysis, data were investigated according to the procedures described in the subsections 3.2.3 , 3.2.5, and 3.2.6, employing GLMMs to explore the layer-specific adaptations in A1 across different conditions and time points over the course of the trial. All analysis related to the multiple reversal phases were carried out exactly as described above by using GLMM on a single trial level to predict the behavioral choices (binary classes) for the complete cortical column (AVREC RMS) and for each cortical layer separately. The difference here is that the GLMMs were applied three times because of the three different pooled data subsets (low, medium and high performance, as described in subsection 3.2.7). To streamline the major effects of the layer-specific analysis and the cortical plastic changes during the multiple reversal training, I have used only the illustrations of the time-resolved GLMM-based effect sizes of behavioral outcomes at the three levels of discrimination performance (similar to Figure 3.12). Nevertheless, it is important to note that each point at each of the lines presented in the following figures corresponds to one logistic regression curve with the probabilities of the binary choices.

Looking at the three different levels of performance it is obvious that the time-resolved R^2m values for the four behavioral choices increased over the trial duration preceding an animals' reaction (Figure 3.12) providing support to the hypothesis of accumulating evidence over the trial duration. A first striking observation is that during the sessions with low sensitivity index $d' < 0$ (Figure 3.12, a), the infragranular layer VI showed extremely large R^2m (0.35 to 0.8) values even 2–3 CS presentations before the actual response (up to 3–4.5 seconds) when comparing the correct (hit) with the incorrect (miss/false alarm) conditioned responses. Supragranular layers appeared also important to predict the occurrence of the same behavioral choices. Also, only during the low performance stage the other cortical layers allowed large effect predictions even 2 CS presentations before the response (for hit vs miss, correct rejection vs false alarm and hit vs correct rejection). Cortical layers were not able to predict the incorrect behavioral choices (false alarm vs miss).

Next, when animals showed medium discrimination performance with $0 < d' < 1$, a global activation of the cortical column (all layers) allowed us to correctly predict the occurrence of correct rejections up to 3 CS presentations before the animals' reaction. However, the highest was the activity of cortical layers I/II. In general, here the time-resolved GLMM effect sizes showed similar trends as those form the discrimination phase (Figure 3.10).

Finally, it can be seen that again during the high performing stage ($d' > 1$), infragranular layer VI showed large R^2m values only 1 CS presentations before the actual hit responses. Therefore, in highly trained states the R^2m curves showed a steeper slope towards the decision time point (RT). Moreover, largest effects were found for layers I/II when comparing hit vs. correct rejection trials. Interestingly, for the incorrect decisions (false alarm vs miss), the model showed almost no change of low predictability over the trial length at any of the three levels of learning performance. These are important findings in the understanding of the cortical layer-specific synaptic activation patterns during learning, decision-making and choice accuracy.

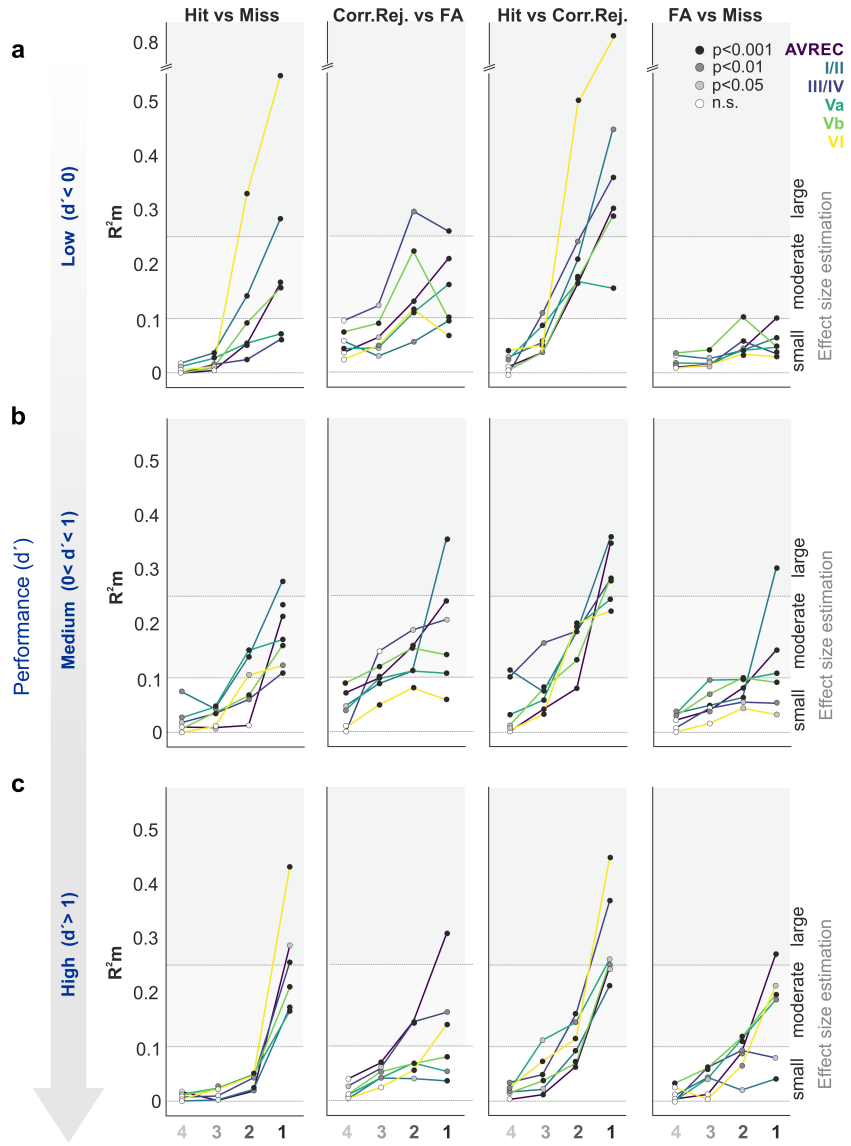

Figure 3.12: Time-resolved GLMM-based effect sizes of behavioral outcomes at the three different performance stages during multiple reversal training. GLMM-based R^2m values for behavioral choices are plotted for time bins before animals reaction (**as described in Figure 3.10**) after pooling the data across all reversal blocks and splitting them according to the three performance levels based on d': **a.** Low performance : layer VI allowed to predict with extremely large R^2m the occurrence of hit responses, **b.** Medium performance: the effect appear similar as those from discrimination phase, and **c.** High performance: layer VI showed large R2m values but smaller than in low performance level at 2-3 CS+ presentations before the actual response was commuted.

4 | Discussion

"We have our strategy in place. A behavior has occurred — one that is reprehensible, or wonderful, or floating ambiguously in between. What occurred in the prior second that triggered the behavior? This is the province of the nervous system. What occurred in the prior seconds to minutes that triggered the nervous system to produce that behavior? This is the world of sensory stimuli, much of it sensed unconsciously."

— Robert Sapolsky[1]

Evolution has enabled organisms to perceive their environments by sensory means. As a consequence, the organisms internally coordinate a range of responses (actions or inactions) to internal and/or external stimuli. The latter is one of the most recent definitions of the term 'behavior' suggested by Levitis et al. (2009). However, defining and understanding the mechanisms underlying behavior has a long history in the fields of philosophy, psychology, ethology, behaviorism, and recently in neuroscience.

Over the past decades, major advances in neuroscience have allowed researchers to combine technologies and discover more about the enigma of behavior. Awareness of the need to look at the brain under the prism of the behavior has been very nicely described by Krakauer et al.. Therefore, examining the brain on microscopic (synapses), mesoscopic (neural circuits) and macroscopic (behavior) level by creating combinatorial experimental protocols will help us to get a holistic interpretation of multiple phenomena related to the behavior (Buzsáki and Christen). One can appreciate that we have now arrived in an era wherein we can explore ethograms in relation to concrete brain activity. In this vein, the overarching goal of my study was to determine how cortical layers contribute to the integrative circuit in the primary auditory cortex (mesoscopic level) in order to code bottom-up and top-down processes (macroscopic level).

[1] From the book "Behave - The biology of humans our best and worst, Chapter 1 - The behavior" Sapolsky

4.1 Combined shuttle-box auditory task with chronic cortical recordings as a tool to study perception and learning

The first question in this study sought to determine whether gerbils are able to readapt their learning behaviors multiple times in a 2-way avoidance auditory Go/NoGo shuttle-box paradigm. The shuttle-box apparatus is well-established and has been used extensively in the past to study animals' behavior on concepts such as detection and categorical discrimination learning, mainly with the aim to better understand the functionality and plasticity of the auditory cortex (Ohl et al., 1999; Wetzel et al., 1998; Weinberger, 1993; Ohl et al., 2001b; Stark et al., 2004; Stark et al., 2008 Deliano et al., 2009b; Happel et al., 2014b).

In those seminal studies the shuttle-box training was combined with various interventions such as lesions, microdialysis, electric mincrostimulation and enzymatic manipulation in order to investigate the role of the A1 in auditory learning. Together, these studies indicate that the A1 plays a crucial role in learning and they provide a great substrate to study even more demanding phenomena, such as reversal learning, decision-making, set shift, and extinction. They also serve to expand our knowledge on the neural correlates of behavioral flexibility. The experimental work presented here provides one of the first shuttle-box long-term protocols (over several weeks) which combines multiple reversals of the choice outcome contingency with parallel *in-vivo* chronic CSD recordings in freely moving gerbils (Happel et al., 2015).

4.1.1 Gerbils are able to discriminate auditory stimuli even after several reversals of choice-outcome contingencies

First, in respect to the behavioral results, learning curves based on the averaged conditioned response rates (Wagner et al., 1989) and the sensitivity index d' (SDT) were used to describe the overall learning progress during the multiple blocks. Additionally, I used the variable *reaction time or response latency* (Figure 3.2) which have been extensively studied as an appropriate variable to interpret behavioral choices and learning progress

in decision making experiments (Young, M.E. & *Crumer, 2006; Donders, 1969). According to those, reaction times decrease with the increase of the performance which is in agreement with what I had observed here (Figure 3.2, c). One of the most interesting findings is that after successful detection of the two pure tone frequencies, gerbils had to abandon their initially learned strategy and 're-associate' one of the two CS with a new meaning during the discrimination phase. This finding was unexpected and suggests that a switch of the task rule caused the animals to completely abandon the previous but still valuable 'knowledge' about parts of the stimulus representation, i.e. the CS which kept the same meaning. Therefore, gerbils had to re-learn a new set of behavioral action-outcome contingencies already from the first task switch (Figure 3.1, Part I).

Similarly, during the multiple reversal tasks, the subjects were re-adapting their learning strategies each time the meaning of the tone was reversed and were finally able to discriminate the two conditioned stimuli (Figure 3.1, Part II). In the beginning of each reversal block — for 1 to 4 initial training sessions — animals were performing poorly and showing a 'perseverative error' (higher false alarm than hit responses) due to previously learned strategies. The phenomenon of 'perseverative error' has been explored broadly in respect to other brain areas (e.g. mediodorsal nuclei of thalamus, striatum, prefrontal cortex, locus coeruleus, and nucleus accumbens core) and certainly under the light of reward systems, dopaminergic, and noradrenergic modulation in a big range of studies from rodents to humans (Block et al., 2007; Waelti et al., 2001; Jarvers et al., 2016; Glennon et al.). Also, Stark et al. (2004) showed that dopamine was increased in the medial prefrontal cortex (mPFC) while gerbils were actively avoiding the aversive stimulus (US, footshock) by initiating a behavior (locomotion) and establishing the avoidance strategy, in a similar shuttle-box Go/NoGo paradigm. It can thus be suggested that the reward signal in the present experiment is the avoidance of the US. Even so, this thesis does not focus on the prediction/perseverative error theories; the established experimental protocol offers the opportunity to further investigate those highly cognitive aspects in the future.

To the best of my knowledge, this is the first study showing that rodents can complete four consecutive reversals. Particularly, in a recent review, Izquierdo et al. (2017) reported a large volume of published studies regarding the neural basis of reversal learning. They

providing evidence on the function of multiple brain circuits of several species during reversal learning. Finally, one must be cautious with the interpretations due to the huge diversity of the modalities, task-designs, brain areas and neuromodolatory systems (Hamilton and Brigman, 2015).

4.1.2 Learning dynamics and strategy adaptations during shuttle-box training

It is interesting to note that after several reversal blocks, the majority of animals followed a more probabilistic strategy by increasing the miss responses (escaping) (Figure 3.2, b) but they still reached the learning performance criterion ($d' = 1$) (Figure 3.1, Figure 3.2) and successfully discriminated between the two pure tones. The reason for the switch to a escaping-like behavior is not clear but it may have something to do with the development of a rapid defensive behavior to the - already known - aversive stimuli and the establishment of an 'economic' way to solve the task (Evans et al., 2018; Evans et al., 2019). Other reasons might be the level of engagement and the sensitization to the aversive stimulus after the long-training protocol.

From the presented data, it can be inferred that the animals were able to reach good discrimination performance in each phase, even after multiple reversals of the choice-outcome contingencies. Nevertheless, the way each animal solves the task and finally reaches our pre-defined learning performance threshold varies from subject to subject. This behavioral variability may be associated with changes in animals ' natural environment (eg. interaction with the experimenter, odors, noises etc.) and the natural tendency to avoid behaviors with high computational effort (Renart and Machens, 2014). Following the trajectories on the ROC strategy planes (Figure 3.3), one can conclude that gerbils show very unique learning strategies and can easily switch them (i.e. from conservative to liberal or from wrong to optimal state etc.). Hence, those findings highlight that animals trained in the exact same tasks in the shuttle-box develop individual learning strategies. One type of learning strategies can have characteristics of an economic and deterministic model, while others can be described as more exploitative and stochastic.

The rationale of this behavioral analysis is to correlate the cognitive and motivational status of the animal from session to session with the recorded cortical activity (data not

shown). This idea reflects that of Berditchevskaia et al. (2015) who also suggest that there are unique motivation levels already within a training session during a Go/NoGo visual task with mice and confirmed by simulations with a new computational model (Motivated Actor-Critic Model). They observed that animals' over-motivation in the beginning of the session was basically driven by Pavlovian mechanisms while at the end of the session a more goal-directed behavior was reported. The optimal performance was noticed during the middle parts of the session, where there was a balance of learning elements (Pavlovian, instrumental and task engagement). Thus, by averaging d' across trials we might underestimate the learning performance of the animals. This view of handling behavioral data on a single-trial level is supported by Deliano et al. (2016), as well. They proposed a random-effects model of the learning process, which consists of multiple stages even in simple tasks and it is based on the estimation of a state-space and history of the trials. Further research on these questions would be a useful way to acquire a full picture of the learning dynamics and the related cortical activity.

4.2 Unraveling the role of the A1 and its integrative function in bottom-up and top-down processes

4.2.1 Beyond tonotopy - Task rule shapes the cortical columnar activity in A1

One of the research questions of this dissertation was to identify if and how the switches in the task rule, for example from detection to discrimination task, impact on the cortical columnar network in A1. Based on the overall columnar AVREC responses, we could show that during discrimination, stimulus-dependent features between Go- and NoGo-stimuli are represented differently as the sound frequency attained a behavioral relevance due to the shift of the task rule.

As expected, it was possible to qualitatively detect some differences between the CSD profiles from several conditions (Figure 3.5,a). The evoked CSD patterns between the two pure-tone stimuli (both CS+) showed no differences during the detection phase. But, when one CS+ switched to CS- (discrimination) considerably different CSD activity was

detected. The observed difference in spatiotemporal current flow was a first, strong hint that the same physical auditory stimulus (4 kHz in this case) involves different cortical circuits when the contingency of that stimulus changes. Further, statistical tests on a group level (AVREC RMS, n=9/8) confirmed our initial hypothesis regarding the stimulus-related activity (Figure 3.5,b). Interestingly, we did not observe any statistical difference merely explained by the tone frequency during detection, which is in line with our qualitative observations.

Based on the existing literature one might argue that the observed effects are due to the tuning properties after training in an auditory task. For example, Guo et al. (2017b) showed that, during sound detection, the A1 tone-evoked responses were enhanced and the tuning was wider. In contrast, the improved discrimination performance was correlated with suppressed A1 responses and sharper frequency tuning. Moreover, the tonotopic map expansion appears to be positively related to the involvement in an auditory behavioral training and to the engagement to the task level (Bao et al., 2004; Carcea et al., 2017b). However, the aforementioned studies investigate the tuning effects on a single-neuron level while we focus on the population mesoscopic network in the present study.

In order to offer other possible explanations, I compared the tuning curves obtained during the passive listening recording sessions before and after each training phase (Figure 2.4, yellow squares). From these measurements, a rather flat frequency tuning (Figure A.2,b) of the dominant early synaptic inputs was observed. In our laboratory we have recently published a study, where we compared CSD-based frequency tunings in the awake A1 and under ketamine anesthesia from animals of the same data set (Deane et al., 2020). The comparison revealed stronger frequency tuning under ketamine anesthesia compared to awake recordings, which might also explain the flat frequency tuning shown in Figure A.2,b. Thus, the findings of this experiment can be explained beyond tonotopic plastic adaptations in A1 (Figure A.1).

In addition, the present results are in line with the opinion from David et al. (2012), who suggested that by keeping identical auditory stimuli and only changing the task rule from an avoidance to a reward structure, the representations in the A1 were differentiated. In my experiment, when the NoGo contingency was introduced for the first time during the discrimination, the task difficulty increased. The task became more aversive (namely,

increased occasions to get the shock, at least during the initial training sessions of each new phase) and the animals had to inhibit their previous jumping behavior. Therefore, it is likely that the differences we observed in the overall CSD cortical activity are related to the changes of task-rule but also to the behavioral inhibition, which promotes states of higher engagement.

This hypothesis seem to be consistent with other research which found that A1 spectrotemporal receptive fields (STRF) in ferrets change in relation to the behavioral performance and increasing task difficulty leads to weaker STRF patterns (Atiani et al., 2009). Furthermore, similar findings were also reported recently by Bagur et al. (2018) by using spike recordings from A1 in a Go/NoGo licking paradigm with ferrets. They showed that task engagement induces a shift in stimulus encoding from sensory to a behaviourally driven representation, which enhances specifically the target stimulus. They concluded that the A1 is important for extracting task relevant information during a behavioral task. Hence, it could conceivably be hypothesised that the observed adaptive changes in CSD cortical recordings are task-related and not only sensory-related.

4.2.2 Supragranular layer activity better classifies the stimulus contingency than the presented tone frequency

There is a growing body of literature that recognises the importance of the A1 in sensory-guided behaviors and learning. However, we still know very little about the association between the layer-specific changes in the A1 during those top-down processes. The majority of previous studies are based on single unit or multi-unit recordings (MUA) (Buran et al., 2014; Bagur et al., 2018; Parras et al., 2017; Pachitariu et al., 2015) which lack the information we get from the chronic cortical depth recordings and the synaptic current flow plastic adaptations. A number of recent studies have begun to examine the role of sensory cortices in learning and decision-making. This can be done either on the level of single and multi-unit recordings (Fritz et al., 2005; Yin et al., 2020) or on a population and layer-specific manner by implementing two-photon imaging techniques (Henschke et al., 2020; Pakan et al., 2018; Francis et al., 2018b). Despite the valuable information we get from those population measurements, these studies have their specific methodological limitations. While unit recordings lack a certain degree of resolution within which specific

layers' activity is measured, two-photon imaging targets mainly the upper cortical layers. Therefore, the present study contributes to fill the gap in better understanding the representation of such task-related information on the level of layer-specific processing in the A1 complementing our knowledge on the multifactorial role of cortical microcircuits during cognitive tasks.

In respect to the main aim of this dissertation, I have applied GLMMs to find out the layer-specific changes while animals perform in the shuttle-box task. The first obvious finding to emerge from the GLMM analysis is that the representation of two different pure tone frequencies is distinguishable on the level of the A1 population activity only if there is the behavioral need to discriminate between stimuli. Thus, the model seems to confirm the findings from the statistical tests of variance (rmANOVA, Figure 3.7). It is necessary at this point to mention the reasons I preferred to use the GLMMs in order to test the relationship of a dependent variable of cortical layer-specific activity with the behavioral outcome of the animal. The corresponding R^2m value of each GLMM model allowed us to evaluate how well the respective synaptic activity can explain the variation in the behavioral outcomes of the animals. With this approach, it is possible to investigate the underlying circuit mechanisms of the relationship between the physiological data and behavioral outcomes by utilizing statistical models. These models help us to evaluate the usefulness of different physiological variables in this prediction (with the R^2m), while accounting for within-animal variability (Bakeman, 2005).

More specifically, during the initial detection phase, the initiation of the active avoidance response was reflected in all cortical layers (Figure 3.8,b - left). The task-irrelevant sound frequency was not differentially represented on a columnar response level (Figure 3.7,b - left). On the other hand, after switching to the more demanding discrimination task employing the same pure tone stimuli, synaptic circuits within mainly granular input layers and supragranular layers reflected the behaviorally observed discriminability between the stimulus classes 'Go' and 'NoGo' (Figure 3.7, Figure 3.8,a). Hence, the task structure affected the columnar representation of auditory information to otherwise identical pure tones. These task-dependent representations emerge as accumulating evidence throughout the trial and are most strongly represented right before a behavioral choice of the animal, based on the reaction time (see Figure 3.6 and Figure 3.10).

By switching to a more cognitively demanding task, e.g. the discrimination phase, the animals needed to re-adapt their strategy and differentially represent the sound frequency of the two conditioned stimuli to successfully perform the task. It is possible, therefore, that spectral integration was behaviorally more important during phases with higher task difficulty (eg. discrimination). Here, it seems that thalamic input layers III/IV and supragranular layers I/II were particularly strongly recruited during trials that led to an active conditioned response. Activity during hits and false alarms was higher compared to misses and correct rejections, respectively. This might reflect the need for more crosscolumnar communication within supragranular layers in order to integrate the spectral content of a presented conditioned stimulus, and its behavioral relevance in auditory-guided action selection (eg. motor initiation) (Happel et al., 2014a; Francis et al., 2018b).

Furthermore, we found that the cortical activity was modulated in supragranular layers well before a behavioral choice was made (Figure 3.10). This observation may support the hypothesis that the representation of stimulus features in the sensory cortex, such as tone frequency in the A1, does not depend only on the transmission process of the sensory information via the primary sensory pathways, but it is significantly modulated by the behavioral need and the behavioral relevance of a stimulus. Data from several other studies suggest that such influence is based on the recurrent circuitry between auditory cortex and higher order top-down regions e.g. parietal and frontal areas (Caras and Sanes, 2017; Polley et al., 2006; Rodgers and DeWeese, 2014; Runyan et al., 2017; Steinmetz et al., 2019; Plakke and Romanski, 2014; Fritz et al.). This might reflect a neuronal basis for auditory response properties of frontal lobe neurons (Romanski and Goldman-Rakic, 2002), its involvement in auditory detection and discrimination (Poremba et al; Zatorre et al., 2004), and fast top-down response modulation of A1 neurons during behavior via the frontal cortex (Winkowski et al., 2018).

4.2.3 Correlates of motor initiation dominate A1 population activity during detection

Most early studies as well as current work suggest an association between motor initiation and other primary sensory cortices depending on region, system, and task-engagement (Steinmetz et al., 2019; Busse et al., 2017). For example, in this recent study *Steinmetz et al.* prove, by using the Neuropixels probe recordings in the mouse brain, that although the responses to sensory stimuli are confined to a restricted sensory pathway, the neural correlates of action initiation are essentially global.

According to the presented data, we can infer that during the detection, the tone-evoked activity in the primary auditory cortex may be modulated by auditory-guided motor initiation. These results support previous research on spiking activity from the A1 area of macaque monkeys which links the motor initiation and sensory-guided behavior in auditory experiments (Huang et al., 2019; Brosch et al., 2015; Niwa et al., 2012). The distinct sound frequency of a pure tone seems less determining on the activity strength. Deep output layer activity (layers Va-VI) showed a significant increase of activity during hit trials. This is in accordance with the findings that neurons in these layers convey information to downstream motor centers, as the basal ganglia or the striatum, which play an important role for the control of motor decisions by the sensory cortex (Znamenskiy and Zador, 2013; Xiong et al., 2015; Ayaz et al., 2019).

Additionally, the selection of an appropriate action might also be conveyed directly to motor cortex via direct anatomical projections (Huang et al., 2019; Matyas et al., 2010). Ample evidence argues that our findings reflect a motor-related modulation of the cortical physiology, rather than a movement artifact. In the described data, auditory cortex activity reflected the initiation of motor actions during detection learning most prominently in deeper layers. Hence, motor-related signals were reflected on a layer-specific level while showing a conserved spatiotemporal profile of the tone-evoked CSD, which is in strong favor of a motor-related modulation of the cortical physiology. A muscle artifact would affect the LFP across all the recording channels in a similar manner. Hence, the reference-free CSD transformation, as the 2nd spatial derivative over the artifact on the LFP level, would be less affected. Nevertheless, we controlled this by a trial-by-trial analysis excluding such trials (Figure 3.5,a).

Moreover, during discrimination the cortical activity was less accurate in predicting motor response initiation but was more accurate in predicting correct choice options (Figure 3.6 and Figure 3.9). Cortical population activity did not differ during false alarm and miss trials. Also, cortical activity was elevated between the consecutively presented CS during hit trials. This argues for an accumulative evidence about the stimulus contingency that the animals kept persistently over the trial, which was instructive for an auditory-guided action (Figure 3.10). Differences between hit and false alarms argue that the motor-related preparatory signal cannot fully explain the variability in our data set. Rather, we find a combinatorial representation of stimulus contingency, task rule, selection accuracy, and motor initiation that accumulates in its richness over the duration of a trial until the actual decision (Figure 3.10).

The question that then naturally arises is whether other movements, such as gerbils' grooming or thumping during task performance, is related with the decision making. An interesting answer to this comes from a recent study on mice using neuropixel recordings, wide-field one photon imaging and video tracking shows that the uninstructed movements or 'fidgets' during a task were better predictors for the trial-by-trial neural variance and dynamics but there was a clear task-related modulation for the stimulus locked time windows (Musall et al.). Finally, this promising line of research approaches would be useful in the future to find out more about the relationship between multiplexed representations in sensory cortices and the motion.

4.2.4 Choice accuracy is represented throughout the cortical column

A recent study by Francis et al. (2018b) suggests that layer II/III activity in mice A1 is highly correlated, not only with sensory processing, but also with the attentional gain and behavioral choices during a tone detection paradigm. By using *in vivo* 2-photon imaging and functional connectivity via Granger causality they were able to show that during the sensory-based decision-making a small clustered neural network was formed in A1 layers II/III. To our knowledge, this is the first study proposing that A1 subnetworks can be modulated separately and contribute to several behavioral aspects (eg.choice accuracy).

In this vein, the current study focuses on the A1 layer-specific subnetworks and their contribution to sensory-guided decision-making. An important finding was that the mod-

ulation of the cortical activity by contingency and motor initiation reflects a cortical correlate of choice accuracy. For example, in the discriminant auditory Go/NoGo-paradigm all cortical layers were more strongly activated during correct hits compared to correct rejections (Figure 3.9 and Figure 3.10). In contrast, the cortical activity recorded in any layer during false alarms and miss responses did not differ. This result now provides evidence that the cortical representation of spectral information during discrimination training (see Figure 3.6) was dependent on the accuracy of the promoted behavior.

In accordance with these findings, previous studies have demonstrated an enhanced representation of target stimuli that initiated an auditory-guided motor response in various Go/NoGo discrimination tasks (Bagur et al., 2018; Gold et al., 1999; Fritz et al., 2003). We found that the cortical activity during correct rejection trials was lower than the activity during other choices. This result ties well with previous studies wherein rats and humans were trained in a Go/NoGo paradigm and lower activity during correct rejections was observed (Nanda et al., 2020; Smith et al., 2008). A possible explanation for this is that cortical activity during those trials might reflect an active inhibition of motor or cognitive responses during a Go/NoGo task. On the other hand, others found higher cortical recruitment during correct rejections compared to hit trials in a Go/NoGo task in the macaque A1 (Huang et al., 2019). This discrepancy could be attributed to the task design, aversive or appetitive reinforcing regimes, or stimulus characteristics (David et al., 2012; Osmanski and Wang, 2015). Further studies, which take these variables into account, will need to be undertaken.

Another relevant aspect to take into account is the temporal relation of the observed effects to the repetitive tone presentation throughout the trial in our task design. The time windows of 500 ms around the consecutively presented CS covered the sensory-dominated columnar response (Figure 3.5,a). The results of that analysis are in accord with other studies indicating that representation of the choice-related activity in the auditory cortex during discrimination of tone events also accumulates until the animal's decision (Niwa et al., 2012; Bizley and Cohen). Further, we have analysed the data for 500-1000 ms after each stimulus presentation so as to separate the relative modulation of cortical layer activity by sensory-driven effects from the task-related, but potentially temporally distributed, information. This additional analysis found evidence for a comparable mod-

ulation of the columnar cortical activity (Figure A.3). From this standpoint, it can be considered that choice accuracy is represented across all cortical layers as accumulating evidence across the entire trial length independent of the stimulus-dominated auditory response.

In order to evaluate how these representations emerge over the trial duration, in agreement with the concept of accumulating evidence in sensory cortex we used a time-resolved analysis based on the GLMMs (Figure 3.10). These results reflect those of Jaramillo and Zador (2011) who found a clear enhancement of activity evoked by stimuli close to a task-relevant moment by using single-unit tetrode recordings from the primary auditory cortex, of behaving rats. In short, it seems that the primary auditory cortex encodes predictions of "what" and "when" sensory events are going to occur and accumulates sensory evidence which lead to a behavioral choice (Jaramillo and Zador, 2011; Tsunada et al., 2015; Bizley and Cohen). A similar conclusion was reached in a computational study by Cone and Shouval (2020). They suggest a layer-specific model for sensory cortices which is able to learn temporal sequences and afterwards increases the corticocortical connections within the same module. Together with these, the presented results provide further support for the hypothesis that there is a multiplexed representation of stimulus- and task-related features distributed across cortical layers.

4.2.5 Cognitive flexibility is correlated with activity in infragranular cortical layers

In a world full of stimuli and rapidly changing environments, cognitive flexibility is a crucial skill for the organisms to shift associations, adapt their behaviors, and survive. In humans, cognitive flexibility is often examined in the context of development and pathology of neurological disorders eg. ADHD (Gelfo, 2019; Dajani and Uddin). Recent advantages in brain imaging techniques (eg. fMRI) allow researchers to design proper experiments in order to study the neural basis of cognitive flexibility (Armbruster et al., 2012).

To asses cognitive flexibility in rodents, reversal learning or attention set-shifting tasks are usually used (Brigman et al.; Nilsson et al.). Although, the reversal learning-related literature has increased in the last years (Talpos and Shoaib, 2015), much uncertainty still ex-

ists about the relationship between a flexible behavior and its neural substrates.

Research to date has associated reversal learning with functions mainly in the prefrontal cortex, the orbitofrontal cortex but also the amygdala and the striatum of rodents (Kesner and Churchwell; Izquierdo et al., 2017; Costa et al., 2015; Hamilton and Brigman, 2015). It has been shown that the A1 is involved in re-associating same physical stimuli with new contingencies (Rothe et al., 2009) and that A1 plasticity is fundamental providing the neural substrate for cognitive flexibility of strategy change (Happel et al., 2014c). However, how the corresponding neuronal circuits of the A1 are actually reflecting the behavioral flexibility during strategy change remains unclear. One purpose of this thesis was to assess the extent to which cortical layers are involved in such highly cognitive behaviors. The presented results go beyond previous reports, showing that during the multiple reversal of choice-outcome contingency task, behavioral choices affect the global cortical recruitment based on the level of discrimination performance. Namely, it is possible that the increasing performance enhances the cortical activity, especially for the correct active responses (hit trials) (Figure 3.11).

What stands out in this analysis is that, from the A1, there emerges a clear layer-specific modulation over the different states of reversal learning (Figure 3.12). During high uncertainty phases (eg. start of each reversal block, $d' < 0$, Figure 3.12, a) with high perseverative error rates, certainly the infragranular layer VI appeared vastly important to predict the occurrence of correct behavioral choices (Hit). Interestingly, layer VI could predict largely the behavioral outcomes even up to 3-4.5 seconds before the CS presentation. A possible explanation for these findings might be that, at this stage of learning, cognitive flexibility is determining because the animals need to inhibit the previous successfully learned strategies.

It is known that neocortical layer VI consists of two distinct patterns of neuronal circuits: the excitatory and the inhibitory (Zhou et al., 2010; Thomson, 2010). *Zhou et al.(2010)* highlight that during conditioning, rodents' layer VI can be strongly inhibitory by activating a feedback loop which consequently initiates the thalamic plasticity. Therefore, it may be hypothesised that the reported strong infragranular activity (layer VI) is related not only with the excitatory circuits, but also with the inhibitory in order to suppress the previous learned motor responses and re-learn the task-rule. It has been demonstrated that frontal dopamine increases during novel learning and strategy estab-

lishment of a Go/NoGo auditory task in the shuttle-box (Stark et al., 2004). Further, it is proved that dopaminergic neurons lay in the deeper cortical layers and electrical stimulation in deeper layers causes enhanced tone detection performance during shuttle-box training (Happel et al., 2014a). Thus, we hypothesize that observed higher infragranualar activity during the low performing state might be related to the dopamine release during predictive coding and high perseverative errors.

Furthermore, during the intermediate level of discriminability in the reversal learning ($0 < d' < 1$, Figure 3.12, b), a more global circuitry activation was observed. Nevertheless, supragranular layers (I/II) were able to predict the occurrence of the behavioral choices with larger effect sizes comparing to other cortical layers. At this stage, animals were re-acquiring the task by increasing their correct responses and reducing the false alarms. Thus, during this 'eureka' moment and re-establishment of a new rule, we observed that cortical circuits in A1 are highly activated. There was a network rearrangement and especially the supragranular layer appeared the strongest in activity even some seconds before a behavioral choice was executed. This finding connects well with the ideas of crosscolumnar communication via supragranular synaptic activation and the corticocortical integrative signals from other high brain areas (eg.mPFC, dPFC), as they are already described in the section 4.2.2, when animals were performing in the first discrimination task (Happel et al., 2014a; Happel, 2016; Francis et al., 2018b; Kato et al.; Rodgers and DeWeese, 2014; Fritz et al.; Berditchevskaia et al.).

Next, at trials with high learning performance ($d' > 1$, Figure 3.12, c) again the infragranular layer VI activity contributes most to the prediction of almost all behavioral choices. It is important to mention that during the low performance stage the infragranular layer activity was highlighted because it was the only layer predicting the behavioral choices and longer before the actual response. In contrast during high discrimination performance sessions, while animals were already engaged to the task, all layers seem to be important in the prediction of hit versus miss trials. Especially, layer VI showed high effect only right before the active response. This observation may support the hypothesis that while animals learned the new rule, there is still the need of layer VI involvement to constantly update the network during predictive coding of the two tone frequencies. At the same time, a global cortical activation with strong supragranular power is required in order to facilitate the choice-accuracy (Hit vs Miss) (Francis et al.,

2018b).

During the reversal phases, gerbils showed a more probabilistic behavioral, reflecting the recent and long-term history of stimulus-specific reinforcement regimes, which led to a generally pronounced avoidance behavior. As final point, we speculate that this phenomenon might be related to this probabilistic behavioral strategy and, hence, the cortical layers in A1 may continuously optimize the discrimination learning (Chéreau et al.). Several reports have shown that there is a bidirectional modulation of A1 sensory representations wherein inhibitory neurons –somatostatin-expressing (SOM) and paralvumin (PV)– are highly involved in auditory-guided learning behaviors (Kato et al.; Aizenberg and Geffen, 2013; Aizenberg et al., 2015). Nevertheless, this is an important issue for future research.

4.3 Conclusion

Previous research and the current study show that neuronal activity in the primary auditory cortex encodes sounds in ways that are directly relevant to behavior (King et al., 2018). The current work has revealed how the specific synaptic circuits across cortical layers in the A1 cooperate on a mesoscopic level to code task-relevant information of the stimulus features, the task rule, and the consequential behavioral choice. One key finding of the present study is that the cortical contribution to auditory-guided decision-making is not only circuit-specific, but also depends on learning. During phases of learning and re-learning, the A1 activity is more involved in the promotion of flexible behaviors. This might help to integrate former studies that often investigated cortical processing during decision-making in highly trained animals (cf. Francis et al., 2018a). Therefore, we can derive a better understanding of the instructive role of the auditory cortex for complex auditory-guided decision-making and learning.

We observed that infragranular layers dominated the cortical processing modes during action selection within a detection context while supragranular layers gained relevance when stimulus features needed to be integrated during discrimination. Moreover, cognitive flexibility was reflected during the multiple contingency reversal of the pure tone stimuli. In such highly cognitive processes, the infragranular layer VI steadily contributes to the optimization of the strategy switches and discrimination performance, while supragranular layers promote the choice accuracy, especially at states with higher task-engagement and performance. Our study thereby expands our understanding of the layer-specific cortical circuit processing modes which code task-relevant information in order to guide sensory-based decision making and behavioral adaptation during strategy change. Future studies will enunciate the more widespread brain networks for mediating perceptual decision making, in which the A1 circuitry reflects only one important hub.

4.4 Perspectives and outlook

This doctoral project was undertaken to design a novel experimental approach, which combines the auditory shuttle-box paradigm with chronic, long-term CSD recordings using the animal model Mongolian gerbil. The ultimate goal of this novel approach was to evaluate how individual cortical layers contribute to the integrative circuit in the sensory auditory cortex (A1) in order to code task-relevant information and guide sensory-based decision making (Happel et al., 2015; Zempeltzi et al., 2020). The present study has gone some way towards enhancing our understanding of the role of the A1 during auditory-guided and cognitively flexible behaviors. The new established experimental pipeline and outcomes of the study open a fruitful area for further work and collaborative projects (Figure 4.1).

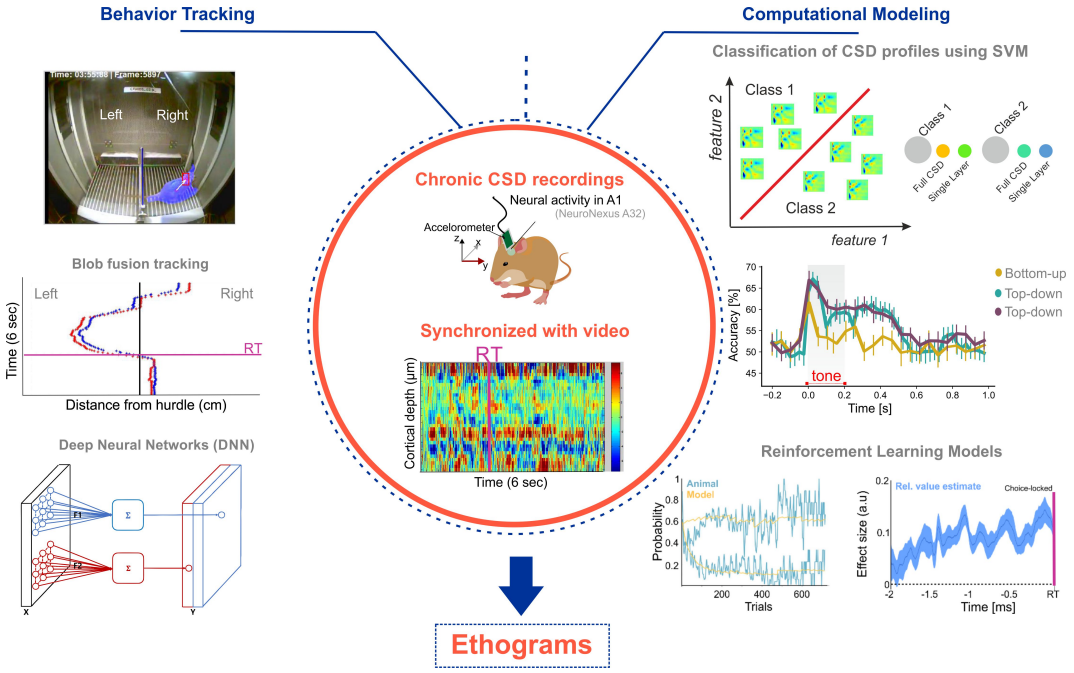

Figure 4.1: Ongoing work and perspectives of the current project. (Convolutional Neural Network clipart source: https://www.hiclipart.com)

These large-scale *in vivo* recordings of neuronal population activity during complex task-designs and decision making provides a large amount of labeled (by the experimenter) data which can be used to run machine learning algorithms, such as linear support vector machines (SVM). In a collaborative project, we have applied linear SVM classifiers to layer-specific, time-binned subsets of CSD data (Figure 4.1, top-right and middle). Targets of the classifiers were reflecting either stimulus-related aspects of au-

ditory processing, or processing of task-dependent information. We could demonstrate significant class separation of distinct layer-specific CSD distributions over time with respect to the presented tone frequency, the learning rule or the ultimate decision made by the animal. The SVM-based information can be used to add more evidence in the hypothesis of a differential representation of auditory stimulus processing *(bottom-up)* and task- and choice-related information *(top-down)* via the synaptic population activity distributed across cortical layers in the A1. In particular, we found that classifiers were most accurate at tone onset with a peak reaching around 80% accuracy. At tone offset (200 ms) 70% accuracy was observed. Additionally, classifiers trained on data from individual layers showed pronounced differences depending the specific *(bottom-up)* and *(top-down)* targets (eg. 'correctness','performance' etc.). Thus, we are able to draw conclusions upon the role of individual cortical layers during learning the auditory task. *[Collaborators: S.Maurya and Prof. Dr. M. Spiliopoulou - Faculty of Computer Science, Otto-von-Guericke University (OvGU), Magdeburg), Maurya*,Zempeltzi* et al. - in preparation.]*

Additionally, according to reinforcement learning theories, goal-directed behavior requires the estimation of the reward expected from a particular stimulus or action. Such value estimates can be identified by the prediction error: the difference between expected reward and reward actually obtained (Schultz et al.). Therefore, more modelling work will have to be conducted in order to evaluate the synaptic patterns representing option values and their temporal dynamics underlying choice. We have now started using a reinforcement learning model developed for human data (Klein et al.) to the layer-specific rodent data. The model is based on a relative value Q-learning algorithm and can be used to model the discrimination behavior of the animals. Further, by using the time-resolved multiple regression with behavioural and CSD data, we will gain more insights about the relative value representation within the auditory cortex and the temporally aligned decision of the animal (Figure 4.1, bottom-right). *[Funding: SFB779, Collaborator: Prof. Dr. G. Jocham - Heinrich Heine University, Düsseldorf]*

Furthermore, a greater focus on the video recordings could produce interesting findings that account more for the individual explorative behaviors within subjects, which results in goal-oriented strategies. By synchronizing the video files with the corresponding electropysiological data will be able to unravel new insights of behavioral influence within the corti-

cal recordings. To achieve this we have established a new pipeline based on video tracking algorithms eg. Blob fusion (Arroyo et al.) for detecting the temporal trajectory of the animal's head and body position on a trial-by-trial manner (Figure 4.1, bottom-left). We are now at the initial stage of visualizing the acquired videos together with the CSD data of each corresponding trial per session. As next, we could integrate signals of an accelerometer (included in NeuroNexus probes) as a qualitative marker of head 3D-movements, e.g. attentional responses. *[Collaborators: B. Auer and M. Brunk - LIN, Magdeburg | project funded by the institutional grant LIN-seeds]*

Next, we envisage the inclusion of deep neural networks for the classification of certain behavior, such as waiting, approaching, and grooming, based on feature extraction (Mathis et al., 2018). Another perspective is to apply the the brand-new algorithm Variational Animal Motion Embedding (VAME) (Luxem et al., 2020) to properly associate ethograms within the corresponding large scale recordings. Another fascinating technique that could be used is the depth imaging to show the 3D animals' pose dynamics structured at the sub-second time-scale (Wiltschko et al.). Altogether, these methods are a new era wherein by identifying individual behavioral strategies we could predict phenotypes caused by genes or neuronal functions. The ultimate diversity of ethologically complex behaviors is of uttermost importance to expand our understanding of individual behavioral decision making and learning strategies in animal models (Baguette et al.). Only then we might be closer to a holistic understanding of the brain mechanisms during behavior or as R. Dawkins vividly describes "the neurophysiologist's nirvana"[2](Gris et al., 2017; Gomez-marin et al., 2014;). *[Collaborators: B. Auer, P. Bauer - LIN, A. Enaya, A. Hashaam, Dr. F. Kramer Farahat - Initos, Magdeburg, Prof. Dr. Stober - OvGU, Magdeburg]*

A natural progression of this work is to establish an 'upgraded' version of the task design, but with the same animal model and type of recordings. In order to increase the complexity in sensory processing, as well as in learning and decision-making, we designed a new paradigm with frequency modulated (FM) tones and sequential blocks of cognitive complex tasks. The upgraded design aims to assess the layer-specific modulations during FM tone discrimination, categorial discrimination, set-shift, reversal and extinction learning, all very central concepts for the discipline (Ohl et al., 2001a; Wetzel et al.,

[2]Dawkins, R. (1976). Hierarchical organisation: A candidate principle for ethology. In Growing Points in Ethology, P. Bateson and R.A. Hinde, eds. (Cambridge University Press), pp. 7–54

1998). The new data-set has been already acquired and it will undergo similar analysis with the one described in this thesis. The major reason of delaying the analysis lies in the fact that the enormous amount of new data (n=10, 75.000 trials) need to be labeled (layer assignment) and then controlled for artifacts on a trial-by-trial level. Till now, this time consuming procedure has been done by the experimenters manually. Only recently we started using deep neural network methods (eg. Autoencoder) to semi-automatize the process, which will allow faster execution of our analysis pipelines. *[Experimenters:S.Aksit - LIN and F.Abela - University of Piza, Italy | Collaborators: A. Faraht, A. Enaya, A. Hashaam, Dr. F. Kramer - Initos, Magdeburg, A. Ofner, Prof. Dr. Stober - OvGU, Magdeburg]*

Finally, to acquire more information on the exact neuromodulatory systems and cellular types during auditory-guided behavior, it would be helpful to make causality interpretations and establish a greater degree of accuracy on the matter. For example, we know from studies in anesthetized gerbils that dopaminergic modulation induced a stimulus specic and layer-dependent phase-resetting in granular input layers, which might be a key step in the recruitment of cortical activity modes interpreting sensory input (Deliano et al., 2018). Also, in an experiment using optogenetic stimulation of the ventral tagmental area (VTA), it is shown that value-related modulation of auditory signal processing in the auditory cortex is relayed via a gain modulation of thalamic inputs in infragranular layers Vb and VIa (Brunk et al., 2019), which subsequently strengthened cross-columnar corticocortical processing via supragranular circuits (Happel et al., 2014a). A key policy to describe the neuromodulation and the precise cortical cellular types would be either via pharmacological, c-fos blocking, or optogenetic manipulations while animals performing in the shuttle-box (de Hoz et al., 2018; Ceballo et al., 2019; Kuchibhotla et al., 2017; Aizenberg et al., 2015).

A | Appendix

A.1 Results - Supplementary information

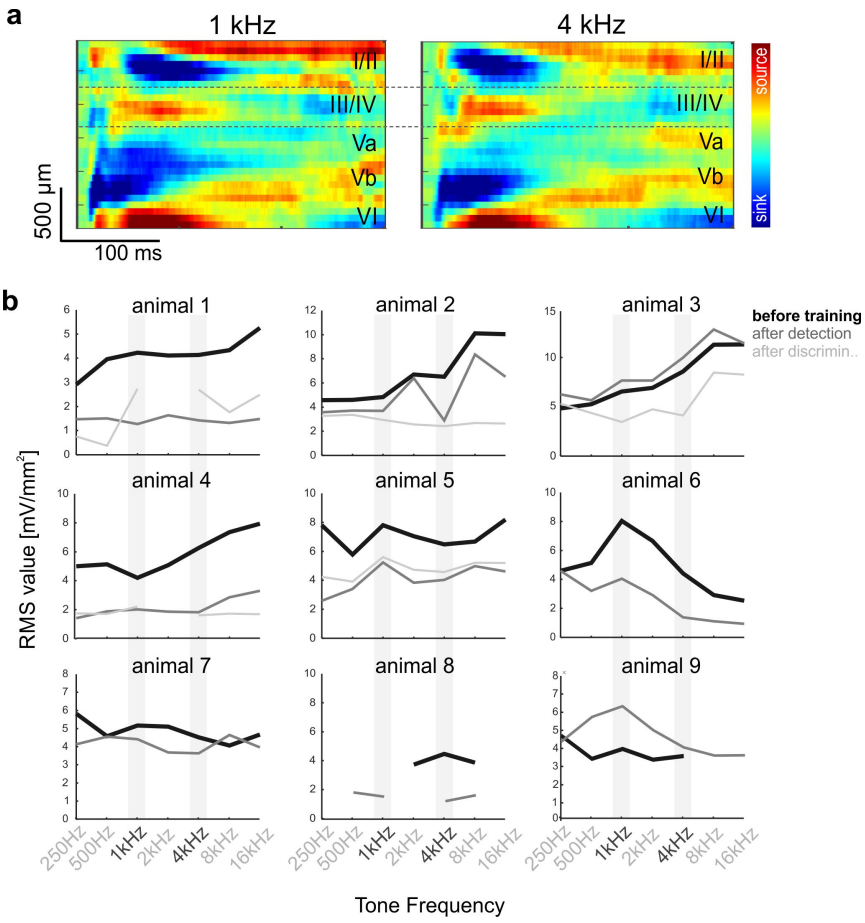

Figure A.1: Characterization of tuning properties in primary auditory cortex in recordings from individual animals. a. Representative example of an averaged CSD profile during the first awake, but passively listening measurement before the actual start of the behavioral training. CSD activity is shown for the two pure tone frequencies also used during the later training, namely 1 kHz (left) and 4 kHz (right; tone duration: 200 ms, ISI 800 ms, 50 pseudorandomized repetitions, sound level 70 dB SPL). **b.** Individual tuning curves of mean CSD RMS values from dominant early synaptic inputs (averaged over 50 trials per frequency) are plotted as a function of stimulation frequency (n=9). We found a generally broad frequency tuning in awake, passively listening subject (cf.**?**). We repeated measuring passively recorded tuning curves after the consecutive detection and discrimination phase (grey curves). Associative training with two pure tone frequencies, hence, did not lead to systematic changes of the general tuning properties.

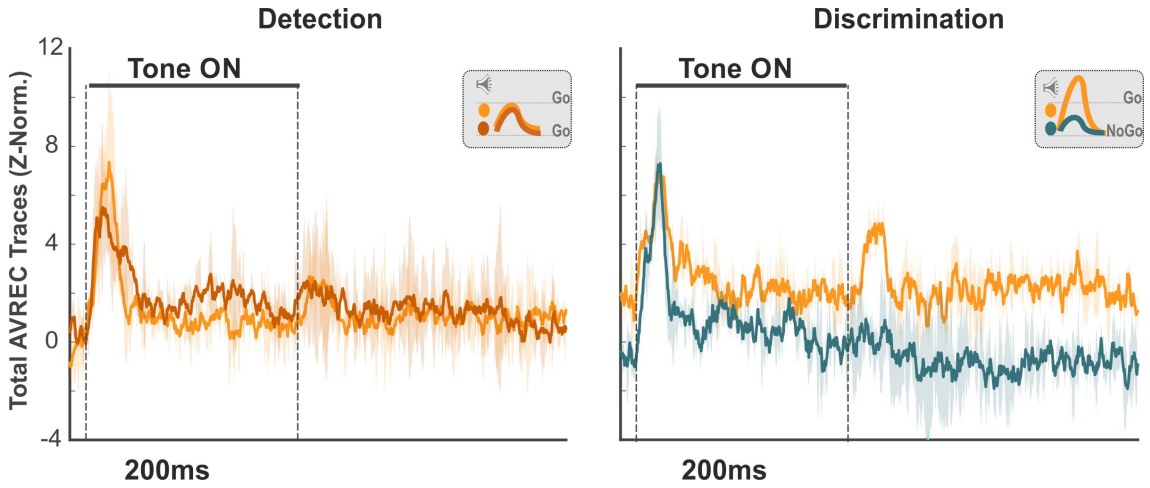

Figure A.2: Representative example of raw AVREC traces for the detection and discrimination phase. Averaged AVREC traces (z-norm.) across all trials of the detection (left) and discrimination (right) phase of the same subject shown in (Figure 3.5,a). The AVREC traces show the activity after the presentation of the two Go-stimuli (1kHz in yellow and 4kHz in brown) during the detection phase (left) and the Go/NoGo stimuli (1kHz in yellow and 4kHz in blue, respectively) during the discrimination phase (right). The shaded error bars indicate the standard error of mean (± s.e.m) of the averaged AVREC traces. The raw traces between the two pure tones frequencies showed no obvious differences during the detection phase, but considerably different activity between CS+ and CS- trials during discrimination. Simplified illustrations of the raw data are shown the grey insets and are used as insets.

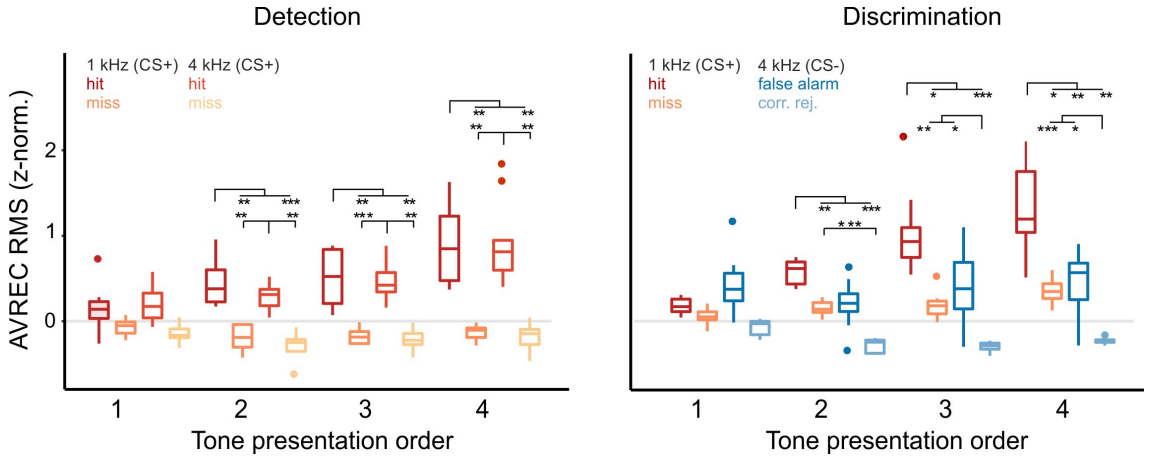

Figure A.3: Behavioral choices and contingency are represented in population activity of the A1 during time windows after the stimulus presentation. Averaged AVREC RMS values (at 500-1000 ms window after CS presentation) plotted with respect to the conditioned stimuli and behavioral choice. Left, During the detection phase evoked activity was significantly higher during hit trials compared to miss trials independent of the stimulation frequency (detection/ discrimination: n=9/8). Right, In the discrimination phase, cortical activity was strongest during correct hit trials and lowest during correct rejections. During trials of incorrect behavioral choices (miss/false alarm) tone-evoked activity was characterized by intermediate amplitudes and did not differ. These results show a very similar pattern with those from Figure 3. Box plots represent median (bar) and interquartile range, and bars represent full range of data. Dots represent outliers. Significant bars indicate differences revealed by a two-way rmANOVA and corresponding post-hoc tests with Holm-corrected levels of significance (see Table A.5)

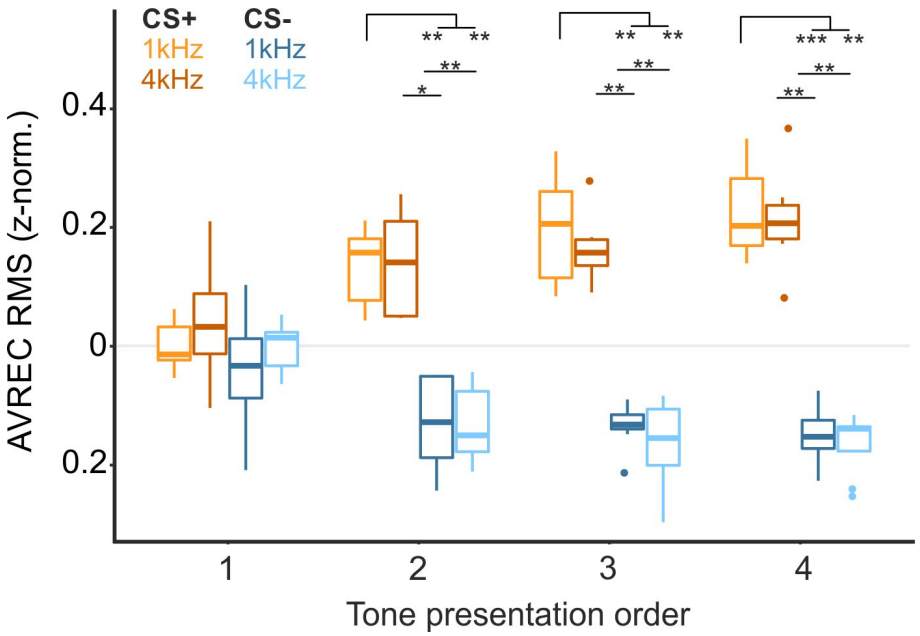

Figure A.4: Contingency is represented in population activity of the A1 during the multiple reversal of choice-outcome contingency. RMS values of the AVREC (time window of 500 ms beginning at each tone presentation and z-normalized) shown for each of the four consecutive CS and separated by the two different tone-frequencies after pooling all Go-trials (yellow-range colors) and all NoGo-trials (blue-range colors) from the reversal phases (reversal 1-4, n=8/7). Box plots represent median (bar) and interquartile range, and bars represent full range of data. Significant bars indicate differences revealed by a two-way rmANOVA and corresponding post-hoc tests with Holm-corrected levels of significance (see Table A.6).

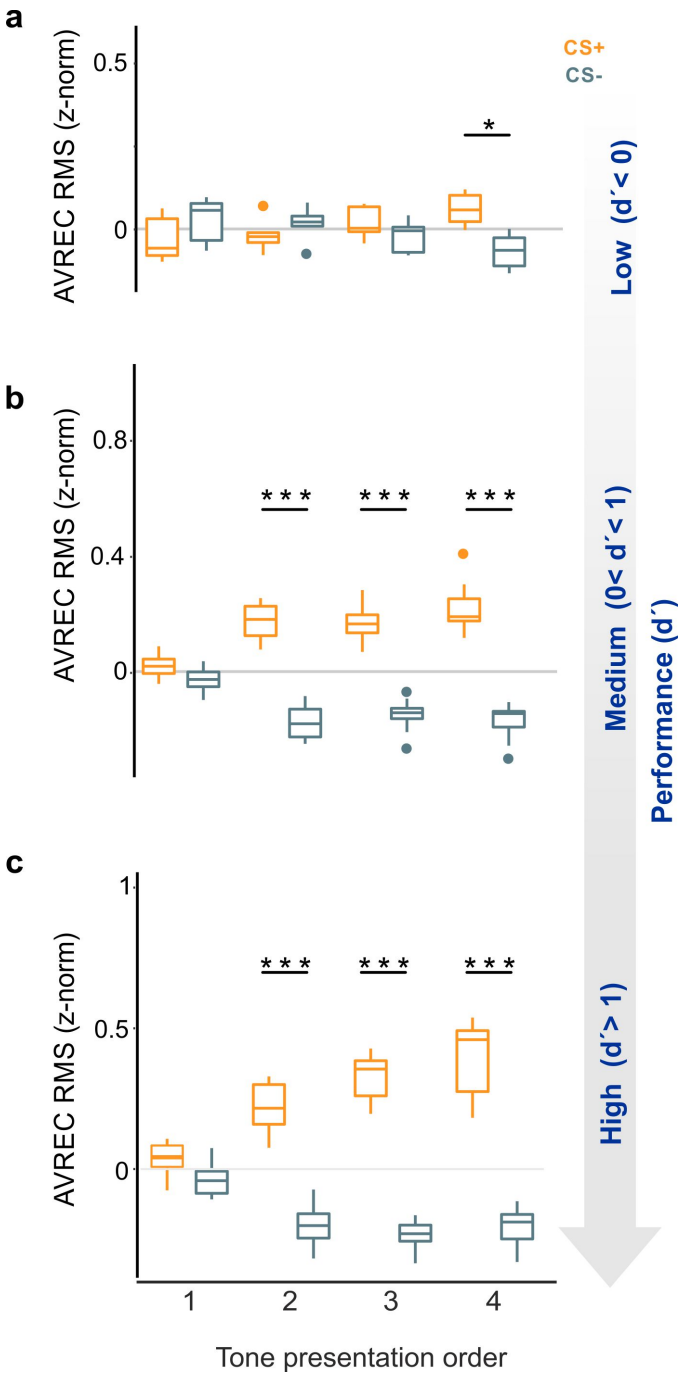

Figure A.5: Contingency-related activity during several performance levels of the reversal learning. RMS values of the AVREC (time window of 500 ms beginning at each tone presentation and z-normalized) shown for each of the four consecutive CS and separated by the different contingencies (CS+ and CS-) during the combined reversal phases(n=8/7) and the performance level based on the d' values. In all cases, cortical activity after the 1st CS presentation remains same irrelevant of the contingency and the the differences emerge during trial duration. **a.** During the low performance stage ($d' < 0$) cortical activity differ slightly between the two contingencies, only after the last CS presentation.**b.** During the medium performance stage ($0 < d' < 1$) cortical activity appeared significant higher at Go trials comparing to the NoGo trials **c.** During the high performance stage ($d' > 1$) cortical activity showed increased amplitudes and remained significantly stronger at Go trials comparing to the NoGo trials. Box plots represent median (bar) and interquartile range, and bars represent full range of data. Significant bars indicate differences revealed by a two-way rmANOVA and corresponding post-hoc tests with Holm-corrected levels of significance (see Table A.7).

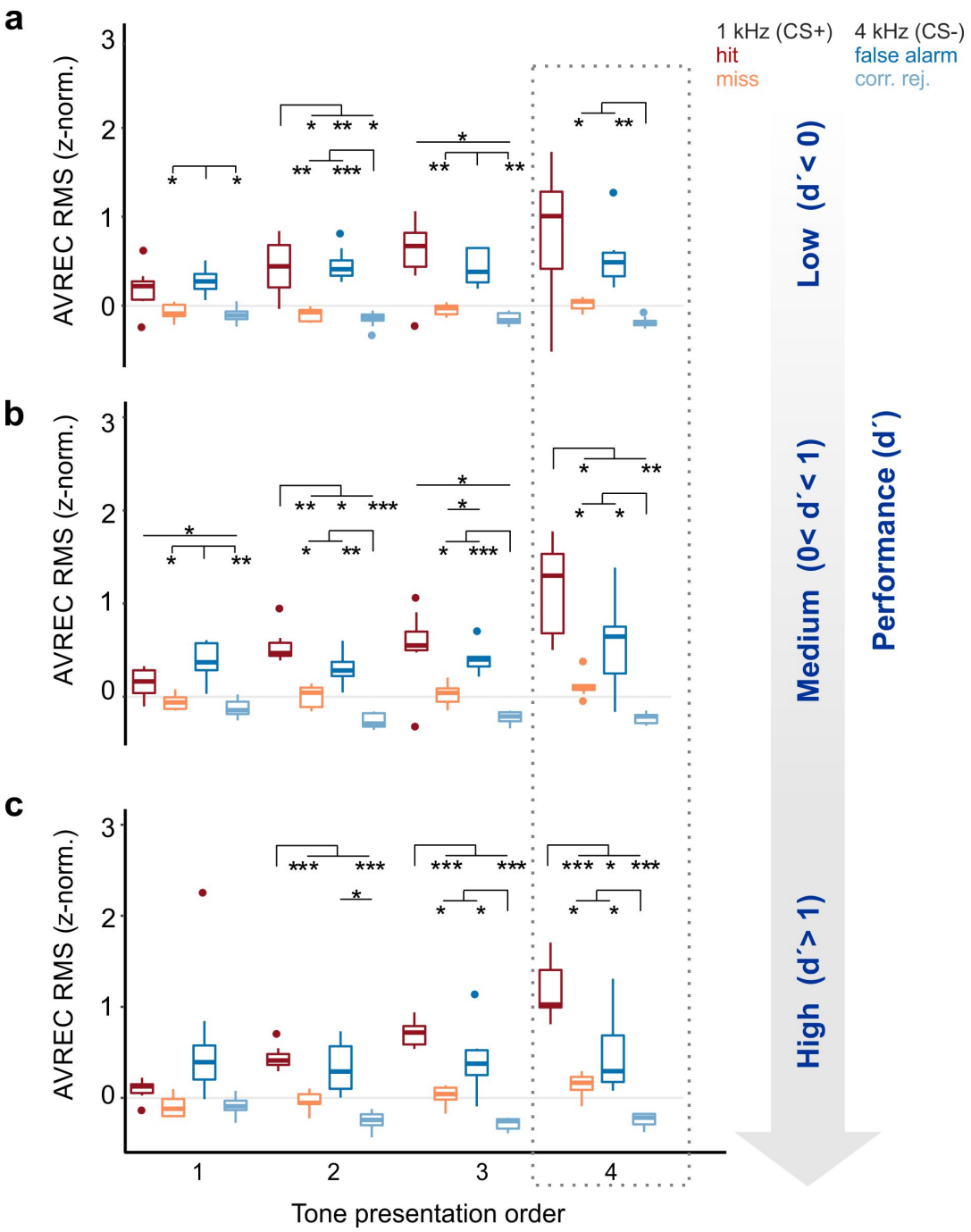

Figure A.6: Representations of behavioral choices in population activity of the A1 during reversal learning at multiple performance levels. Averaged AVREC RMS values (at 0-500 ms window after CS presentation) plotted with respect to the conditioned stimuli and behavioral choice (n=8/7). **a.** During the low performance stage ($d' < 0$) cortical activity was strongest during correct hit trials and lowest during correct rejections. **b.** During the medium performance stage ($0 < d' < 1$) cortical activity was emerging during the trial duration and significant differences were observed within almost all behavioral choices. **c.** During the high performance stage ($d' > 1$) cortical activity was strongest during correct hit trials and lowest during correct rejections. During trials of incorrect behavioral choices (miss/false alarm) tone-evoked activity was characterized by intermediate amplitudes and differ only after the fourth CS presentation. Box plots represent median (bar) and interquartile range, and bars represent full range of data. Dots represent outliers. Significant bars indicate differences revealed by a two-way rmANOVA and corresponding post-hoc tests with Holm-corrected levels of significance (see Table A.8). The dashed-line box indicates the extracted plots used for the (Figure 3.11, b), as a simplified version of the figure.

A.2 Statistical Tables

Choice-related contingencies AVREC RMS (cf. Figure 3.6)			
Detection			
Outcome	$F_{3,24}$= 40.63	$p < 0.001$	η^2_{gen}= 0.66
Tone order	$F_{3,96}$= 26.58	$p < 0.001$	η^2_{gen}= 0.25
Interaction	$F_{9,96}$= 10.05	$p < 0.001$	η^2_{gen}= 0.27
Discrimination			
Outcome	$F_{3,21}$= 31.67	$p < 0.001$	η^2_{gen}= 0.68
Tone order	$F_{3,84}$= 26.39	$p < 0.001$	η^2_{gen}= 0.23
Interaction	$F_{9,84}$= 17.52	$p < 0.001$	η^2_{gen}= 0.38

Table A.1: 2-way from rmANOVA of choice-related contingencies AVREC RMS

GLMM applied to the CS 1 kHz vs 4 kHz (cf. Figure 3.7,b)			
Detection			
Layer I/II	$R^2m = 0$	$R^2c = 0$	$p = 0.549$
Layer III/IV	$R^2m = 0$	$R^2c = 0$	$p = 0.649$
Layer Va	$R^2m = 0$	$R^2c = 0$	$p = 0.703$
Layer Vb	$R^2m = 0$	$R^2c = 0$	$p = 0.836$
Layer VI	$R^2m = 0$	$R^2c = 0$	$p = 0.754$
Discrimination			
Layer I/II	$R^2m = 0.065$	$R^2c = 0.080$	$p < 0.001$
Layer III/IV	$R^2m = 0.121$	$R^2c = 0.219$	$p < 0.001$
Layer Va	$R^2m = 0.095$	$R^2c = 0.175$	$p < 0.001$
Layer Vb	$R^2m = 0.076$	$R^2c = 0.118$	$p < 0.001$
Layer VI	$R^2m = 0.034$	$R^2c = 0.058$	$p = 0.001$

Table A.2: Layer-wise GLMM applied to the conditioned stimuli 1 kHz vs 4 kHz

GLMM applied to the behavioral choices (cf. Figure 3.8,b)			
Detection 'Hit vs Miss'			
Layer I/II	$R^2m = 0.113$	$R^2c = 0.537$	$p < 0.001$
Layer III/IV	$R^2m = 0.190$	$R^2c = 0.406$	$p < 0.001$
Layer Va	$R^2m = 0.242$	$R^2c = 0.512$	$p < 0.001$
Layer Vb	$R^2m = 0.258$	$R^2c = 0.569$	$p < 0.001$
Layer VI	$R^2m = 0.200$	$R^2c = 0.396$	$p < 0.001$
Discrimination 'Hit vs Miss'			
Layer I/II	$R^2m = 0.144$	$R^2c = 0.240$	$p < 0.001$
Layer III/IV	$R^2m = 0.188$	$R^2c = 0.361$	$p = 0.001$
Layer Va	$R^2m = 0.086$	$R^2c = 0.214$	$p = 0.216$
Layer Vb	$R^2m = 0.049$	$R^2c = 0.152$	$p = 0.001$
Layer VI	$R^2m = 0.033$	$R^2c = 0.212$	$p = 0.118$
Discrimination 'False alarm vs Correct Rejection'			
Layer I/II	$R^2m = 0.164$	$R^2c = 0.465$	$p < 0.001$
Layer III/IV	$R^2m = 0.170$	$R^2c = 0.318$	$p < 0.001$
Layer Va	$R^2m = 0.118$	$R^2c = 0.234$	$p < 0.001$
Layer Vb	$R^2m = 0.105$	$R^2c = 0.263$	$p < 0.001$
Layer VI	$R^2m = 0.096$	$R^2c = 0.239$	$p < 0.001$

Table A.3: Layer-wise GLMM applied to the behavioral choices

GLMM applied to the choice accuracy (cf. Figure 3.9,b)			
Discrimination 'Hit vs Correct Rejection'			
Layer I/II	$R^2m = 0.517$	$R^2c = 0.607$	$p < 0.001$
Layer III/IV	$R^2m = 0.435$	$R^2c = 0.573$	$p < 0.001$
Layer Va	$R^2m = 0.380$	$R^2c = 0.509$	$p < 0.001$
Layer Vb	$R^2m = 0.378$	$R^2c = 0.479$	$p < 0.001$
Layer VI	$R^2m = 0.193$	$R^2c = 0.287$	$p < 0.001$
Discrimination 'Miss vs False alarm'			
Layer I/II	$R^2m = 0.028$	$R^2c = 0.184$	$p = 0.004$
Layer III/IV	$R^2m = 0.049$	$R^2c = 0.202$	$p = 0.047$
Layer Va	$R^2m = 0.039$	$R^2c = 0.225$	$p = 0.058$
Layer Vb	$R^2m = 0$	$R^2c = 0.21$	p =0.98
Layer VI	$R^2m = 0.015$	$R^2c = 0.178$	$p = 0.322$

Table A.4: Layer-wise GLMM applied to the choice accuracy

Offset(500-1000ms) choice-related AVREC RMS (cf.Figure A.3			
Detection			
Outcome	$F_{3,24}= 34.95$	$p < 0.001$	$\eta^2_{gen}= 0.60$
Tone order	$F_{3,96}= 18.75$	$p < 0.001$	$\eta^2_{gen}= 0.23$
Interaction	$F_{9,96}= 6.03$	$p < 0.001$	$\eta^2_{gen}= 0.22$
Discrimination			
Outcome	$F_{3,21}= 30.82$	$p < 0.001$	$\eta^2_{gen}= 0.66$
Tone order	$F_{3,84}= 19.88$	$p < 0.001$	$\eta^2_{gen}= 0.21$
Interaction	$F_{9,84}= 10.28$	$p < 0.001$	$\eta^2_{gen}= 0.29$

Table A.5: 2-way from rmANOVA of choice-related contingencies AVREC RMS

Stimulus-related activity during reversal learning (cf. Figure A.4)			
Low performance			
Contingency	$F_{1,7}$= 51.77	p < 0.001	η^2_{gen}= 0,84
Tone order	$F_{3,42}$= 3.13	p = 0.035	η^2_{gen}= 0.04
Interaction	$F_{3,42}$= 90.78	p < 0.001	η^2_{gen}= 0.59

Table A.6: 2-way rmANOVA of stimulus-activity during reversal learning

Contingency-related activity during reversal learning (cf. Figure A.5)			
Low performance			
Contingency	$F_{1,7}$= 0.44	p = 0,524	η^2_{gen}= 0,02
Tone order	$F_{3,42}$= 0.012	p = 0.998	η^2_{gen}= 0.00
Interaction	$F_{3,42}$= 14.88	p < 0.001	η^2_{gen}= 0.36
Medium performance			
Contingency	$F_{1,7}$= 65.16	p < 0.001	η^2_{gen}= 0.83
Tone order	$F_{3,42}$= 1.01	p = 0.396	η^2_{gen}= 0.03
Interaction	$F_{3,42}$= 38.76	p < 0.001	η^2_{gen}= 0.55
High performance			
Contingency	$F_{1,7}$= 64.77	p < 0.001	η^2_{gen}= 0.86
Tone order	$F_{3,42}$= 12.88	p < 0.001	η^2_{gen}= 0.17
Interaction	$F_{3,42}$= 108.10	p < 0.001	η^2_{gen}= 0.63

Table A.7: 2-way rmANOVA of contingency-related activity during reversal learning

Choice-related activity during reversal learning (cf. Figure A.6)			
Low performance			
Outcome	$F_{3,21}$= 30.39	p < 0,001	η^2_{gen}= 0,57
Tone order	$F_{3,84}$= 5.24	p = 0.002	η^2_{gen}= 0.10
Interaction	$F_{9,84}$= 2.57	p = 0.001	η^2_{gen}= 0.14
Medium performance			
Outcome	$F_{3,21}$= 76.98	p < 0.001	η^2_{gen}= 0.68
Tone order	$F_{3,84}$= 12.04	p < 0.001	η^2_{gen}= 0.23
Interaction	$F_{9,84}$= 6.30	p < 0.001	η^2_{gen}= 0.32
High performance			
Outcome	$F_{3,21}$= 62.10	p < 0.001	η^2_{gen}= 0.63
Tone order	$F_{3,84}$= 7.37	p < 0.001	η^2_{gen}= 0.15
Interaction	$F_{9,84}$= 6.82	p < 0.001	η^2_{gen}= 0.34

Table A.8: 2-way rmANOVA of choice-related activity during reversal learning

Bibliography

Aizenberg, M. and Geffen, M. N. (2013). Bidirectional effects of aversive learning on perceptual acuity are mediated by the sensory cortex. *Nature Neuroscience*, 16(8):994–996.

Aizenberg, M., Mwilambwe-Tshilobo, L., Briguglio, J. J., Natan, R. G., and Geffen, M. N. (2015). Bidirectional Regulation of Innate and Learned Behaviors That Rely on Frequency Discrimination by Cortical Inhibitory Neurons. *PLoS Biology*, 13(12):1–32.

Armbruster, D. J., Ueltzhöffer, K., Basten, U., and Fiebach, C. J. (2012). Prefrontal cortical mechanisms underlying individual differences in cognitive flexibility and stability. *Journal of Cognitive Neuroscience*, 24(12):2385–2399.

Arroyo, R., Yebes, J. J., Bergasa, L. M., Daza, I. G., and Almazán, J. Expert video-surveillance system for real-time detection of suspicious behaviors in shopping malls. *Expert Systems with Applications*, 42.

Atiani, S., Elhilali, M., David, S. V., Fritz, J. B., and Shamma, S. A. (2009). Task Difficulty and Performance Induce Diverse Adaptive Patterns in Gain and Shape of Primary Auditory Cortical Receptive Fields. *Neuron*, 61(3):467–480.

Ayaz, A., Stäuble, A., Hamada, M., Wulf, M. A., Saleem, A. B., and Helmchen, F. (2019). Layer-specific integration of locomotion and sensory information in mouse barrel cortex. *Nature Communications*, 10(1):1–14.

Baguette, M., Legrand, D., and Stevens, V. M. An Individual-Centered Framework For Unravelling Genotype-Phenotype Interactions. *Trends in Ecology and Evolution*, (12):709–711.

Bagur, S., Averseng, M., Elgueda, D., David, S., Fritz, J., Yin, P., Shamma, S., Boubenec, Y., and Ostojic, S. (2018). Go/No-Go task engagement enhances population representation of target stimuli in primary auditory cortex. *Nature Communications*, 9(1).

Bakeman, R. (2005). Recommended Effect Size Statistic. *Behavior Research Methods*, 37(3):379–384.

Bandyopadhyay, S., Shamma, S. A., and Kanold, P. O. (2010). Dichotomy of functional organization in the mouse auditory cortex. *Nature Neuroscience*, 13(3):361–368.

Bao, S., Chang, E. F., Woods, J., and Merzenich, M. M. (2004). Temporal plasticity in the primary auditory cortex induced by operant perceptual learning. 7(9):974–981.

Barton, K. (2019). MuMIn: Multi-Model Inference, Version 1.43.6. (1):1–75.

Berditchevskaia, A., Cazé, R. D., and Schultz, S. R. Performance in a GO/NOGO perceptual task reflects a balance between impulsive and instrumental components of behaviour. *Scientific Reports*, (August 2015):1–15.

Bizley, J. K. and Cohen, Y. E. The what, where and how of auditory-object perception. *Nature Reviews Neuroscience*, (10):693–707.

Bizley, J. K. and Cohen, Y. E. (2013). The what, where and how of auditory-object perception. *Nature Reviews Neuroscience*, 14(10):693–707.

Block, A. E., Dhanji, H., Thompson-Tardif, S. F., and Floresco, S. B. (2007). Thalamic-prefrontal cortical-ventral striatal circuitry mediates dissociable components of strategy set shifting. *Cerebral Cortex*, 17(7):1625–1636.

Brigman, J. L., Powell, E. M., Mittleman, G., and Young, J. W. Examining the genetic and neural components of cognitive flexibility using mice. *Physiology and Behavior*, (5):666–669.

Brosch, M., Selezneva, E., and Scheich, H. (2005). Nonauditory events of a behavioral procedure activate auditory cortex of highly trained monkeys. *Journal of Neuroscience*, 25(29):6797–6806.

Brosch, M., Selezneva, E., and Scheich, H. (2015). Neuronal activity in primate auditory cortex during the performance of audiovisual tasks. *European Journal of Neuroscience*, 41(5):603–614.

Brunk, M. G., Deane, K. E., Kisse, M., Deliano, M., Vieweg, S., Ohl, F. W., Lippert, M. T., and Happel, M. F. (2019). Optogenetic stimulation of the VTA modulates a frequency-specific gain of thalamocortical inputs in infragranular layers of the auditory cortex. *Scientific Reports*, 9(1):1–15.

Budinger, E. and Kanold, P. O. (2018). *Auditory Cortex Circuits*.

Buran, B. N., Trapp, G. V., Sanes, D. H., von Trapp, G., Sanes, D. H., Trapp, G. V., and Sanes, D. H. (2014). Behaviorally gated reduction of spontaneous discharge can improve detection thresholds in auditory cortex. *Journal of Neuroscience*, 34(11):4076–4081.

Busse, L., Cardin, J. A., Chiappe, M. E., Halassa, M. M., McGinley, M. J., Yamashita, T., and Saleem, A. B. (2017). Sensation during active behaviors. *Journal of Neuroscience*, 37(45):10826–10834.

Buzsáki, G. and Christen, Y. *Micro-, Meso- and Macro-Dynamics of the Brain*. Research and Perspectives in Neurosciences.

Carandini, M. and Churchland, A. K. (2013). Probing perceptual decisions in rodents. *Nature neuroscience*, 16(7):824–31.

Caras, M. L. and Sanes, D. H. (2017). Top-down modulation of sensory cortex gates perceptual learning. *Proceedings of the National Academy of Sciences of the United States of America*, 114(37):9972–9977.

Carcea, I., Insanally, M. N., and Froemke, R. C. (2017a). Dynamics of auditory cortical activity during behavioural engagement and auditory perception. *Nature Communications*, 8:1–12.

Carcea, I., Insanally, M. N., and Froemke, R. C. (2017b). Dynamics of auditory cortical activity during behavioural engagement and auditory perception. *Nature Communications*, 8:1–12.

Castro, J. B. and Kandler, K. (2010). Changing tune in auditory cortex. *Nature Neuroscience*, 13(3):271–273.

Ceballo, S., Piwkowska, Z., Bourg, J., Daret, A., and Bathellier, B. (2019). Targeted Cortical Manipulation of Auditory Perception. *Neuron*, 104(6):1168–1179.e5.

Chang, A., Bosnyak, D. J., and Trainor, L. J. (2018). Beta oscillatory power modulation reflects the predictability of pitch change. *Cortex*, 106(May 2019):248–260.

Chéreau, R., Bawa, T., Fodoulian, L., Carleton, A., Pagès, S., and Holtmaat, A. Dynamic encoding of perceptual features in primary somatosensory cortex upon reversal learning. *bioRxiv*, page 782847.

Cone, I. and Shouval, H. Z. (2020). Learning precise spatiotemporal sequences via biophysically realistic circuits with modular structure.

Costa, V. D., Tran, V. L., Turchi, J., and Averbeck, B. B. (2015). Reversal learning and

dopamine: A Bayesian perspective. *Journal of Neuroscience*, 35(6):2407–2416.

Cutler, M. G. and Mackintosh, J. H. (1989). Epilepsy and behaviour of the Mongolian gerbil: An ethological study. *Physiology and Behavior*, 46(4):561–566.

Dajani, D. R. and Uddin, L. Q. Demystifying cognitive flexibility: Implications for clinical and developmental neuroscience. *Trends in Neurosciences*, (9):571–578.

David, S. V., Fritz, J. B., and Shamma, S. A. (2012). Task reward structure shapes rapid receptive field plasticity in auditory cortex. *Proceedings of the National Academy of Sciences of the United States of America*, 109(6):2144–2149.

de Hoz, L., Gierej, D., Lioudyno, V., Jaworski, J., Blazejczyk, M., Cruces-Solís, H., Beroun, A., Lebitko, T., Nikolaev, T., Knapska, E., Nelken, I., and Kaczmarek, L. (2018). Blocking c-Fos Expression Reveals the Role of Auditory Cortex Plasticity in Sound Frequency Discrimination Learning. *Cerebral cortex (New York, N.Y. : 1991)*, 28(5):1645–1655.

Deane, K. E., Brunk, M. G. K., Curran, A. W., Zempeltzi, M. M., Ma, J., Lin, X., Abela, F., Aksit, S., Deliano, M., Ohl, F. W., and Happel, M. F. K. (2020). Ketamine anesthesia induces gain enhancement via recurrent excitation in granular input layers of the auditory cortex. *The Journal of Physiology*, 0:1–15.

Deike, S., Heil, P., Böckmann-Barthel, M., and Brechmann, A. (2015). Decision making and ambiguity in auditory stream segregation. *Frontiers in Neuroscience*, 9(JUL):1–6.

Deliano, M., Brunk, M. G., El-Tabbal, M., Zempeltzi, M. M., Happel, M. F., and Ohl, F. W. (2018). Dopaminergic neuromodulation of high gamma stimulus phase-locking in gerbil primary auditory cortex mediated by D1/D5-receptors. *European Journal of Neuroscience*, 51(June 2017):1315–1327.

Deliano, M., Scheich, H., and Ohl, F. W. (2009a). Auditory cortical activity after intracortical microstimulation and its role for sensory processing and learning. *Journal of Neuroscience*, 29(50):15898–15909.

Deliano, M., Scheich, H., and Ohl, F. W. (2009b). Auditory cortical activity after intracortical microstimulation and its role for sensory processing and learning. *The Journal of neuroscience : the official journal of the Society for Neuroscience*, 29(50):15898–15909.

Deliano, M., Tabelow, K., König, R., and Polzehl, J. (2016). Improving accuracy and temporal resolution of learning curve estimation for within- and across-session analysis.

PLoS ONE, 11(6):1–23.

Donders, F. C. (1969). On the speed of mental processes. *Acta Psychologica*, 30(C):412–431.

Einevoll, G. T., Kayser, C., Logothetis, N. K., and Panzeri, S. (2013). Modelling and analysis of local field potentials for studying the function of cortical circuits. *Nature Reviews Neuroscience*, 14(11):770–785.

Evans, D. A., Stempel, A. V., Vale, R., and Branco, T. (2019). Cognitive Control of Escape Behaviour. *Trends in Cognitive Sciences*, 23(4):334–348.

Evans, D. A., Stempel, A. V., Vale, R., Ruehle, S., Lefler, Y., and Branco, T. (2018). escape decisions.

Fawcett, T. An introduction to roc analysis. *Pattern Recognition Letters*, (8):861–874.

Fishman, Y. I., Steinschneider, M., Micheyl, C., and Micheyl, C. (2014). Neural representation of concurrent harmonic sounds in monkey primary auditory cortex: implications for models of auditory scene analysis. *Journal of Neuroscience*, 34(37):12425–12443.

Francis, N. A., Elgueda, D., Englitz, B., Fritz, J. B., and Shamma, S. A. (2018a). Laminar profile of task-related plasticity in ferret primary auditory cortex. *Scientific Reports*, 8(1):1–10.

Francis, N. A., Winkowski, D. E., Sheikhattar, A., Armengol, K., Babadi, B., and Kanold, P. O. (2018b). Small Networks Encode Decision-Making in Primary Auditory Cortex. *Neuron*, 97(4):885–897.

Freeman, A. and Nicholson, C. (1975). Experimental optimization of Current Source-Density Thechnique for Anuran Cerebellum.

Frégnac, Y., Bathellier, B., and Fre, Y. (2015). Cortical Correlates of Low-Level Perception: From Neural Circuits to Percepts. *Neuron*, 88(1):110–126.

Fritz, J., Elhilali, M., and Shamma, S. (2005). Active listening: Task-dependent plasticity of spectrotemporal receptive fields in primary auditory cortex. *Hearing Research*, 206(1-2):159–176.

Fritz, J., Shamma, S., Elhilali, M., and Klein, D. (2003). Rapid task-related plasticity of spectrotemporal receptive fields in primary auditory cortex. *Nature Neuroscience*, 6(11):1216–1223.

Fritz, J. B., David, S. V., Radtke-Schuller, S., Yin, P., and Shamma, S. A. Adaptive,

behaviorally gated, persistent encoding of task-relevant auditory information in ferret frontal cortex. *Nature Neuroscience*, (8):1011–1019.

Gelfo, F. (2019). Does experience enhance cognitive flexibility? An overview of the evidence provided by the environmental enrichment studies. *Frontiers in Behavioral Neuroscience*, 13(July).

Gerd, S. R.-s. and Frank, S. (2016). Brain atlas of the Mongolian gerbil (Meriones unguiculatus) in CT / MRI-aided stereotaxic coordinates.

Geva-Sagiv, M., Las, L., Yovel, Y., and Ulanovsky, N. (2015). Spatial cognition in bats and rats: From sensory acquisition to multiscale maps and navigation. *Nature Reviews Neuroscience*, 16(2):94–108.

Givre, S. J., Schroeder, C. E., and Arezzo, J. C. (1994). Contribution of extrastriate area V4 to the surface-recorded flash VEP in the awake macaque. *Vision Research*, 34(4):415–428.

Glennon, E., Carcea, I., Martins, A. R. O., Multani, J., Shehu, I., Svirsky, M. A., and Froemke, R. C. Locus coeruleus activation accelerates perceptual learning. *Brain Research*, pages 39–49.

Gold, J., Bennett, P. J., and Sekuler, A. B. (1999). Signal but not noise changes with perceptual learning. *Nature*, 402(6758):176–178.

Gomez-marin, A., Paton, J. J., Kampff, A. R., Costa, R. M., and Mainen, Z. F. (2014). Big behavioral data : psychology , ethology and the foundations of neuroscience. 17(11):1455–1462.

Green, D. M. and Swets, J. A. (1966). *Signal Detection Theory and Psychophysics*. Wiley, New York.

Gris, K. V., Coutu, J.-P., and Gris, D. (2017). Supervised and Unsupervised Learning Technology in the Study of Rodent Behavior. *Frontiers in Behavioral Neuroscience*, 11(July):1–6.

Guo, L., Ponvert, N. D., and Jaramillo, S. (2017a). The role of sensory cortex in behavioral flexibility. *Neuroscience*, 345:3–11.

Guo, W., Clause, A. R., Barth-Maron, A., and Polley, D. B. (2017b). A Corticothalamic Circuit for Dynamic Switching between Feature Detection and Discrimination. *Neuron*, 95(1):180–194.

Hackett, T. A., Barkat, T. R., O'Brien, B. M., Hensch, T. K., and Polley, D. B. (2011). Linking topography to tonotopy in the mouse auditory thalamocortical circuit. *Journal of Neuroscience*, 31(8):2983–2995.

Hamilton, D. A. and Brigman, J. L. (2015). Behavioral flexibility in rats and mice: Contributions of distinct frontocortical regions. *Genes, Brain and Behavior*, 14(1):4–21.

Happel, M. F. (2016). Dopaminergic impact on local and global cortical circuit processing during learning. *Behavioural brain research*, 299:32–41.

Happel, M. F., Deliano, M., and Ohl, F. W. (2015). Combined Shuttle-Box Training with Electrophysiological Cortex Recording and Stimulation as a Tool to Study Perception and Learning. *Journal of Visualized Experiments*, 2015(104):1–9.

Happel, M. F., Jeschke, M., and Ohl, F. W. (2010a). Spectral integration in primary auditory cortex attributable to temporally precise convergence of thalamocortical and intracortical input. *Journal of Neuroscience*, 30(33):11114–11127.

Happel, M. F. K., Deliano, M., Handschuh, J., and Ohl, F. W. (2014a). Dopamine-Modulated Recurrent Corticoefferent Feedback in Primary Sensory Cortex Promotes Detection of Behaviorally Relevant Stimuli. 34(4):1234–1247.

Happel, M. F. K., Deliano, M., Handschuh, J., and Ohl, F. W. (2014b). Dopamine-Modulated Recurrent Corticoefferent Feedback in Primary Sensory Cortex Promotes Detection of Behaviorally Relevant Stimuli. *Journal of Neuroscience*, 34(4):1234–1247.

Happel, M. F. K., Jeschke, M., and Ohl, F. W. (2010b). Spectral Integration in Primary Auditory Cortex Attributable to Temporally Precise Convergence of Thalamocortical and Intracortical Input. *Journal of Neuroscience*, 30(33):11114–11127.

Happel, M. F. K., Niekisch, H., Castiblanco Rivera, L. L., Ohl, F. W., Deliano, M., and Frischknecht, R. (2014c). Enhanced cognitive flexibility in reversal learning induced by removal of the extracellular matrix in auditory cortex. *Proceedings of the National Academy of Sciences of the United States of America*, 111:2800–5.

Haueis, P. (2016). The life of the cortical column: opening the domain of functional architecture of the cortex (1955–1981). *History and Philosophy of the Life Sciences*, 38(3):1–27.

Hawkins, J., Ahmad, S., and Cui, Y. (2017). A theory of how columns in the neocortex

enable learning the structure of the world. *Frontiers in Neural Circuits*, 11(October):1–18.

He, J. (1997). Modulatory effects of regional cortical activation on the onset responses of the cat medial geniculate neurons. *Journal of Neurophysiology*, 77(2):896–908.

Hechavarría, J. C., Macías, S., Vater, M., Voss, C., Mora, E. C., and Kössl, M. (2013). Blurry topography for precise target-distance computations in the auditory cortex of echolocating bats. *Nature Communications*, 4:1–11.

Henschke, J. U., Dylda, E., Katsanevaki, D., Dupuy, N., Currie, S. P., Amvrosiadis, T., Pakan, J. M., and Rochefort, N. L. (2020). Reward Association Enhances Stimulus-Specific Representations in Primary Visual Cortex. *Current Biology*, 30(10):1866–1880.e5.

Hickmott, P. W. and Merzenich, M. M. (1998). Single-cell correlates of a representational boundary in rat somatosensory cortex. *Journal of Neuroscience*, 18(11):4403–4416.

Holm, S. (1979). A simple rejective test procedure. *Scandinavian Journal of Statistics*, 6(2):65–70.

Homma, N. Y., Happel, M. F., Nodal, F. R., Ohl, F. W., King, A. J., and Bajo, V. M. (2017). A Role for Auditory Corticothalamic Feedback in the Perception of Complex Sounds. *The Journal of Neuroscience*, 37(25):6149–6161.

Huang, Y., Heil, P., and Brosch, M. (2019). Associations between sounds and actions in early auditory cortex of nonhuman primates. *eLife*, 8:1–22.

Hurtado-Parrado, C., González, C. H., Moreno, L. M., González, C. A., Arias, M., Beltrán, L., and Cardona, S. (2015). Catalogue of the behaviour of Meriones unguiculatus f. dom. (Mongolian gerbil) and wild conspecies, in captivity and under natural conditions, based on a systematic literature review. *Journal of Ethology*, 33(2):65–86.

Izquierdo, A., Brigman, J. L., Radke, A. K., Rudebeck, P. H., and Holmes, A. (2017). The neural basis of reversal learning: An updated perspective. *Neuroscience*, 345(March):12–26.

Jaramillo, S. and Zador, A. M. (2011). The auditory cortex mediates the perceptual effects of acoustic temporal expectation. *Nature Neuroscience*, 14(2):246–253.

Jarvers, C., Brosch, T., Brechmann, A., Woldeit, M. L., Schulz, A. L., Ohl, F. W., Lommerzheim, M., and Neumann, H. (2016). Reversal learning in humans and gerbils:

Dynamic control network facilitates learning. *Frontiers in Neuroscience*, 10(NOV):1–17.

Kajikawa, Y. and Schroeder, C. E. (2011). How local is the local field potential? *Neuron*, 72(5):847–858.

Kamarajan, C., Pandey, A. K., Chorlian, D. B., and Porjesz, B. (2015). The use of current source density as electrophysiological correlates in neuropsychiatric disorders: A review of human studies. *International journal of psychophysiology : official journal of the International Organization of Psychophysiology*, 97(3):310–22.

Kato, H. K., Gillet, S. N., Isaacson, J. S., Kato, H. K., Gillet, S. N., and Isaacson, J. S. Flexible Sensory Representations in Auditory Cortex Driven by Behavioral Relevance Article Flexible Sensory Representations in Auditory Cortex Driven by Behavioral Relevance. *Neuron*, (5):1027–1039.

Kesner, R. P. and Churchwell, J. C. An analysis of rat prefrontal cortex in mediating executive function. *Neurobiology of Learning and Memory*, (3):417–431.

King, A. J., Teki, S., and Willmore, B. D. (2018). Recent advances in understanding the auditory cortex. *F1000Research*, 7(0):1555.

Klein, T. A., Ullsperger, M., and Jocham, G. Learning relative values in the striatum induces violations of normative decision making. *Nature Communications*, (May 2016):1–12.

Kössl, M., Voss, C., Mora, E. C., MacIas, S., Foeller, E., and Vater, M. (2012). Auditory cortex of newborn bats is prewired for echolocation. *Nature Communications*, 3.

Krakauer, J. W., Ghazanfar, A. A., Gomez-Marin, A., MacIver, M. A., and Poeppel, D. Neuroscience Needs Behavior: Correcting a Reductionist Bias. *Neuron*, (3):480–490.

Krypotos, A. M., Effting, M., Kindt, M., and Beckers, T.

Kuchibhotla, K. V., Gill, J. V., Lindsay, G. W., Papadoyannis, E. S., Field, R. E., Sten, T. A., Miller, K. D., and Froemke, R. C. (2017). Parallel processing by cortical inhibition enables context-dependent behavior. *Nature Neuroscience*, 20(1):62–71.

Lakatos, P., Shah, A. S., Knuth, K. H., Ulbert, I., Karmos, G., and Schroeder, C. E. (2005). An oscillatory hierarchy controlling neuronal excitability and stimulus processing in the auditory cortex. *Journal of Neurophysiology*, 94(3):1904–1911.

Levitis, D. A., Lidicker, W. Z., and Freund, G. (2009). Behavioural biologists do not agree on what constitutes behaviour. *Animal Behaviour*, 78(1):103–110.

Li, L. Y., Ji, X. Y., Liang, F., Li, Y. T., Xiao, Z., Tao, H. W., and Zhang, L. I. (2014). A feedforward inhibitory circuit mediates lateral refinement of sensory representation in upper layer 2/3 of mouse primary auditory cortex. *Journal of Neuroscience*, 34(41):13670–13683.

Luxem, K., Fuhrmann, F., Kuersch, J., Remy, S., and Bauer, P. (2020). Identifying behavioral structure from deep variational embeddings of animal motion. *bioRxiv*.

Markram, H., Muller, E., Ramaswamy, S., Reimann, M., Abdellah, Marwan, ., Sanchez, C., Ailamaki, J., Hill, S., Segev, I., and Schürmann, F. (2015). Reconstruction and Simulation of Neocortical Microcircuitry. *Cell*, 163(2):456–492.

Mathis, A., Mamidanna, P., Cury, K. M., Abe, T., Murthy, V. N., Mathis, M. W., and Bethge, M. (2018). DeepLabCut: markerless pose estimation of user-defined body parts with deep learning. *Nature Neuroscience*.

Matyas, F., Sreenivasan, V., Marbach, F., Wacongne, C., Barsy, B., Mateo, C., Aronoff, R., and Petersen, C. C. (2010). Motor control by sensory cortex. *Science*, 330(6008):1240–1243.

Mazzoni, A., Logothetis, N. K., and Panzeri, S. (2013). Information content of local field potentials: Experiments and models. *Principles of Neural Coding*, pages 411–430.

McNiel, D. B., Choi, J. S., Hessburg, J. P., and Francis, J. T. (2016). Reward value is encoded in primary somatosensory cortex and can be decoded from neural activity during performance of a psychophysical task. *Proceedings of the Annual International Conference of the IEEE Engineering in Medicine and Biology Society, EMBS*, 2016-October:3064–3067.

Meng, X., Winkowski, D. E., Kao, J. P., and Kanold, P. O. (2017). Sublaminar subdivision of mouse auditory cortex layer 2/3 based on functional translaminar connections. *Journal of Neuroscience*, 37(42):10200–10214.

Mitzdorf, U. (1985). Current source-density method and application in cat cerebral cortex: Investigation of evoked potentials and EEG phenomena. *Physiological Reviews*, 65(1):37–100.

Moss, C. F. and Surlykke, A. (2010). Probing the natural scene by echolocation in bats. *Frontiers in Behavioral Neuroscience*, 4(AUG):1–16.

Mountcastle VB, Berman AL, D. P. (1955). Topographic organization and modality

representation in first somatic area of cat's cerebral cortex by method of single unit analysis. *American Journal of Physiology, 183 : 646*.

Mowrer, O. H. (1951). Two-factor learning theory: summary and comment. *Psychological review*, 58(5):350–354.

Muff, S., Held, L., and Keller, L. F. (2016). Marginal or conditional regression models for correlated non-normal data? *Methods in Ecology and Evolution*, 7(12):1514–1524.

Musall, S., Kaufman, M. T., Juavinett, A. L., Gluf, S., and Churchland, A. K. Single-trial neural dynamics are dominated by richly varied movements. *Nature Neuroscience*, (10):1677–1686.

Nakagawa, S. and Schielzeth, H. (2013). A general and simple method for obtaining R2 from generalized linear mixed-effects models. *Methods in Ecology and Evolution*, 4(2):133–142.

Nanda, P., Morris, A., Kelemen, J., Yang, J., and Wiest, M. C. (2020). Evoked frontal and parietal field potential signatures of target detection and response inhibition in rats performing an equiprobable auditory go/no-go task. *eNeuro*, 7(1):1–18.

Nilsson, S. R., Alsiö, J., Somerville, E. M., and Clifton, P. G. The rat's not for turning: Dissociating the psychological components of cognitive inflexibility. *Neuroscience and Biobehavioral Reviews*, (October 1980):1–14.

Niwa, M., Johnson, J. S., O'Connor, K. N., and Sutter, M. L. (2012). Activity related to perceptual judgment and action in primary auditory cortex. *Journal of Neuroscience*, 32(9):3193–3210.

Ohl, F. W. (2015). Role of cortical neurodynamics for understanding the neural basis of motivated behavior - lessons from auditory category learning. *Current Opinion in Neurobiology*, 31:88–94.

Ohl, F. W. and Scheich, H. Differential frequency conditioning enhances spectral contrast sensitivity of units in auditory cortex (field Al) of the alert Mongolian gerbil. *The European journal of neuroscience*, (5):1001–17.

Ohl, F. W. and Scheich, H. (1997). Learning-induced dynamic receptive field changes in primary auditory cortex of the unanaesthetized Mongolian gerbil. *Journal of Comparative Physiology - A Sensory, Neural, and Behavioral Physiology*, 181(6):685–696.

Ohl, F. W. and Scheich, H. (2005). Learning-induced plasticity in animal and human

auditory cortex. *Current Opinion in Neurobiology*, 15(4):470–477.

Ohl, F. W., Scheich, H., and Freeman, W. J. (2000). Topographic analysis of epidural pure-tone-evoked potentials in gerbil auditory cortex. *Journal of neurophysiology*, 83:3123–3132.

Ohl, F. W., Scheich, H., and Freeman, W. J. (2001a). Change in pattern of ongoing cortical activity with auditory category learning. *Nature*, 412(6848):733–736.

Ohl, F. W., Scheich, H., and Freeman, W. J. (2001b). Change in pattern of ongoing cortical activity with auditory category learning. *Nature*, 412(1997):733–736.

Ohl, F. W., Wetzel, W., Wagner, T., Rech, A., and Scheich, H. (1999). Bilateral Ablation of Auditory Cortex in Mongolian Gerbil Affects Discrimination of Frequency Modulated Tones but not of Pure Tones. *Learning & Memory*, 6:347–362.

Olejnik, S. and Algina, J. (2003). Generalized Eta and Omega Squared Statistics: Measures of Effect Size for Some Common Research Designs. *Psychological Methods*, 8(4):434–447.

Osmanski, M. S. and Wang, X. (2015). Behavioral Dependence of Auditory Cortical Responses. *Brain Topography*, 28(3):365–378.

Otto, G. and Jürgen, S. (2011). The Mongolian Gerbil as a Model for the Analysis of Peripheral and Central Age-Dependent Hearing Loss.

Pachitariu, M., Lyamzin, D. R., Sahani, M., and Lesica, N. A. (2015). State-dependent population coding in primary auditory cortex. *Journal of Neuroscience*, 35(5):2058–2073.

Pakan, J. M., Currie, S. P., Fischer, L., and Rochefort, N. L. (2018). The Impact of Visual Cues, Reward, and Motor Feedback on the Representation of Behaviorally Relevant Spatial Locations in Primary Visual Cortex. *Cell Reports*, 24(10):2521–2528.

Parras, G. G., Nieto-Diego, J., Carbajal, G. V., Valdés-Baizabal, C., Escera, C., and Malmierca, M. S. (2017). Neurons along the auditory pathway exhibit a hierarchical organization of prediction error. *Nature Communications*, 8(1).

Patterson, R. D. (1999). Interdisciplinary auditory neuroscience. *Trends in Cognitive Sciences*, 3(7):245–247.

Petkov, C. I., Kang, X., Alho, K., Bertrand, O., Yund, E. W., and Woods, D. L. (2004). Attentional modulation of human auditory cortex. *Nature Neuroscience*, 7(6):658–663.

Plakke, B. and Romanski, L. M. (2014). Auditory connections and functions of prefrontal cortex. *Frontiers in Neuroscience*, 8(8 JUL):1–13.

Polley, D. B., Steinberg, E. E., and Merzenich, M. M. (2006). Perceptual learning directs auditory cortical map reorganization through top-down influences. *Journal of Neuroscience*, 26(18):4970–4982.

Poremba et al. Species-specific calls evoke asymmetric activity in the monkey's temporal poles. *Nature*, (6973):445–448.

Purves, D. *Neuroscience*.

Puschmann, S., Steinkamp, S., Gillich, I., Mirkovic, B., Debener, S., and Thiel, C. M. (2017). The right temporoparietal junction supports speech tracking during selective listening: Evidence from concurrent EEG-fMRI. *Journal of Neuroscience*, 37(47):11505–11516.

Renart, A. and Machens, C. K. (2014). Variability in neural activity and behavior. *Current Opinion in Neurobiology*, 25:211–220.

Rodgers, C. C. and DeWeese, M. R. (2014). Neural correlates of task switching in prefrontal cortex and primary auditory cortex in a novel stimulus selection task for rodents. *Neuron*, 82(5):1157–1170.

Romanski, L. M. and Goldman-Rakic, P. S. (2002). An auditory domain in primate prefrontal cortex. *Nature Neuroscience*, 5(1):15–16.

Romo, R. and Rossi-Pool, R. (2020). Turning Touch into Perception. *Neuron*, 105(1):16–33.

Rothe, T., Deliano, M., Scheich, H., and Stark, H. (2009). Segregation of task-relevant conditioned stimuli from background stimuli by associative learning. *Brain Research*, 1297:143–159.

Runyan, C. A., Piasini, E., Panzeri, S., and Harvey, C. D. (2017). Distinct timescales of population coding across cortex. *Nature*, 548(7665):92–96.

Sakata, S. and Harris, K. D. Laminar Structure of Spontaneous and Sensory-Evoked Population Activity in Auditory Cortex. *Neuron*, (3):404–418.

Sapolsky. *Behave: The Biology of Humans at Our Best and Worst*.

Schaefer, M. K., Hechavarría, J. C., and Kössl, M. Quantification of mid and late evoked sinks in laminar current source density profiles of columns in the primary auditory

cortex. *Frontiers in neural circuits*, (October):52.

Scheich, H. (1991). Auditory cortex: comparative aspects of maps and plasticity. *Current opinion in neurobiology*, 1(2):236–247.

Scheich, H., Brechmann, A., Brosch, M., Budinger, E., Ohl, F. W., Selezneva, E., Stark, H., Tischmeyer, W., and Wetzel, W. (2011). Behavioral semantics of learning and crossmodal processing in auditory cortex: The semantic processor concept. *Hearing Research*, 271(1-2):3–15.

Schroeder, C. (1998). A spatiotemporal profile of visual system activation revealed by current source density analysis in the awake macaque. *Cerebral Cortex*, 8(7):575–592.

Schultz, W., Carelli, R. M., and Wightman, R. M. Phasic dopamine signals: From subjective reward value to formal economic utility. *Current Opinion in Behavioral Sciences*, pages 147–154.

Seto-Ohshima, A., Ito, M., Kudo, T., and Mizutani, A. (1992). Intrinsic and drug-induced seizures of adult and developing gerbils. *Acta Neurologica Scandinavica*, 85(5):311–317.

Shiell, M. M., Hausfeld, L., and Formisano, E. (2018). Activity in human auditory cortex represents spatial separation between concurrent sounds. *Journal of Neuroscience*, 38(21):4977–4984.

Smith, J. L., Johnstone, S. J., and Barry, R. J. (2008). Movement-related potentials in the Go/NoGo task: The P3 reflects both cognitive and motor inhibition. *Clinical Neurophysiology*, 119(3):704–714.

Stark, H., Rothe, T., Deliano, M., and Scheich, H. (2008). Dynamics of cortical theta activity correlates with stages of auditory avoidance strategy formation in a shuttle-box. *Neuroscience*, 151(2):467–475.

Stark, H., Rothe, T., Wagner, T., and Scheich, H. (2004). Learning a new behavioral strategy in the shuttle-box increases prefrontal dopamine. *Neuroscience*, 126:21–29.

Steinmetz, N. A., Zatka-Haas, P., Carandini, M., and Harris, K. D. (2019). Distributed coding of choice, action, and engagement across the mouse brain. *Nature*, in press(November 2018).

Stevens, K. A. (2012). The vision of david marr. *Perception*, 41(9):1061–1072.

Suga, N. (1984). Neural mechanisms of complex-sound processing for echolocation. *Trends in Neurosciences*, 7(1):20–27.

Szymanski, F. D., Garcia-Lazaro, J. A., and Schnupp, J. W. H. (2009). Current source density profiles of stimulus-specific adaptation in rat auditory cortex. *Journal of neurophysiology*, 102(3):1483–90.

Tajima, S., Koida, K., Tajima, C. I., Suzuki, H., Aihara, K., and Komatsu, H. (2017). Task-dependent recurrent dynamics in visual cortex. *eLife*, 6:1–27.

Talpos, J. and Shoaib, M. (2015). Executive function. *Handbook of Experimental Pharmacology*, 228:191–213.

Tchabovsky, A. V., Savinetskaya, L. E., Ovchinnikova, N. L., Safonova, A., Ilchenko, O. N., Sapozhnikova, S. R., and Vasilieva, N. A. (2019). Sociability and pair-bonding in gerbils: a comparative experimental study. *Current Zoology*, 65(4):363–373.

Teki, S., Chait, M., Kumar, S., Shamma, S., and Griffiths, T. D. (2013). Segregation of complex acoustic scenes based on temporal coherence. *eLife*, 2013(2):1–16.

Thomas, H., Tillein, J., Heil, P., and Scheich, H. (1993). Functional organization of auditory cortex in the mongolian gerbil (Meriones unguiculatus). I. Electrophysiological mapping of frequency representation and distinction of fields. *The European journal of neuroscience*, 5(7):882–897.

Thomson (2010). Neocortical layer 6, a review. *Frontiers in Neuroanatomy*, 4(March):1–14.

Tischbirek, C. H., Noda, T., Tohmi, M., Birkner, A., Nelken, I., and Konnerth, A. (2019). In Vivo Functional Mapping of a Cortical Column at Single-Neuron Resolution. *Cell Reports*, 27(5):1319–1326.

Town, S. M., Wood, K. C., and Bizley, J. K. (2018). Sound identity is represented robustly in auditory cortex during perceptual constancy. *Nature Communications*, 9(1).

Tsunada, J., Liu, A. S., Gold, J. I., and Cohen, Y. E. (2015). Causal contribution of primate auditory cortex to auditory perceptual decision-making. *Nature Neuroscience*, 19(1):135–142.

Wadenberg, M.-l. G. (2010). Encyclopedia of Psychopharmacology. *Encyclopedia of Psychopharmacology*, pages 1–6.

Waelti, P., Dickinson, A., and Schultz, W. (2001). Dopamine responses comply with basic assumptions of formal learning theory. *Nature*, 412(6842):43–48.

Wagner, A., Brandon, S., Klein, S., and Mowrer, R. (1989). Contemporary learning theo-

ries: Pavlovian conditioning and the status of traditional learning theory. In *Evolution of a Structured Connectionist Model of Pavlovian Conditioning (AESOP)*, page 149. Erlbaum Hillsdale, NJ.

Waiblinger, E. and König, B. (2004). Refinement of gerbil housing and husbandry in the laboratory. *ATLA Alternatives to Laboratory Animals*, 32(SUPPL. 1A):163–169.

Weinberger, N. M. (1993). Learning-induced changes of auditory receptive fields. *Current Opinion in Neurobiology*, 3(4):570–577.

Weinberger, N. M. and Weinberger, N. M. (2007). Associative representational plasticity in the auditory cortex : A synthesis of two disciplines. pages 1–16.

Wetzel, W., Wagner, T., Ohl, F. W., and Scheich, H. (1998). Categorical discrimination of direction in frequency-modulated tones by Mongolian gerbils. *Behavioural Brain Research*, 91:29–39.

Wiltschko, A. B., Johnson, M. J., Iurilli, G., Peterson, R. E., Katon, J. M., Pashkovski, S. L., Abraira, V. E., Adams, R. P., and Datta, S. R. Mapping Sub-Second Structure in Mouse Behavior. *Neuron*, (6):1121–1135.

Winer, J. (1992). *Handbook of Auditory Research, volume 1, The Mammalian Auditory Pathway: Neuroanatomy.* Springer.New York.

Winkowski, D. E., Nagode, D. A., Donaldson, K. J., Yin, P., Shamma, S. A., Fritz, J. B., and Kanold, P. O. (2018). Orbitofrontal Cortex Neurons Respond to Sound and Activate Primary Auditory Cortex Neurons. *Cerebral cortex (New York, N.Y. : 1991)*, 28(3):868–879.

Wrobel, C., Dieter, A., Huet, A., Keppeler, D., Duque-Afonso, C. J., Vogl, C., Hoch, G., Jeschke, M., and Moser, T. (2018). Optogenetic stimulation of cochlear neurons activates the auditory pathway and restores auditory-driven behavior in deaf adult gerbils. *Science Translational Medicine*, 10(449).

Xiong, Q., Znamenskiy, P., and Zador, A. M. (2015). Selective corticostriatal plasticity during acquisition of an auditory discrimination task. *Nature*, 521(7552):348–351.

Yang, H., Kwon, S. E., Severson, K. S., and O'Connor, D. H. (2015). Origins of choice-related activity in mouse somatosensory cortex. *Nature Neuroscience*, 19(1):127–134.

Yin, P., Strait, D. L., Radtke-Schuller, S., Fritz, J. B., and Shamma, S. A. (2020). Dynamics and Hierarchical Encoding of Non-compact Acoustic Categories in Auditory and

Frontal Cortex. *Current Biology*, 30(9):1649–1663.e5.

Young, M.E. & *Crumer, A. (2006). *Reaction time*, volume 7.

Yuste, R. (2015). From the neuron doctrine to neural networks. *Nature Reviews Neuroscience*, 16(8):487–497.

Zatorre, R. J., Bouffard, M., and Belin, P. (2004). Sensitivity to Auditory Object Features in Human Temporal Neocortex. *Journal of Neuroscience*, 24(14):3637–3642.

Zempeltzi, M. M., Kisse, M., Brunk, M. G., Glemser, C., Aksit, S., Deane, K. E., Maurya, S., Schneider, L., Ohl, F. W., Deliano, M., and Happel, M. F. (2020). Task rule and choice are reflected by layer-specific processing in rodent auditory cortical microcircuits. *Communications Biology*, 3(1):1–12.

Zhou, Y., hua Liu, B., Wu, G. K., Kim, Y. J., Xiao, Z., Tao, H. W., and Zhang, L. I. (2010). Preceding Inhibition Silences Layer 6 Neurons in Auditory Cortex. *Neuron*, 65(5):706–717.

Znamenskiy, P. and Zador, A. M. (2013). Corticostriatal neurons in auditory cortex drive decisions during auditory discrimination. *Nature*, 497(7450):482–485.

List of Publications

- **Task rule and choice are reflected by layer-specific processing in rodent auditory cortical microcircuits** - **M. M. Zempeltzi**, M. Kisse, M. G. K. Brunk, C. Glemser, S. Aksit, K. E. Deane, S. Maurya, L. Schneider, F. W. Ohl, M. Deliano, M. F. K. Happel – **Communications Biology (2020)**
- **Ketamine anesthesia induces gain enhancement via recurrent excitation in granular input layers of the auditory cortex** - K. E. Deane, M. G.K. Brunk, A. Curran, **M. M. Zempeltzi**, M. Deliano, F. W. Ohl, M. F.K. Happel - **Journal of Physiology (2020)**
- **Dopaminergic neuromodulation of high-gamma stimulus phase-locking in gerbil primary auditory cortex mediated by D1/D5-receptors** - M. Deliano*, M. G.K. Brunk*, M. El-Tabbal, **M. M. Zempeltzi** , M. F.K. Happel, F. W. Ohl - **European Journal of Neuroscience (2018)**
- **Wide distribution of CREM immunoreactivity in adult and embryonic human brain, with an increased expression in Dentate gyrus neurons of Alzheimer's as compared to normal aging brains** - H-G. Bernstein, E. Kirches, G. Keilhoff, B. Bogerts, J. Steiner, U. Lendeckel, **M. M. Zempeltzi**, V. Dobrowolny, C. Kyttaris, K. Tenbrock, C. Mawrin - **Amino Acids (2013)**